This is to certify that the
dissertation entitled

BIOPOLYMER-BASED OCULAR DRUG DELIVERY SYSTEMS

presented by

WEIPENG LIU

has been accepted towards fulfillment
of the requirements for the

Ph.D. degree in CHEMICAL ENGINEERING

Kamani Narayan
Major Professor's Signature

Nov 22, 2008
Date

BIOPOLYMER-BASED OCULAR DRUG DELIVERY SYSTEMS

By

Weipeng Liu

A DISSERTATION

Submitted to
Michigan State University
in partial fulfillment of the requirements
for the degree of

DOCTOR OF PHILOSOPHY

Chemical Engineering

2008

ABSTRACT

BIOPOLYMER-BASED OCULAR DRUG DELIVERY SYSTEMS

By

Weipeng Liu

A major problem in ocular therapeutics is the attainment of an optimal drug concentration at the site of action. Because of the specific structure of the eye, the treatment of ocular diseases is often a drug delivery problem. This dissertation represents a systematic study of molecular structure-property-performance relationship of chemically modified starch-based ocular drug delivery systems.

The specific polymers investigated were Dihydroxyl Starch (DHS) and DHS Esters including acetates and propionates. The DHS was prepared through a two-step method. Starch was first oxidized by $NaIO_4$ to form Dialdehyde Starch (DAS) and DAS was reduced to form the corresponding hydroxyls with $NaBH_4$. After this modification, polymers with increased solubility in water were obtained. By varying the ratio between starch and oxidant in the first step, the content of Dialdehyde groups was controlled; thereafter 20DHS, 60DHS, and 100DHS were prepared. Among them, 100DHS was further esterified to obtain DHS acetates (DHSA) and DHS Propionates (DHSP). During esterification, the degree of substitution (DS) of DHSA and DHSP was controlled and in this work DHSA and DHSP with DS equal to 0.1 and 0.4 were prepared.

The specific aspects investigated in this research were surface property, mucoadhesion, rheological behavior, controlled drug release, and their effects on ocular drug delivery systems' performance in animal tests. (1) Surface property. Previous work was focused on lowering surface tension (ST) to help spreading. In this work, we took the

ST's effect on both spreading and adhesion into account and suggested an ideal ST should be moderately lower than that of the cornea. (2) Mucoadhesion. A strong adhesion with mucus in the eye helps a drug delivery system to achieve a prolonged retention time and form a strengthened network that sustains the release of drug. In this work, the mucoadhesion of synthesized polymers was studied through a typical rheological approach. (3) Rheological properties. Flow properties were thoroughly studied by other researchers. However, it is rare for ophthalmic solutions to undergo only steady state shear rate in situ. Thus, it was necessary to investigate their viscoelastic properties as well, which were omitted by previous researchers. Therefore, in this work both steady shear and dynamic behaviors of synthesized polymers were studied to investigate their effects on ocular drug delivery systems. (4) Controlled drug release. The drug release profile is important for achievement of sustained drug release and they were studied with a standard USP dissolution method in this work. None of the four concepts we investigated is new and some of them have been introduced to the study of ocular drug delivery systems, however, no work has been done to study their effects systematically. As the first work of systematic study of biopolymer-based ocular drug delivery systems, we studied how these properties were affected by molecular structures, how they should be designed by engineering chemical structures accordingly, and how they affected the performance of ocular drug delivery systems, both theoretically and experimentally. The work described in this dissertation helps fill the knowledge gaps, which exist for the design of effective ocular drug delivery systems with modified starch.

ACKNOWLEDGMENTS

I would like to first thank my advisor, Dr. Narayan, for the opportunity to work on such an interesting project and for his guidance, help, and support for this work. Thank Dr. Townsend for her help on the medical aspects of the project. Thank Dr. Steffe for providing lab, equipments, and answering rheological questions. Thank Dr. Drzal for help on surface tension analysis. I would also like to thank all of my friends in the department for helping me in the many ways that you did. And finally I would like to thank my parents and my wife, Tingting, for all of the support they have provided me as well as my wife's help with statistics.

TABLE OF CONTENTS

LIST OF TABLES

LIST OF FIGURES

Chapter 1 Introduction and Background

1.1 Introduction

Drug delivery is usually a problem in ocular therapeutics because of the specific structure of the eye. Eye diseases can cause patients anxiety and discomfort, or even worse, loss of vision or facial disfigurement. One of the most important concerns in ocular therapeutics is the attainment of an optimal drug concentration at the site of action. Poor bioavailability of active agents from ocular dosage forms is mainly due to two major constraints[1] the precorneal loss factions and the relative impermeability of the corneal epithelial membrane. Due to these physiological and anatomical barriers, only a very small fraction of the drug, usually 1-5% or even less of the instilled dose[2], is effectively absorbed. While there are many topical ophthalmic solutions, all of them have very poor bioavailability. Therefore, there is a need for ocular drug delivery systems with long retention times, relatively high bioavailability, ease of use, ease of manufacture, and overall acceptance by the patient.

1.1.1 Objectives

This project was focused on fundamental aspects of the ocular drug delivery process as well as structure-property performance relationship of ocular drug delivery systems using modified starch-based biopolymers. As such, this is the first work to systemically study modified starch-based ocular drug delivery systems. Generally, the ocular drug delivery process can be divided into four subprocesses: (1) spreading or wetting; this subprocess is important for minimizing irritancy and further forming of mucoadhesion. It is affected and can be optimized by controlling the interfacial properties of the ocular drug delivery system. (2) Mucoadhesion; this subprocess is important for

prolonging the retention time in the eye, which is the bottleneck of most current ocular drug delivery systems. (3) Retention: this subprocess is significantly affected by rheological properties of the ocular drug delivery system, which are important for both reducing irritancy and increasing the retention time. (4) Optimized drug release; this subprocess is important to achieve an effective treatment and to avoid any side effects. Based on these design principles, a series of polymers with tailored chemical structures have been synthesized to achieve optimized properties for the starch-based ocular drug delivery. Successful completion of this work should lead to improved design of modified starch-based ocular drug delivery systems and will also help understanding fundamental aspects of ocular drug delivery process and their relationships with molecular structures.

1.1.2 Organization of this Thesis

The thesis is divided into five main parts. In Chapter 1, the need for new ocular drug delivery systems is addressed. This chapter also includes comprehensive reviews and background information of current problems as well as current research activities in this field.

In Chapter 2, detailed experiment procedures are given including the synthesis of these novel polysaccharide-based polymers, which are water soluble and suitable for ophthalmic solution preparation. This chapter also includes detailed structural analyses of the products using FT-IR, NMR, and other chemical methods.

In Chapter 3, property characterizations of ophthalmic solutions made of synthesized polymers are described. Properties investigated include surface tension, mucoadhesion, rheological properties, drug release, and stability.

In Chapter 4, the focus is on animal tests, including irritancy, tear break-up time,

and drug release tests to characterize the performance of selected candidates.

Chapter 5 draws conclusions based on the finished work and suggests future research plans.

1.2 Background

The fact that drug delivery to the eye is an important and active research topic has attracted many researchers into this field. In order to further understand this topic, in this section, the anatomy of the eye, common eye diseases, drug diffusion model and the tear film structure in the eye are discussed.

1.2.1 Anatomy of the eye

To understand the unique drug delivery issues associated with the eye, the structure of the eye is the first consideration. Figure 1 shows a schematic cross section of the eye.

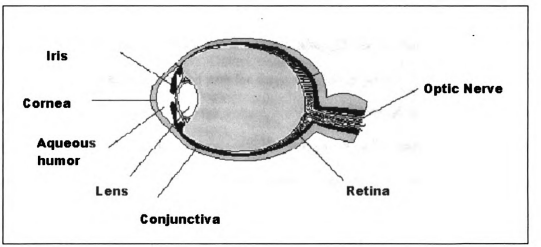

Figure 1 Anatomy of the eye

The three areas of interest in the eye with respect to topical application of drugs are the cornea, the conjunctiva, and the nasolachrymal drainage system[3]. The cornea is the main pathway for the permeation of drugs into the eye[4]. In terms of drug delivery, the

cornea consists of three main barriers in series: the epithelium, the stroma, and the endothelium. The outer epithelium is lipophilic in nature and consists of 5-6 layers of cells. It is the most significant barrier to hydrophilic drug delivery. The stroma accounts for approximately 90% of the corneal thickness and is a relatively open hydrophilic region. The final important region, the inner endothelium, consists of a single layer of flattened cells and is in direct contact with the anterior chamber. Because of both the hydrophilic and hydrophobic regions, the cornea provides an effective barrier to drug transport.

The second major region of the eye with importance to drug delivery is the conjunctiva, which is a thin mucous membrane that lines the posterior surface of the eyelids and the outer regions of the cornea. It is involved in the formation and the maintenance of the precorneal tear film and it is involved in the protection of the eye. The epithelium of the conjunctiva is somewhat different from that of the cornea. The human conjunctiva is 15-25 times more permeable to hydrophilic drugs than the cornea and it provides an alternative absorption path for drugs applied topically[1].

The nasolachrymal drainage system accounts for most of the drug loss in the precorneal region. It consists of three parts: the secretory system, distributive system, and the excretory system. It is thought that tears are largely absorbed by the mucous membranes of the ducts and that only a small amount reaches the nasal passages[5]. This absorbtion by the mucous membranes provides another route of systemic absorption of the applied drugs. The *cul-de-sac* of the eye normally holds 7-9 µl of tears and can contain up to 20-30 µl if care is taken not to blink. The normal tear flow rate is 1 µl per minute and the pH is maintained at 6.5-7.6. The high turnover of tear fluid and the

limited capacity of the sacs can lead to a high clearance rate of drugs once applied[3].

1.2.2 Common eye diseases

In this section, we will review some common eye diseases which need topical therapies by targeting the outer surface or anterior chamber of the eye. They are introduced as follows.

Dry eye. According to the definition by Brewitt and Sistani[6], dry eye is a disease of the ocular surface attributable to different disturbances of the natural function and protective mechanism of the external eye, leading to an unstable tear film during the open eye state. This disease can be caused by tear deficiency or excessive evaporation and is associated with symptoms of discomfort. The definition of dry eye has been further expanded by Albietz to include any functional or component anomaly of the lids or glands associated with tear production in which the quality and/or quantity of the tear film is adversely affected and there is an inability to maintain a healthy ocular surface[7]. Clinically dry eye disease can be assigned to two major classes: aqueous deficient dry eye, due to a reduced aqueous tear secretion; and evaporative dry eye. No matter what the initial cause is, chronic dryness of the ocular surface results in an inflammatory reaction, which is the key mechanism of chronic ocular surface injury. Patients often complain about grittiness, foreign body sensation, burning, soreness, stinging, scratchiness, dryness, blurry vision, a "film over the eyes," paradoxical reflex tearing, and photophobia. Absolute tear deficiency can lead to blindness due to severe ocular surface disease and attempts of surgical reconstruction frequently fail in this situation[8]. The global features in common for both forms of dry eye are (1) a set of characteristic

symptoms, (2) ocular surface damage, (3) reduced tear film stability, and (4) tear hyperosmolarity[9].

The goals of dry eye treatment are to reduce symptoms, to improve tear film quantity and quality, and to reverse the ocular surface damage. Therapeutical approaches include (1) tear substitution, (2) pharmacological stimulation of tear secretion, and (3) tear preservation through reduction of tear evaporation or drainage[10]. The latter two approaches are beyond the scope of this study. We will focus our discussion on the tear substitution approach.

The goal of using tear substitutes is to increase humidity at the ocular surface and to improve lubrication. This approach is currently the most widely used therapy for dry eye. It includes a variety of components to formulate a considerable number of commercially available preparations. Cellulose ethers are most commonly used in dry eye solutions and have good retention time on the ocular surface[11], sodium hyaluronate has been found particularly beneficial in corneal wound healing[12], carbomers provide excellent adhesive behavior and higher retention time,[13] and recently lipid containing drops aim to rebuild the lipid layer[14].

Glaucoma is a group of disorders characterized by progressive damage to the eye at least partly due to intraocular pressure damaging the optic nerve. Because glaucoma comes in many forms, there is not a universal treatment for it. Treatments can be categorized by either increasing outflow or by decreasing aqueous production.

Conjunctivitis is inflammation of the conjunctiva or the mucous membrane surrounding the eye, also known as pinkeye.

Keratitis is inflammation of the cornea characterized by loss of luster and transparency, as well as cellular infiltration.

Iritis (anterior uveitis) is inflammation of the iris; can be caused by systemic diseases (such as rheumatoid arthritis), systemic infections (such as measles, syphilis, and tuberculosis), trauma, or idiopathic (unknown) sources.

1.2.3 Drug diffusion in the eye

For ailment of the eye, topical administration is usually preferred. The topically administered ocular drugs have to reach inner parts of the eye to obtain therapeutic effects. The transcorneal penetration is believed to be the major route for ocular drug absorption. Diffusion is thought to be the process by which most drugs penetrate the cornea.

As shown in Figure 2, topically applied drugs are cleared from the precorneal area in three different ways: tear drainage, diffusion across the conjunctiva, and diffusion across the cornea. Both tear drainage and diffusion across the conjunctiva account for drug loss in the precorneal area.

Eyedrops mix with the tear fluid when they are administered to the precorneal area. After administration the extra solution volume rapidly flows from the precorneal area into the nasolachrymal drainage system. The drainage of instilled solution is rapid. The drainage rate constant in rabbits increases with instilled volume to $0.31 min^{-1}$ and $0.82\ min^{-1}$ for eyedrops of 5 µl and 50 µl, respectively. Futhermore, the rate of solution drainage decreases with elevated solution viscosity and mucoadhesiveness.[15]

Another important route of drug loss from the precorneal area is drug diffusion across the conjunctiva. Since the conjunctival permeability is fairly high compared to that

of the cornea most drugs diffuse across the conjunctiva easily.

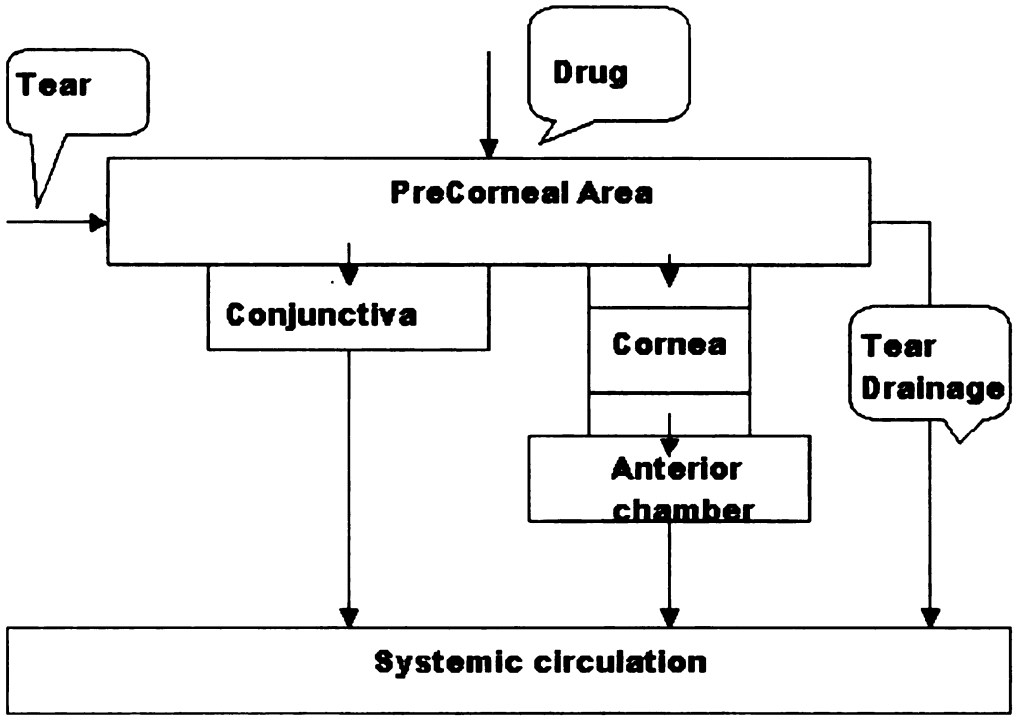

Figure 2 Schematic representation of topical drug delivery model

According to research done by A. Urtti[15], a mass balance equation is induced to describe the drug release in the precorneal area.

$$dQ/dt = C_{pc} (Cl_{tf} + Cl_{cj} + Cl_{co}) \qquad (1.1)$$

where

dQ/dt: drug release rate from polymer matrix

C_{pc}: precorneal drug concentration

Cl_{tf}: drug clearance via tear turnover

Cl_{cj}: drug clearance from fluid to conjunctiva (Cl_{cj} = $Permeability_{cj}$ * $Area_{cj}$)

Cl_{co}: drug clearance from fluid to cornea (Cl_{co} = $Permeability_{co}$ * $Area_{co}$)

Based on the Equation (1.1), the quantity of drug diffusing across the cornea can be figured out as,

$$C_{pc}\, Cl_{co} = dQ/dt - (C_{pc}\, Cl_{tf} + C_{pc}\, Cl_{cj}) \quad (1.2)$$

Therefore, the quantity of the drug absorbed through the cornea can be optimized by controlling drug release rate from polymer matrix and/or by decreasing drug loss through tear drainage and conjunctival absorption. In summary, the strategies to increase the bioavailability of topically applied drug to the eye, involve (1) increasing contact time between drug and cornea, and (2) increasing corneal permeability without a correspondence increase in the conjunctival permeability.

Based on the above discussion, we concluded that both precorneal loss and corneal permeation barrier account for poor performance with current ocular drug delivery systems. In order to significantly improve bioavailability the drug delivery system should have a prolong drug/cornea contact time and/or high corneal permeability. Some synthesized polymer candidates that can be utilized as drug delivery matrices to potentially improve the bioavailability are discussed later.

1.2.4 Tear film

The production and turnover of tears is important for maintaining the health of the ocular surface. Tears clean, lubricate, and nourish the surface of the eye and provide physical and immune protection against infection and mechanical trauma. A small change in tear film stability and/or volume will result in a significant alteration of the quality of the retinal image; thus, maintenance of a stable tear film is essential to healthy vision. The tear film is composed of three main components mucin, water, and lipids. More than 98% of the total tear volume is water[16].

The inner mucin layer is produced by conjunctival goblet cells and epithelial cells of the conjunctiva and cornea. It allows for the wetting of the ocular surface and stabilizes the tear film against the stresses exerted by blinking. The aqueous layer is produced by the main and accessory lacrimal glands. It is responsible for carrying essential growth factors to the epithelium and washing away the epithelial debris, toxic elements, and foreign bodies. The outer lipid layer contains a variety of lipids that protect the tear film against evaporation. In the classical view, the film is thought to have a three-layered architecture. More recently, an aqueous–mucus gel with a mucin gradient has been proposed.[16]

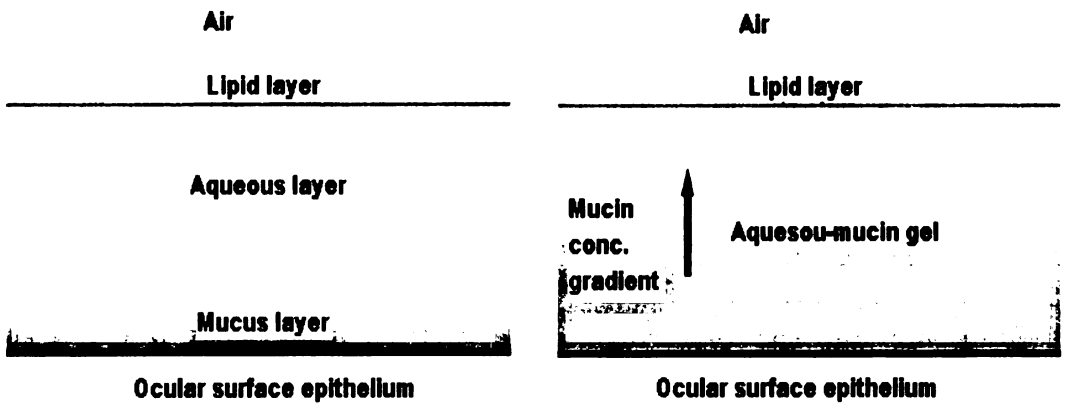

Figure 3: Schematic representations of the structure of the tear film.

1.3 Recent research topics on ocular drug delivery

Scientists involved in ophthalmic pharmaceutical are facing the challenge to improve ocular drug bioavailability from less than 1-5% to at least 15-20%. Investigations aimed at improving topical bioavailability are being pursued along the following principles. First is to minimize precorneal drug loss and maximize corneal absorption by controlling drug release profile, prolonging drug contact time with ocular

surface, and/or transiently changing corneal structure. Second is the use of solid matrices and drug delivery devices, which provide the controlled and continuous delivery of ophthalmic active agents to the pre- and intra-ocular tissues. In this section, some typical ocular drug delivery systems are discussed.

Aqueous gels/Hydrogels: Hydrogels, colloidal gels with water as the dispersion medium, are of particular interest because they can offer controlled drug release according to specific needs. However, difficulty in sterilization and/or easy bacterial contamination has limited their large-scale production and clinic use[1].

Bioadhesive polymer: Bioadhension refers to the attachment of a drug carrier to a specific biological tissue for drug delivery purposes. Coating the external surface of the globe of the eye is a thin film of glycoprotein referred to as mucus. Therefore, bioadhension is also referred to as mucoadhension. Increasing the contact time in the precorneal area appears to be governed by both the mucoadhensive agent as well as the viscosity effects of the polymer. Therefore, in designing the ocular drug delivery systems using mucoadhensives, a vehicle needs to be found that imparts good mucoadhensive strength as well as appropriate viscosity at a low concentration.

Microparticles and nanoparticles: Particulate systems have the potential to become promising for ophthalmic drug delivery by offering an approach to combine extended drug release and improved patient compliance. However, formulation stability, control of particle size, control of the rate of drug release, and large-scale manufacturing of sterile preparations are still major issues in the development of ophthalmic particulate systems.

Penetration enhancers: In order to design a more specific penetration enhancer, it is necessary to have a better understanding of membrane transport, physiology of tight junction, etc. In addition, other approaches such as increasing residence time and inhibition of metabolizing enzymes should be taken into account in conjunction with a penetration enhancer.

Noncorneal route: Relatively high conjunctival and scleral permeability make it possible to put the conjunctival/scleral pathway for the intra-ocular entry of drugs. Much progress has been made in understanding the fundamental basis of drug penetration via those noncorneal pathways. The greatest potential for the concept appears to be the intra-ocular delivery of drugs to treat posterior segment eye diseases, which currently has not been effectively treated by topically administered drugs.

Drug delivery devices: Besides the "pulse entry" type of drug release systems, some systems providing controlled and continuous ocular drug delivery have been developed. These systems can achieve therapeutic action with a smaller dose and fewer side-effects. Typical systems include inserts, implantable systems, and contact lenses. However, patient resistance to surgery and placing an object in the precorneal region should be given particular attention in order to improve overall patient acceptance.

Although a number of polymers have been utilized for ocular drug delivery, none of them provides an optimal approach for this application. In this project, we synthesized a series of starch-based polymers based on the fundamental understanding of the ocular drug delivery process and characterized their properties and performance through both in vitro and in vivo methods.

Chapter 2 Synthesis and Structural Analysis

The objective of this project was to synthesize a safe, water soluble, and biocompatible material that would have the ability to prolong the drug-eye contact time and give controlled drug release profile. Some natural polysaccharides exhibit some of these characteristics, such as biocompatibility and water dispersibility, but they are not optimized for the use of ophthalmic solutions. Waxy starch was chosen as the starting material because of its abundance and current acceptance in pharmaceutical applications. Its chemical structure is shown in Figure 4.

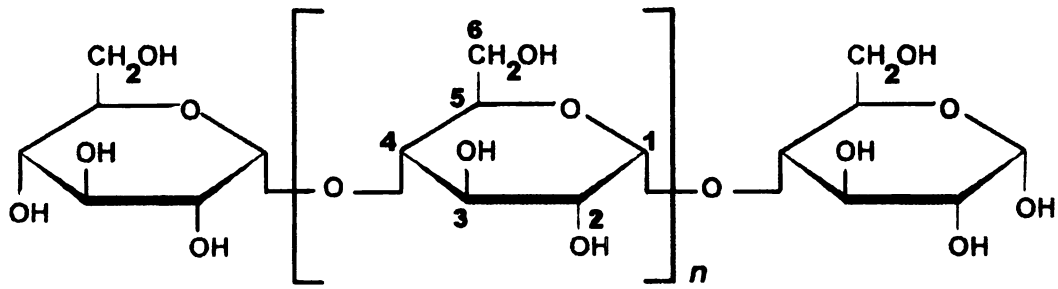

a: amylose

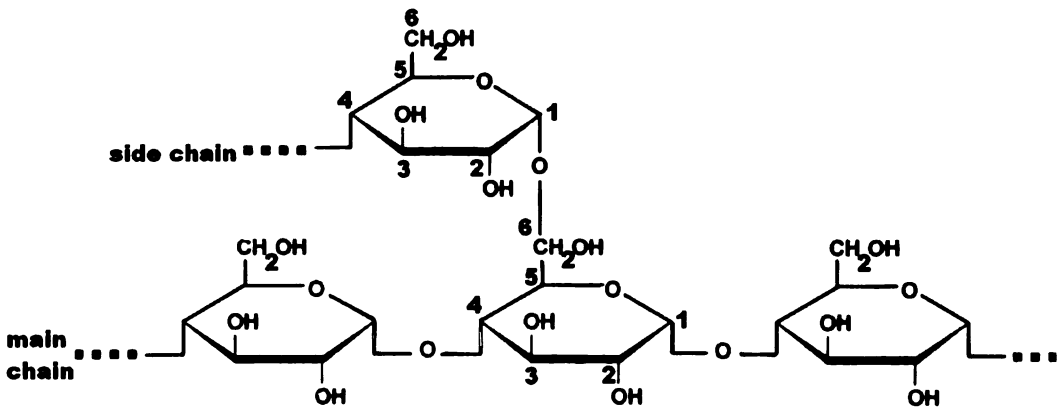

b: amylopectin

Figure 4: Chemical structure of starch

In this study, our objective was to obtain a water soluble product with opened glucose rings in the starch backbone. This was achieved in two steps: (1) Oxidation of starch with sodium periodate to produce Di-Aldehyde-Starch (DAS) and (2) Reduction of DAS by sodium borohydride to the corresponding hydroxyls. In the periodate oxidation step, the starch ring was opened between the C-2 and C-3, which formed a dialdehyde structure. Next, the dialdehyde was reduced and hydroxyl groups were formed at C2 and C3. The product was denoted as DHS (Di-Hydroxyl-Starch).

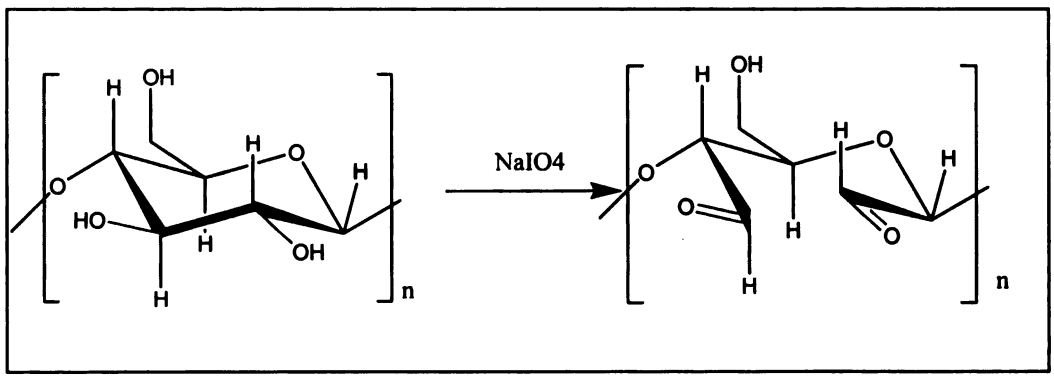

Figure 5: Periodate oxidation of starch

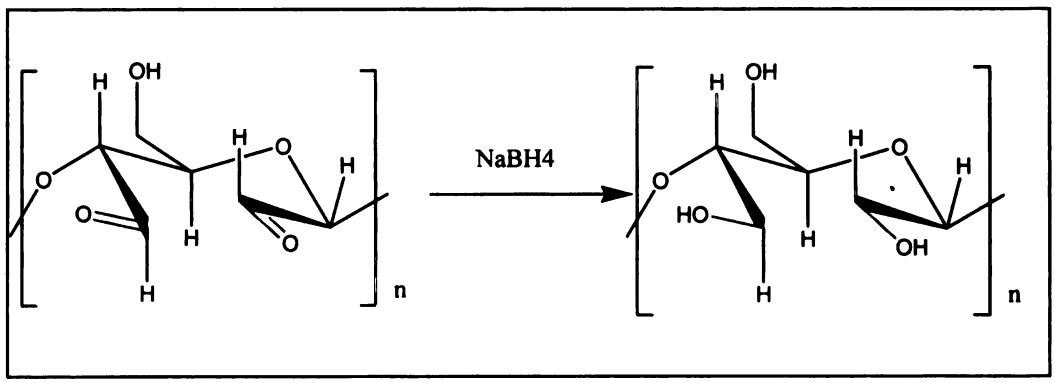

Figure 6: Borohydride reduction of DAS

By effectively controlling the periodate oxidation step, copolymers were formed that contain both the structure of the glucose ring and the flexibility of the open ring structure with C–OH groups on them. In this work a number along with DAS or DHS is used to represent products with different degrees of modifications. For example, 20DAS means periodate oxidized starch with 20% of its ring open and the borohydride reduction product of 20DAS is called 20DHS accordingly. In this project three final products, 20DHS, 60DHS, and 100DHS, were synthesized.

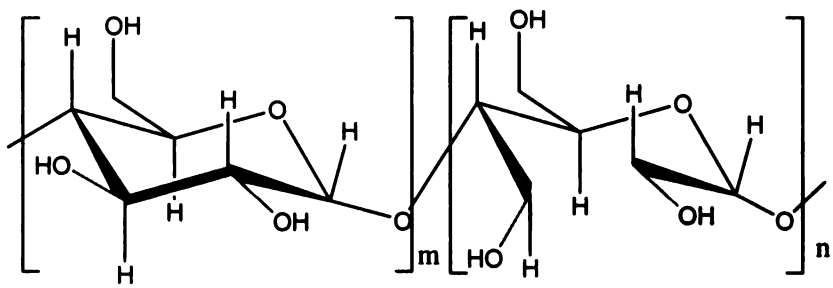

Figure 7: Chemical structure of glucose-c-DHS

Among the three final products, 100DHS was further modified to achieve altered surface activity. The product, 100DHS, was esterified with acetic and propionic anhydride to obtain grafted ester groups with different chain length. In addition, by controlling the amount of anhydride added, esters with various degree of substitution were achieved.

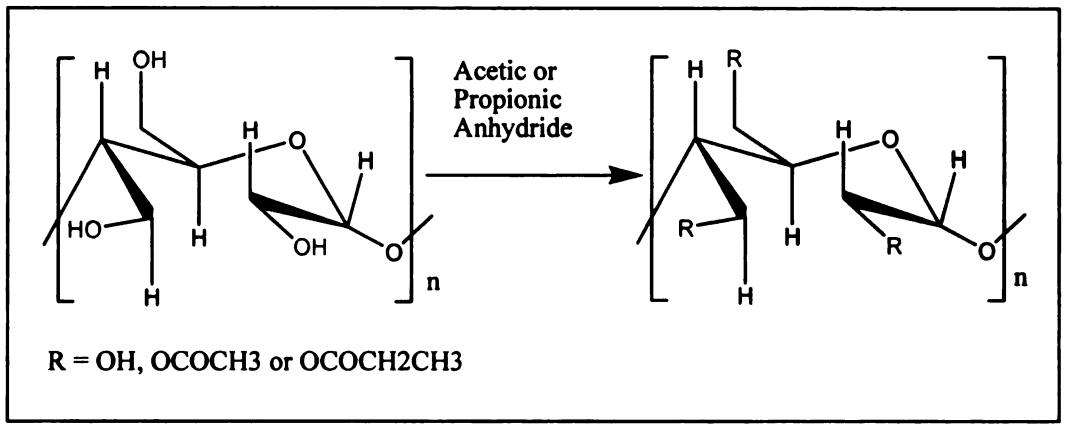

Figure 8: Esterification of 100DHS

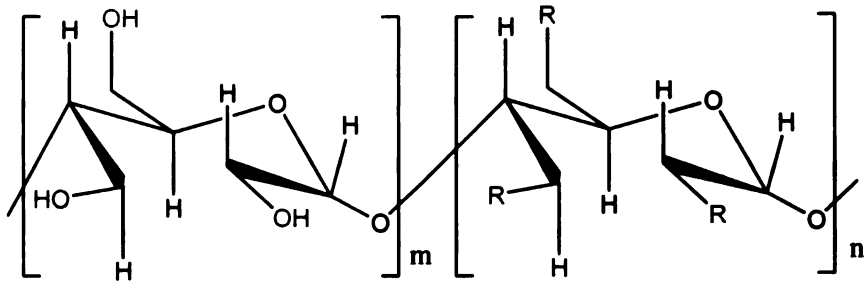

Figure 9: Chemical structure of DHS Esters

2.1 Experiments

2.1.1 DHS preparation

DAS was prepared by oxidizing 8.1 g starch powder suspended in 400 mL of water with sodium periodate at ambient temperature in the dark. Sodium periodate with 1.2 times as much as the theoretical amount (12.8g) was used for preparation of completely oxidized starch (100DAS). Partially oxidized starch was also prepared by the addition of sodium metaperiodate of 0.6 and 0.2 times of theoretical amount (2.1 and 6.4g respectively). The oxidant concentration of each solution prepared was 0.025 M, 0.075 M, and 0.15 M, respectively. The oxidation was performed under magnetic stirring for

six hours. Oxidized products were recovered by filtering and were washed at least 3 times with 400 ml distilled water to remove inorganic salts.

Oxidized product (DAS) was added to a solution containing sodium borohydride, which was 1.5 times as much as the theoretical amount. The reduction was performed at room temperature with magnetic stirring for two hours and the excess borohydride was destroyed with acetic acid. Both 100DHS and 60DHS were completely soluble in water, whereby 20DHS was only partially soluble and thus was separated through filtration into the supernatant solution and an undissolved portion. All the solutions were dialyzed against distilled water to remove inorganic salts and were then concentrated and dried to recover the products. The undissolved portion was suspended in distilled water, filtered, and thoroughly washed with distilled water, and then dried to constant weight. The final weights of the dried samples (20DHS, 60DHS, and 100DDHS) were recorded for yield calculation and further analysis.

2.1.2 DHS Esterification

In this project, DHS esters were synthesized by reacting 100DHS with acetic or propionic anhydride in alkalic aqueous solution. The procedure was as follow:

1. 8 g of 100DHS was dissolved in a beaker with 80 ml of distilled water.
2. Then was stirred on a magnetic plane for 30 minutes until complete dissolution.
3. The beaker was transferred with 100DHS solution into a water bath with temperature set at 15°C.
4. Acetic anhydride (AA) or propionic anhydride (PA) was added into the solution in droplets.

5. Meanwhile, 10% Sodium Hydroxyl solution was added in droplets to keep the pH between 8 and 9.

6. After all AA or PA was added, the solution was transferred into a dialysis tube and was left the tube in distilled water to remove inorganic salts.

7. The dialyzed solution was dried to recover final products: DHS Acetate (DHSA) and DHS Propionate (DHSP).

To obtain products with various DS, AA, or PA was added as shown in Table 1.

Table 1: Esterification of 100DHS

Sample	N(Anhydride)/N(DHS)	AA or PA, gram
DHSA1	0.1	0.255
DHSA2	0.4	1.021
DHSP1	0.1	0.325
DHSP2	0.4	1.301

2.1.3 Carbonyl content determination of DAS

Measurement of the aldehyde groups in DAS was achieved in a procedure by quantitative reduction with sodium borohydride. The relatively rapid method used by Lindberg and Misiorny[17] for estimation of reducing monosaccharides was found to be convenient and applicable to the analysis of the DAS sample. The procedure was based on the hydrogen consumed in the conversion of carbonyl (C=O) to alcohol (C-OH) groups. The difference between the hydrogen evolved on hydrolysis of a sodium borohydride blank containing no DAS and of a mixture after reaction of excess reagent with the DAS sample was the amount of hydrogen required for reduction of the carbonyl groups in the dialdehyde units of DAS.

A DAS sample of 0.10 g was placed in a flask with 0.0280 g sodium borohydride, which was more than the theoretical amount. A 100 ml buret filled with water was connected with the flask to measure the volume of evolved hydrogen. The reduction was performed at room temperature with magnetic stirring for two hours and the stirring was stopped and hydrogen volume was recorded before it was released. Excess acetic acid was added to the flask to destroy unreacted sodium borohydride and the volume of evolved hydrogen was recorded. The sum of both recorded hydrogen volumes was the volume of hydrogen generated by the portion of sodium borohydride, which did not react with DAS. In a separate flask, a blank experiment without DAS was run under the same conditions and the total volume of evolved hydrogen was recorded as well. The difference in total hydrogen volume between the two runs gave the amount of sodium borohydride reacted with DAS, therefore carbonyl content.

2.1.4 NMR

The ^{13}C NMR spectrums of 20DHS, 60DHS, and 100DUS were recorded with a Varian 500 MHz superconducting NMR-Spectrometer operating at 499.738 MHz interfaced with a Sun Microsystems Ultra5 UNIX console. Measurement of NMR spectra was performed in D_2O (99.9% purity) at 25°C. The 3-(Trimethylsilyl)- Propionic acid-D4, sodium salt (TSP) was used as a reference, with a peak at 0 ppm.

Also, Proton NMR was used to determine the DS of DHS esters. This was done on the Varian 500 also. The solvent used was Dimethyl sulfoxide (DMSO). Triflouroacetic acid was added into the test samples to remove the hydroxyls.

2.1.5 FTIR

A Perkins Elmer System 2000 FTIR was used to characterize all samples. The samples were pressed in KBr pellets and run for various amount of scans to achieve high quality spectra. The wavelength range was between 4000 cm^{-1} to 450 cm^{-1}.

2.1.6 DS determination by Titration

The degree of substitution (*DS*) indicates the average number of substitutions per anhydroglucose unit in starch. The highest possible *DS* is three since there are three OH groups available per anhydroglucose unit. The *DS* of esterified starch can be determined by hydrolyzing substituted groups with 0.1 N NaOH and then titrating back with 0.1 N HCl to the original pH prior to the NaOH addition.[18]

Ten grams of the sample were added to a 250 ml conical flask covered with 25 ml of distilled water. The mixture was conditioned in a Tecator 1024 shaking water bath for 1 hour at 30°C and then the pH of the mixture was measured. The pH of the samples ranged from 6 to 7. Next, 150 ml of 0.1 N NaOH were added to each flask. The sample was then conditioned for 48 h at 50°C to hydrolyze the fatty acids substitutes. The excess NaOH of the samples was titrated with HCl back to the original pH. The *DS* was calculated as follows:

$$DS=(M_{FA}*MW_{AN})/[W-M_{FA}(MW_{FA}-MW_{H2O})] \quad (2.1)$$

where *DS*=degree of substitution; *W*=weight of the sample (g); M_{FA}=mols of titrated fatty acid (HCl); MW_{FA}=molecular weight of the fatty acid (HCl); MW_{H2O}=molecular weight of water (18); and MW_{AN}=molecular weight of a repeat unit (164).

2.1.7 Molecular weight measurement

In this project the molecular weight distribution of all synthesized polymers was determined by Gel permeation chromatography (GPC) and their intrinsic viscosity was measured to estimate their viscosity average molecular weight.

GPC involves passing a dilute polymer solution through a tubular column packed with polymeric gel (crosslinked) beads. Under high pressure flow some of the polymer chains are forced into the pores of the gel, while others pass by the gel beads. The residence time of a given polymer chain in the packed column depends on the path it takes through the gel. The output of a GPC reflects the number of chains at a given retention volume, which is directly related to the molecular weight of the sample. From a GPC output, the number average molecular weight, weight average molecular weight and polydispersity index were calculated in comparison to standards. The polydispersity index (PDI) is a measure of the distribution of molecular mass in a given polymer sample. The PDI calculated is the weight average molecular weight divided by the number average molecular weight. The PDI indicates the distribution of individual molecular masses in a batch of polymers. The PDI value is always greater than 1, but as the polymer chains approach is uniform chain length, the PDI approaches unity (1). The PDI from polymerization is denoted as:

$$PDI = M_w/M_n \qquad (2.2)$$

M_n, the number average molecular weight, is the total weight of all the polymer molecules in a sample, divided by the total number of polymer molecules in a sample. M_w, the weight average molecular weight, is based on the fact that a bigger molecule

contains more of the total mass of the polymer sample than the smaller molecules do. These average molecular weights are calculated based on the following two equations:

$$M_n = \frac{\sum_i N_i M_i}{\sum_i N_i} \quad (2.3)$$

$$M_w = \frac{\sum_i N_i M_i^2}{\sum_i N_i M_i} \quad (2.4)$$

Molecular weight can also be calculated from the viscosity of a polymer solution whereby bigger polymers' molecules make the solution more viscous than small polymers. The molecular weight obtained by measuring the viscosity is different from either the number average or the weight average molecular weight. It is between M_n and M_w and it is usually closer to the weight average than the number average molecular weight. Viscosity average molecular weight is determined by intrinsic viscosity and the Mark Houwink equation:

$$[\eta] = KM_v^{\alpha} \quad (2.5)$$

where $[\eta]$ is intrinsic viscosity, K and α are constants and M_v is the experimental viscosity average molecular weight.

Here, α and K are constants for a specific polymer/solvent/temperature system. At the theta condition α should approach 1/2, for non-theta conditions $\alpha>1/2$ and for good-solvent scaling α is expected to be 3/5. α varies from the values of 1/2 or 3/5 due to short-range interactions and their implied effect on the definition of M. Branched

polymers can have a value of a less than 1/2. Values greater than 0.6 are usually associated with the chain rigidity and asymmetry of the coil due to features such as helical coiling.

The viscometer used to measure dilute solutions in this project was an Ubbelohde capillary viscometer. In this viscometer the Poiseuille equation for laminar pressure flow in a capillary tube is used. The volumetric flow rate, Q, under gravity for constant volume is given by Poiseuille's law:

$$Q = \rho g \pi r^4 / (8\eta) \quad (2.6)$$

Where ρ is density, g is gravitational constant, r is the capillary radius, and η is the absolute viscosity. Since the flow time is proportional to the viscosity ($t = k\eta$) the specific viscosity can be calculated as following:

$$\eta_{sp} = [t - t_o] / t_o \quad (2.7)$$

Where t is the efflux time of the solution and t_o is the efflux time of the solvent. The intrinsic viscosity can be calculated from the equation derived by Solomon and Ciuta[19].

$$[\eta] = [2(\eta_{sp} - \ln(\eta_{sp} + 1))]^{1/2} / c \quad (2.8)$$

2.2 Results and discussion

2.2.1 Yield of DHS

In the absence of any side reactions and provided all the products were collected with no loss, 8.08 g 20DHS, 8.04 g 60DHS or 8.00 g 100DHS should have been

recovered given 8.10 g starch was used as the starting material. In practice the actual yield was derived from the weight of collected products divided by the theoretical weight. The yields of DHS are shown in Figure 10.

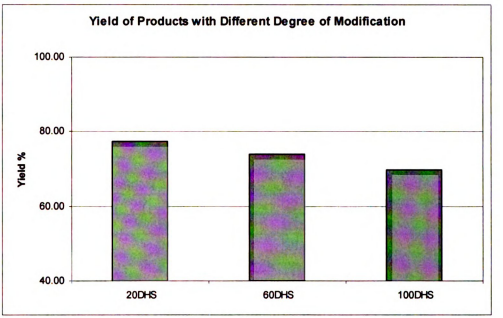

Figure 10: Yield of DHS

It is apparent that the actual yields were between 70-78%. These low yields can be explained by the following reasons: (1) Moisture in the starch. According to the information provided by the manufacturer, there is approximately 11% moisture in the starch. Although it was dried before reaction, there could still have been moisture left, which contributed weight to the starting material. (2) Side reactions. Degradation caused by side reactions were observed during both periodate oxidation and borohydride reduction steps[20]. The second reason also explains why the yield of a high modification product is lower than that of a low modification product.

2.2.2 Carbonyl content determination of DAS

The results of carbonyl contents determination are given in Table 2. The carbonyl contents of 20DAS and 60DAS are slightly higher than the theoretical values because of the moisture in starch. However, the carbonyl content of 100DAS is slightly lower than 100%, most likely due to the fact that the oxidation of starch was not completely finished in the six hours the reaction was run. However, considering the production cost and time, 98.66% yield is acceptable for this study.

Table 2: Dialdehyde unit content of DAS

Sample #	N(NaIO4)/N(AGU)	% Dialdehyde	Std. Dev.
1	20	22.18	0.02
2	60	63.34	0.08
3	100	98.66	0.05

2.2.3 ^{13}C NMR of DHS

The spectrums of starch, 20DHS, 60DHS and 100DHS are shown in Figure 11, 12, 13 and 14. Herein, we focus our discussion on starch and 100DHS, since 20DHS and 60DHS can be seen as copolymers with anhydride-glucose unit and Di-Hydroxyl-Glucose unit, which are the repeat units of starch and 100DHS respectively, and their spectra are the combinations of starch and 100DHS. The ^{13}C NMR spectrum of 100DHS agrees with the work previously done by Narayan[21]. It shows four carbon signals, two of which integrate to two carbons each. The most downfield signal at 104 ppm is obviously the C-1 carbon, which is at 100 ppm in the spectrum of starch. The next signal appears at 78 ppm and is assignable to the C-4 and C-5 carbons. The next two signals appear at 63 ppm representing C2 carbon, and 60.5 ppm, which is assigned to carbons C-3 and C-6.

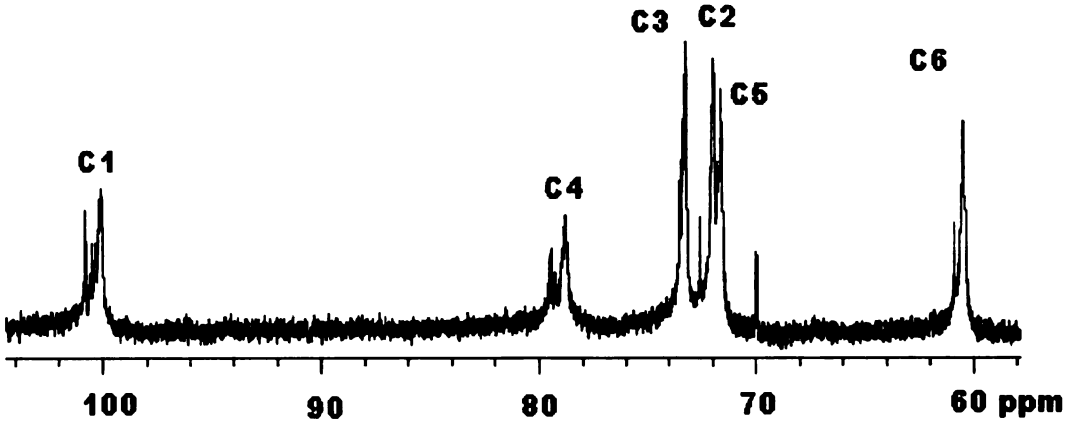

Figure 11: ^{13}C NMR spectrum of corn starch

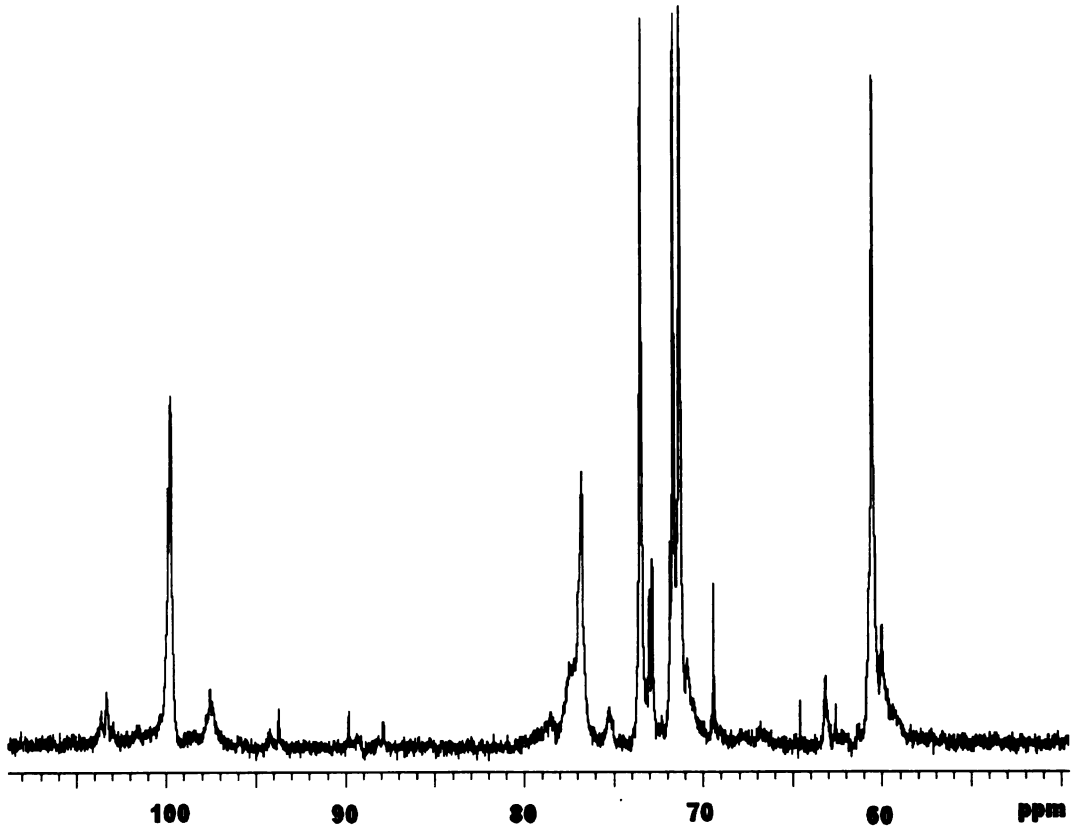

Figure 12: ^{13}C NMR spectrum of 20DHS

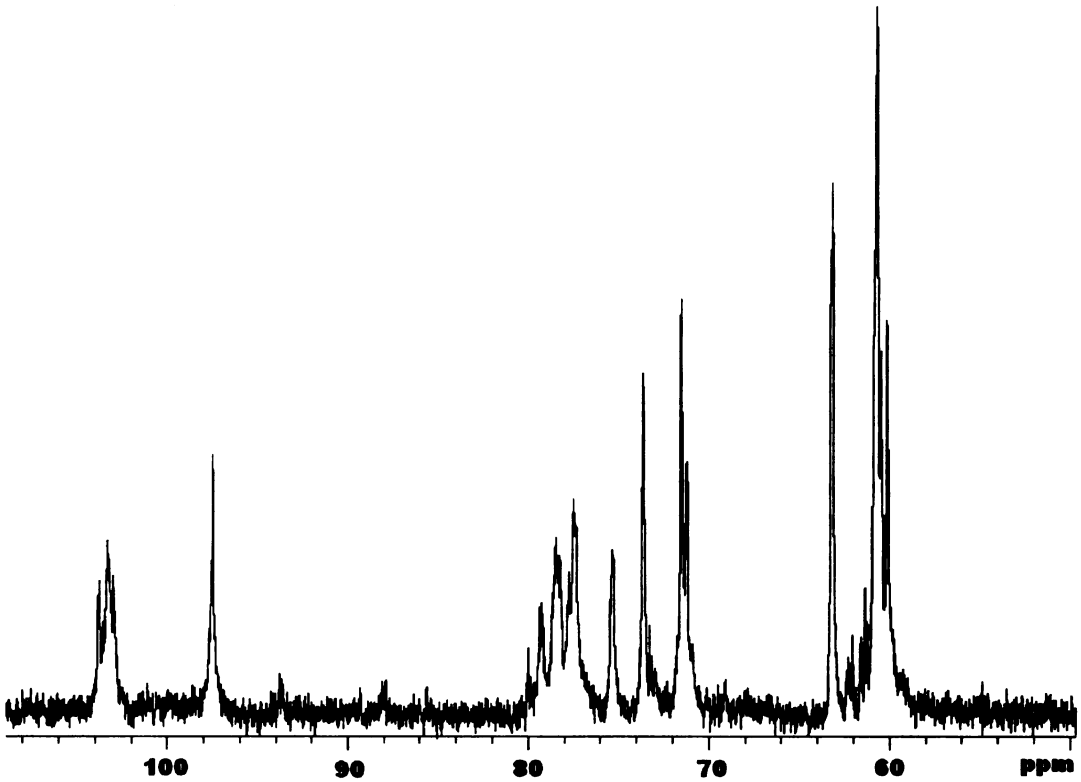

Figure 13: ^{13}C NMR spectrum of 60DHS

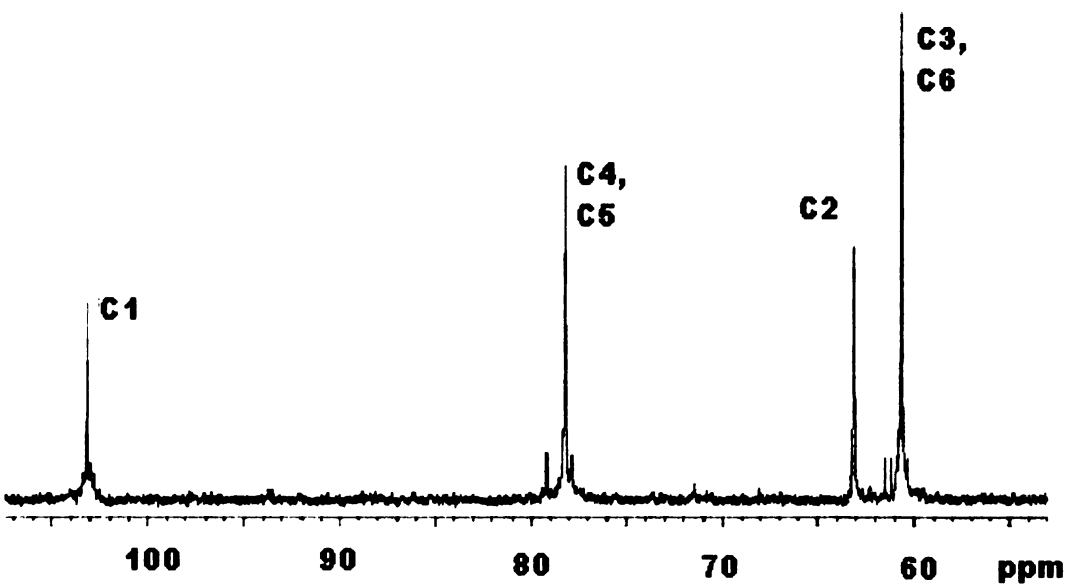

Figure 14: ^{13}C NMR spectrum of 100DHS

2.2.4 FTIR of DHS

In Figure 15, 16, and 17 the spectrum of starch as the starting material is shown at the top. The wide band observed at 3348 cm^{-1} can be attributed to the O-H stretching of the amylopectin and its width is ascribed to the formation of inter- and intra-molecular hydrogen bonds. The bands at 2935 and 2887 cm^{-1} are attributed to the asymmetric stretching of C-H, the band at 1656 cm^{-1} is ascribed to absorbed water and the bands at 1421 and at 1357 cm^{-1} ascribed to the angular deformation of C-H. The C-O ether bond shows stretching at 1156 cm^{-1}, while the C-O alcohol bond shows stretching at 1015 cm^{-1}.

The spectrums of the products after periodate oxidation are shown in the middle of Figure 15, 16, and 17. A band around 1730 cm^{-1} represents stretching of the C=O group was observed. According to Narayan's work[25] most of the aldehyde groups were not in the free state, but probably involved in the formation of hemialdol structure. That is why the peak is not as strong as a regular aldehyde group. Also the C-O alcohol peak at 1015 cm^{-1} is smaller than the corresponding peak of starch. This confirms the structure change from C-O alcohol to C=O carbonyl group.

The spectrums of products after reduction by borohydride are at the bottom of Figure 15, 16, and 17. It is apparent that the carbonyl peak at 1730 cm^{-1} disappeared and the C-O alcohol peak changed back to be as strong as that of starch. Both of these peaks confirmed the borohydride reduction from carbonyl group to hydroxyl group.

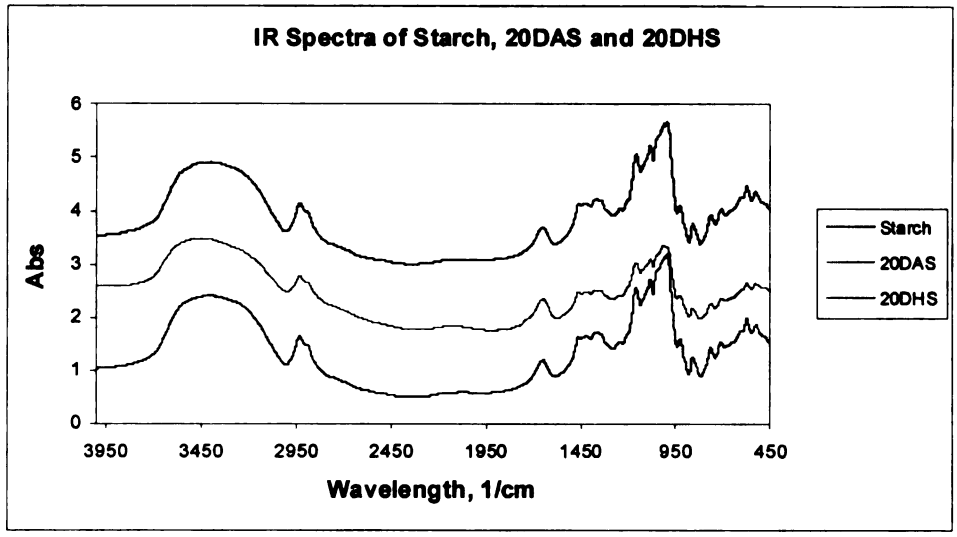

Figure 15: FTIR spectrum of starch, 20DAS and 20DHS

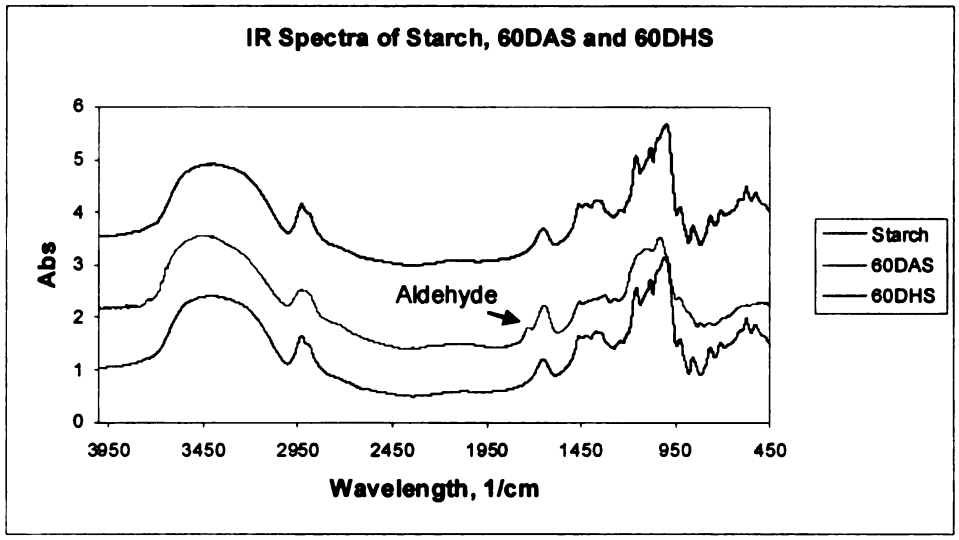

Figure 16: FTIR spectrum of starch, 60DAS and 60DHS

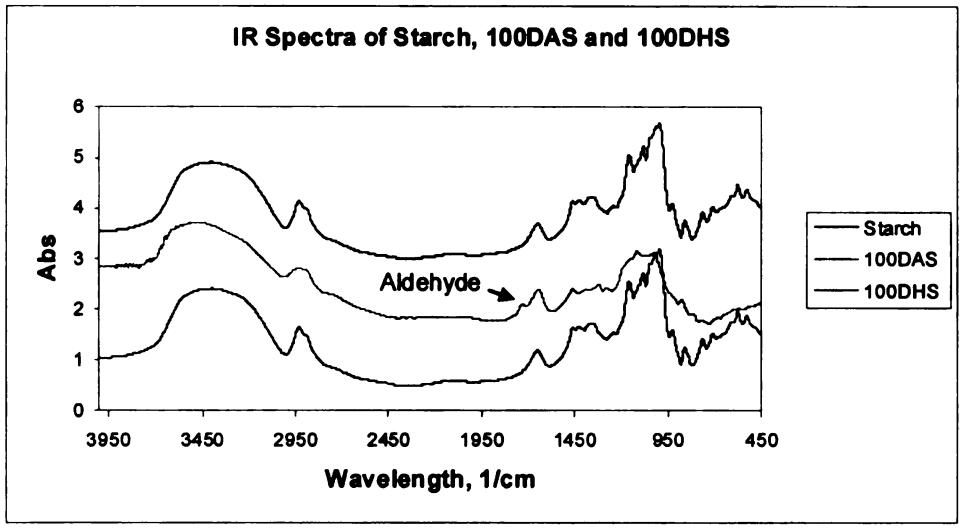

Figure 17: FTIR spectrum of starch, 100DAS and 100DHS

In Figure 18 the spectra of DAS with different degrees of modification are shown. The height differences of carbonyl peak indicate that various degrees of modification were achieved as we expected. The 20DAS shows a very weak carbonyl peak, because only 20% repeat units of starch was oxidized. The 60DAS shows a stronger carbonyl peak and the 100DAS has the strongest carbonyl peak.

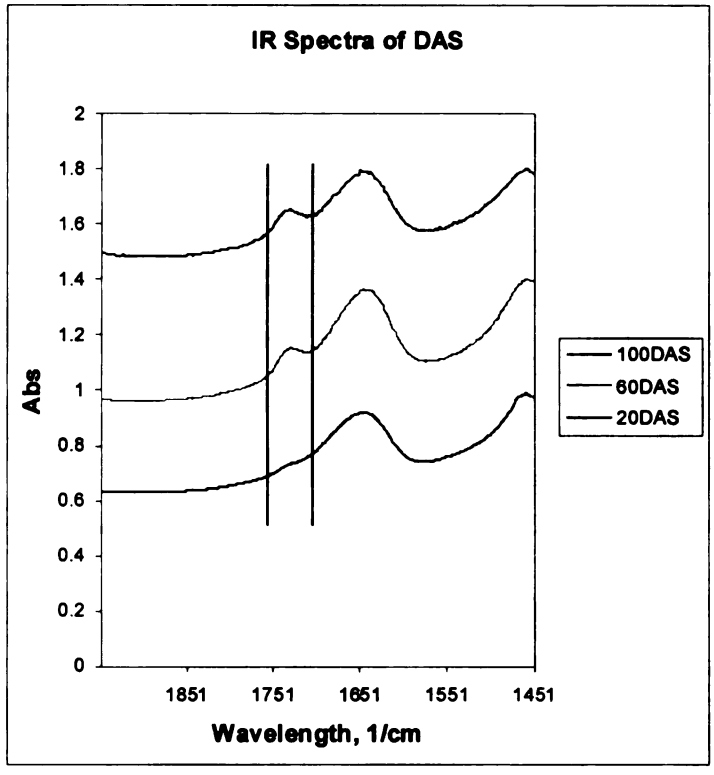

Figure 18: FTIR spectrum of DAS with increasing degree of modification

2.2.5 DS Determination of DHS Esters

The DS was determined by two methods: titration and NMR. It was observed (Table 3) that the measured DS were very close to the theoretically calculated values, especially for products with low DS. Although the esterification was done by following a similar method for esterification of starch in aqueous environment, we obtained much higher DS than that of starch esters. According to the review of Tessler and Billmers[22], typical restriction of an aqueous esterification process is a low substitution level with a DS less than 0.2. This is believed to be because of primary hydroxyl group content difference. In starch there is only one primary hydroxyl group in each anhydrous glucose unit. However, all three hydroxyl groups in the repeat unit of 100DHS are primary.

Although the efficiency of 100DHS esterification was much higher than that of starch, we still need to point out that the efficiency decreases as the DS increases, which is similar to the esterification of starch.

Table 3: DS of DHS esters

Sample	DS(Calculation)	DS(Titration)	STDEV(Titration)	DS(NMR)	STDEV(NMR)
DHSA1	0.10	0.11	0.027	0.10	0.010
DHSA2	0.40	0.38	0.026	0.37	0.014
DHSP1	0.10	0.08	0.034	0.09	0.016
DHSP2	0.40	0.37	0.035	0.36	0.016

In addition, compared to the titration method the NMR method offered a few advantages. As can be seen from the above table, NMR gave much more reliable results with lower standard deviations. Also, this method was much easier and less time consuming.

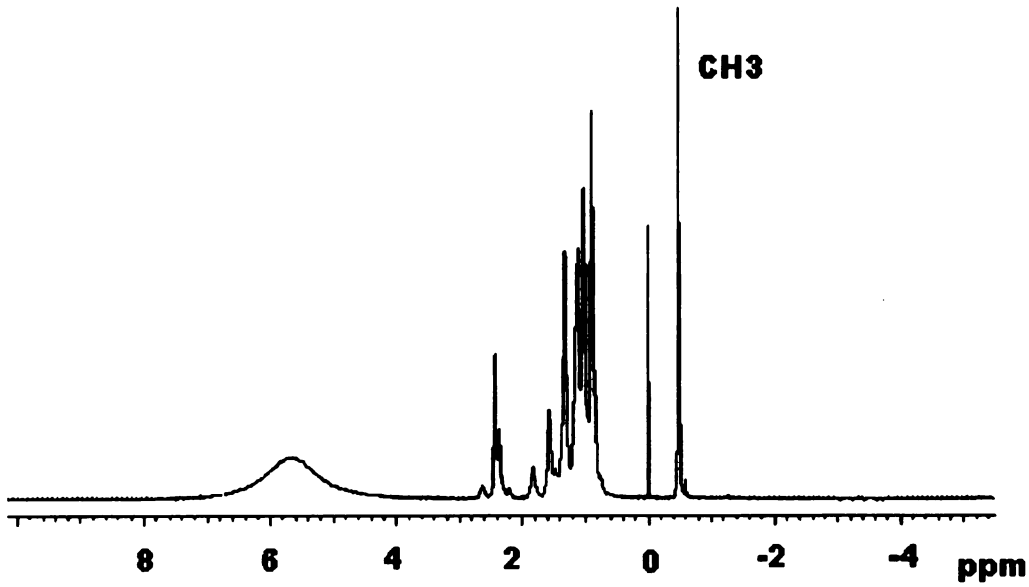

Figure 19: ^{1}H NMR Spectra of DHSA

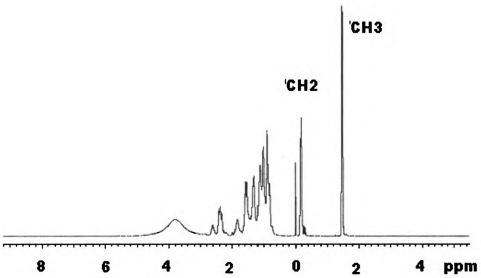

Figure 20: ^{1}H NMR Spectra of DHSP

2.2.6 FTIR of DHS esters

The spectra of DHS esters (DHSA, DHSP and 100DHS) are shown Figure 21. A band around 1730 cm^{-1} represents stretching of the C=O that was observed in all of the esterified products. Also we can see the peak height difference between products with different DS (DHSA1 vs. DHSA2, and DHSP1 vs. DHP2). This further confirms the presence of C=O from ester groups.

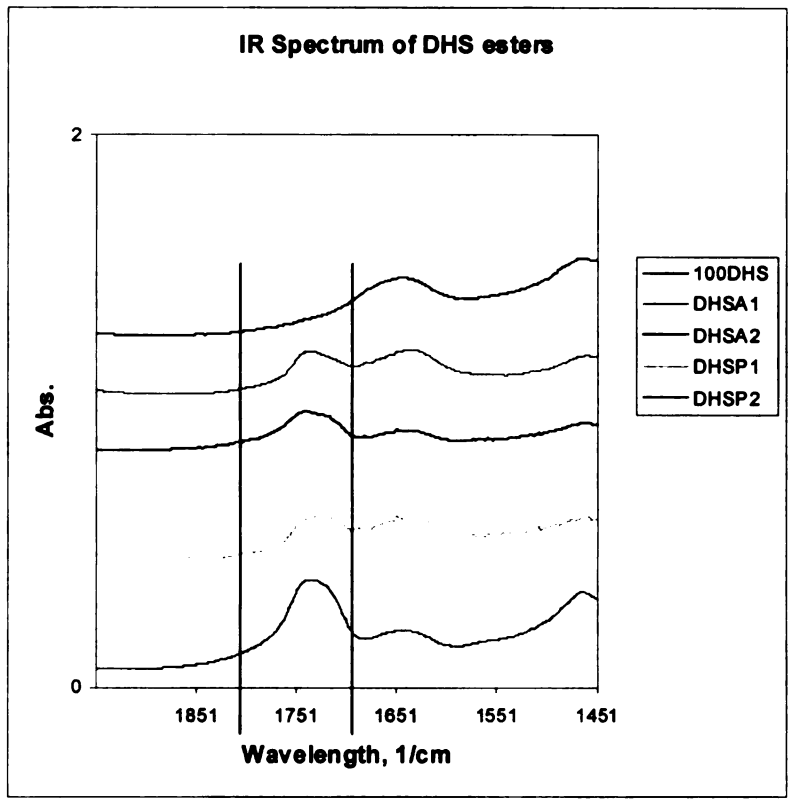

Figure 21: The FTIR Spectrums of DHS Esters

2.2.7 Molecular Weight

The calculated average molecular weights and viscosity of starch, DHS, DHSA and DHSP are shown in Tables 4 and 5:

Table 4: Molecular weight by GPC

Sample	Mn, Da	Mw, Da	PDI
20DHS	878,000	1,047,400	1.19
60DHS	151,800	351,600	2.32
100DHS	139,000	371,600	2.67
DHSA1	138,900	347,000	2.50
DHSA2	133,100	344,400	2.59
DHSP1	151,400	379,300	2.51
DHSP2	146,200	367,100	2.51

Table 5: Intrinsic viscosity

Sample	Intrinsic Viscosity (dl/g)
starch	88.24
20DHS	82.60
60DHS	19.10
100DHS	18.14
DHSA1	9.00
DHSA2	10.68
DHSP1	11.10
DHSP2	11.94

Since K and a are not known for our products, it is not possible to calculate a viscosity average molecular weight. However, the data indicate good correlation between the results from the GPC and the intrinsic viscosity, particularly for DHS. The molecular weight of DHS further confirmed that some degradation occurred during the modification of starch as was also observed from the yielded data. Furthermore, the degree of modification of the starch was directly proportional to the extent of degradation and both GPC and intrinsic viscosity results showed the same trend. During esterification of 100DHS, the molecular weight of DHS esters was shown to be the similar or greater than that of 100DHS. This means there was little or no degradation during the reaction, which agreed with our stability test results that DHS was stable in basic solutions. Although the intrinsic viscosity of DHS esters is much lower than that of 100DHS, it is believed that the K and α constants, not molecular weight, contributed to the difference.

In summary, the modified products, DHS and DHS esters, were synthesized and characterized by FTIR, NMR, and chemical methods to analyze the degree of modification. The degree of modification is controllable by varying the reaction conditions and the products are water dispersible or soluble, depending on the degree of modification.

Chapter 3 Property Characterization

In this chapter some key properties of our starch-based polymers are reported as they relate to the intended application., The surface tension was measured to predict the spreading ability on the ocular surface and the adhesion strength. Mucoadhesion testing was used to predict the retention time in the eye and Rheological analysis was done to study the flow characteristics and the viscoelastic properties, which are important indicators for comfort and retention time. *In vitro* release study was studied to estimate drug release profiles. In addition, the effect of storage and autoclaving were also measured.

3.1 Experiments

3.1.1 Surface properties measurement

Surface tension (ST) is defined as the force acting on the surface of a liquid that tends to minimize the area of the surface or the force that appears to act across a line of unit length on the surface. It is also known as interfacial force, interfacial tension, or surface tensity. The cohesive forces between liquid molecules are responsible for this phenomenon. The spreading or coating ability of the substance can be characterized to some extent by measuring the ST. The ability of ophthalmic solutions to spread on the cornea is important for of two reasons. (1) It helps to lower irritation and (2) It helps to develop an intimate contact with the mucus layer and improves the adhesion to the mucus in the eye. Given this, it is obvious that ST is an important physical property of ophthalmic solutions as it influences the formation and stability of the preocular tear film.

Previous research was focused on obtaining low ST for ophthalmic solutions, however, an ophthalmic solution with low ST also means low thermodynamic adhesion

work and therefore, low adhesion strength, which can result in short retention time in the eye. In this work we take both spreading and adhesion into account and study the ST's effect on the performance.

3.1.1.1 LITERATURE REVIEW

Wetting

The wetting theory, which was developed predominantly in regard to liquid adhesives, was in this study to predict spreading by using interfacial tensions.

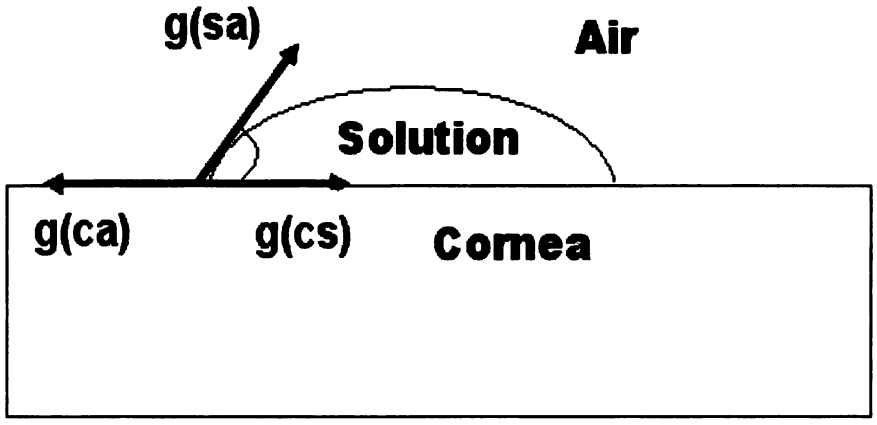

Figure 22: Schematic diagram showing the interfacial tensions involved in spreading an ophthalmic solution over the cornea

Figure 22 is an example showing schematically an ophthalmic solution spreading over the cornea. The contact angle, θ, which should be zero or near zero for proper spreading, is related to interfacial tensions through Young's equation:

$$g_{ca} = g_{cs} + g_{sa}\cos\theta \quad (3.1)$$

where the subscripts c, s, and a represent the cornea, solution, and air. For spontaneous wetting to occur θ must be equal to 0, and therefore

$$g_{ca} >/= g_{cs} + g_{sa} \quad (3.2)$$

The spreading coefficient, S, of an ophthalmic solution over the cornea can be used to predict spreading and can be determined as

$$S = g_{ca} - g_{cs} - g_{sa} \quad (3.3)$$

For an ophthalmic solution to spread over the cornea, S must be positive. Therefore, it is advantageous to maximize g_{ca} while minimizing g_{cs} and g_{sa}.

The corneal epithelium was previously[23] considered as a hydrophobic surface on which water would not spontaneously form a thin film. This notion was subsequently shown to be based on artefactual observations[24]. In contrast, current evidence indicates that the epithelium is highly wettable[25] and the surface tension of intact cells is much closer to that of water leading to a cornea/tear system that is close to a total wetting situation. Therefore, given the fact that g_{ca} is fixed, it is essential to lower g_{cs} and/or g_{sa} in order to obtain spontaneous spreading.

Thermodynamic work of adhesion, Wa

In addition to the spreading coefficient, another important parameter that is affected by interfacial tensions is the specific work of adhesion. According to the Dupre equation, the work of adhesion is equal to the sum of the surface tensions of the cornea and mucoadhesive minus the interfacial tension.

$$W_a = g_{sa} + g_{ca} - g_{cs} \quad (3.4)$$

Therefore, in order to maximize the W_a, we will have to maximize g_{sa}, and minimize g_{cs}.

Given the considerations of both spreading and adhesion, our goal is to minimize g_{cs}, and moderately lower g_{sa}, so that both spontaneous spreading and considerable adhesion strength can be obtained simultaneously. g_{cs} and g_{sa} are discussed as follows.

g_{cs}, Interfacial tension between the cornea and ophthalmic solution

According to the work by Good and Girifalco[26], g_{cs} can be theoretically predicted according to the following equation:

$$g_{cs} = g_c + g_s - 2\Phi(g_c g_s)^{0.5} \quad (3.5)$$

Φ is a molecular parameter. They suggested that higher values of Φ and hence, lower values of g_{cs} are expected to increase the mutual solubility. Generally, a solubility parameter of a polymer can be estimated by a group contribution method. In this work, all polymers were based on modified starch and all were based on similar structures containing grafts of glycopeptide. Therefore, it is reasonable to expect that they are all mutually soluble as they have similar solubility parameters. Based on their structure, we can further expect a low interfacial tension between the cornea and the polymer solution.

Given that g_{cs} can be estimated based on the above discussion, in the above spreading (equation 3.3), and work of adhesion (equation 3.4) equations, two of the three parameters on the right hand side are known or can be theoretically estimated and the only unknown key parameter is g_{sa}, the interfacial tension between polymer solutions and the air. It significantly affects the spreading and the strength of adhesion.

g_{sa}, Interfacial tension between the air and ophthalmic solution

Based on the above discussion, it is essential to moderately reduce g_{sa} to at least lower than the ST of water, rather than to minimize it. Surface tension reduction in water-based systems is generally achieved through the addition of surface active agents called surfactants, which have a characteristic molecular structure consisting of a structural group that has very little attraction for water, known as hydrophobic group, together with a group that has a strong attraction to water, called the hydrophilic group. This is known as amphiphilic structure. When they are dissolved in water the presence of the hydrophobic group in the interior of the solvent causes a distortion of the water structure, increasing the free energy of the system, which requires less work to bring a solute molecule than a water molecule to the surface. Therefore, the solute molecules concentrate at the surface. Since less work is needed to bring molecules to the surface, the presence of surface active molecules decreases the work needed to create unit area of surface. On the other hand, the presence of the hydrophilic group prevents the solute from being expelled completely from the solvent as a separate phase, since that would require desolvation of the hydrophilic group. The amphiphilic structure of surface active molecules therefore causes, not only concentration of the surfactant at the surface and reduction of the surface tension of the solution, but also orientation of the molecules at the surface with its hydrophilic group residing in the aqueous phase and its hydrophobic group oriented away from it.

The hydrophobic group of surfactants is usually a long-chain hydrocarbon residue and to a lesser extent a halogenated group, oxygenated hydrocarbon, or a siloxane chain. The hydrophilic group is usually an ionic or highly polar group. Since both starch and

DHS are hydrophilic in nature, it is feasible to make it more amphiphilic by introducing hydrophobic groups as side chains. Since our goal was to lower the ST moderately, we needed only to introduce short hydrophobic chains onto the starch backbone. In this work, polymers with short hydrophobic chains were grafted. The effects of chain length and degree of substitution on the ST were studied and then correlated with performance as ophthalmic solutions.

In summary, the interfacial tension between the cornea and air is known. DHS and their derivatives have similar structures as grafts of mucin, which helps lower interfacial tension between the drug delivery systems and mucin/cornea. It is essential to control the surface tension of polymer solutions so that both spreading and adhesion strength can be optimized.

3.1.1.2 Method

The surface tension of polymer solutions at the air-water was measured at different concentrations. Surface tension was measured by the pendant drop technique with the Kruss DSA-10. Polymer solutions were loaded into a syringe, pendant drops were produced, and their shapes were recorded by a camera. According to the Young-Laplace equation, the shape of the pendant drop is related with the solutions' surface tension. The shape of a drop is determined by its radii of curvature, R_1 and R_2. In the case of a spherical drop these are equal. The relationship between interfacial pressure (the pressure across the interface) and these radii of curvature is called the Young-Laplace equation:

$$\Delta P = \gamma(1/R_1 + 1/R_2) \quad (3.6)$$

where

ΔP = interfacial pressure difference

γ = interfacial tension

R_1, R_2 = surface's radii of curvature.

3.1.2 Mucoadhesion

Mucoadhesion refers to bonds formed between mucus and polymers that improves the attachment of drug carriers to mucus for drug delivery purposes. Mucus is a substance secreted by various tissues in the body made up of water, mucin (a glycoprotein), salts, and some cells. The mucus glycoproteins consist of hundreds of short polysaccharide chains, which usually constitute about 70% of the weight of the molecule, attached to a polypeptide backbone[27].

For many years mucoadhesion has attracted the attention of ocular researchers who have sought to control it and profit from the concepts and techniques of this novel approach. Since the ocular bioavailability of drugs administrated by conventional eye drops is low due to the small area for absorption and the short contact time in the eye, any modification resulting in increased contact time will improve the drug bioavailability. Therefore, the concept of mucoadhesion was applied in the field of ocular drug delivery to prolong the residence time in the preocular area, potentially increasing the drug bioavailability.

3.1.2.1 Literature review

Formation of mucoadhesion involves two steps: (1) the contact stage where an intimate contact is formed, and (2) the consolidation stage where various interactions occur to consolidate and strengthen the adhesive joint[28]. The first step can be explained by the wetting theory. This theory uses interfacial tensions to predict spreading and in turn adhesion. The second step has been explained by a few different theories[29]. That is,

the electronic theory relies on the assumption that mucoadhesive and mucus have different electronic structures. Therefore the mucoadhesive force is originated from the attractive forces across the interface. The adsorption theory states that the mucoadhesion is due to the van der Waals interactions, hydrogen bonds, and some other related forces between mucoadhesive and mucus. It is the most widely accepted theory of adhesion. The diffusion theory states that mucoadhesion is produced through interpenetration and entanglement of mucoadhesive polymer chains and mucus polymer chains. Therefore, according to this theory the bond strength increases in proportion to the degree of penetration of the polymer chains into the mucus layer. Between all these theories, the diffusion theory and adsorption theory are of particular interest for this study and they are discussed in further details below.

Diffusion theory

The diffusion theory supports that bond strength increases with the degree of penetration of the polymer chains into the mucous layer[30]. The penetration depth, l, can be estimated with the following relationship:

$$l = (tD_b)^{1/2} \quad (3.7)$$

Where t is the time of contact and D_b is the diffusion coefficient of the bioadhesive material in mucus. The bond strength for a given polymer is believed to be attained when the depth of penetration is approximately equal to the end-to-end distance of the polymer chain[31]. Therefore, to achieve the desired bond strength we will have to either choose an adhesive polymer with relatively short end-to-end distance or increase D_b.

According to research done by Voyutskii[30], for diffusion to occur it requires that the polymers possess sufficient mobility and are mutually soluble. This latter requirement

may be restated by the condition that they possess similar value of solubility parameter, which is an index of the compatibility of two components. Thus, the more structurally similar a bioadhesive is to its target, the greater the mucoadhesive bond will be. In order to improve diffusion both chain flexibility/mobility and similar structure with mucin are important.

Adsorption theory

The adsorption theory of adhesion is the most widely applicable theory to describe the adhesive joint. It is proposed that given sufficiently intimate molecular contact at the interface a material will adhere due to inter-atomic and inter-molecular forces. The adhesion can be divided into two categories: (1) chemical bonds and (2) secondary bonds. Chemisorption is defined when chemical bonds are formed across the interface and is beyond this study. We will mainly focus on secondary bonds based on Van der Waal and hydrogen force. Although these forces are relatively weak compared with other bonds (Table 6), the sheer number of interactions, as a whole can, produce intense adhesive strength.

Huntsberger[32] has calculated the attractive forces between two planar bulk phases due to solely dispersion forces. For example, they showed that even at the separation of one nanometer the attractive force would result in a joint strength in tension of approximately 100 MPa. Also, the formation of hydrogen bonds across the interface appears to enhance the intrinsic adhesion and has often been observed. Given the structure of mucin, it is reasonable to assume it can form hydrogen bonds with the starch-based polymers.

Table 6: Typical bond energy

Bond	Bond Energy kJ/mol
Primary bonds	
Ionic	600~1100
Covalent	60~700
Metallic	110~350
Secondary bonds	
Hydrogen bonds	10~40
Van der Waals bonds	0.08~40

A large number of polymers have been studied thoroughly as mucoadhesive drug delivery systems. It is generally agreed that polymer-related factors influencing mucoadhesion include hydration or degree of swelling, molecular weight, the nature of the functional groups, molecular conformation or chain flexibility, and mobility of the polymer and its concentration. Polymer hydration results in the relaxation of stretched, entangled, or twisted macromolecules exposing the adhesive sites. Furthermore, chain interdiffusion is favored by polymer–water interactions dominating the corresponding polymer–polymer interactions.

A critical chain length is necessary to obtain interpenetration and molecular entanglement between the polymer and the mucus layer. The threshold required for successful mucoadhesion is a molecular weight of at least 100,000 Da. Excessive cross-linking in the polymer, however, decreases the chain length available for interfacial penetration. Also, excessive formation of interchain physical entanglement and hydrogen bonding within the polymer itself can lead to conformation that hinders polymer diffusion into the mucus network. As a result, chain flexibility is critical for interpenetration and entanglement with the mucus gel. The mobility of the chain segment is directly

proportional to the interdiffusion and the interpenetration of the polymer within the mucus network. Coiling of polymer chains, due to pH or osmolality of the medium, can result in the shielding the active groups necessary for the adhesion process.

In summary, in order to form mucoadhesive bonds the selected polymer(s) should have at least one of the following characteristics: (a) high molecular weight, (b) high chain flexibility, (c) surface intention that induces spreading into the mucous layer, (d) sufficient quantities of hydrogen-bonding chemical groups, and (e) anionic surface charges.

3.1.2.2 Method

Determination of mucoadhesive bond strength is important in the development of ophthalmic solutions, as it can quantitatively compare different mucoadhesive materials. Hassan and Gallo[33] are considered to have pioneered the work on the rheological assessment of mucin-polymer bioadhesive bond strength. They observed that there was a synergistic increase in viscosity when a mucoadhesive polymer and mucin were mixed together. The viscosity of a dispersion containing mucin and a bioadhesive polymer is determined by the contribution of the different components, as in the following equation:

$$\eta_t = \eta_m + \eta_p + \eta_b \quad (3.8)$$

where

η_t: viscosity of the system

η_m: individual viscosity of mucin

η_p: individual viscosity of polymer

η_b: viscosity component due to bioadhesion

Therefore, the viscosity component contributed by mucoadhesion can be obtained by rearranging the last equation,

$$\eta_b = \eta_t - (\eta_m + \eta_p) \quad (3.9)$$

For these two equations to be valid, η_t, η_m and η_p should be measured at the same concentration, temperature, time, and shear rate. In this study steady state controlled rate flow curves, with shear rate varying from 15 to 300 1/s, of polymer solutions, 5% mucin dispersion, and the mixture of polymer and mucin were collected. η_b was calculated and used as a direct estimate of the force of mucoadhesion.

3.1.3 Rheology

After a drop of ophthalmic solution is applied into the eye, it experiences two processes: blinking, and process between blinking. The process between blinking can be seen as a steady process with low (close to 0) shear rate. The process of blinking can further be divided into two sub-processes: steady and dynamic processes. Part of the process during moving between the upper and lower edge of the eye can be seen as a steady process with a high shear rate. The shear rate associated with the eye has been estimated to range from 0 to as high as 28500 $1/s$[34]. When the eyelid is moving close from/to the upper or lower edge of the eye, it can be seen as a dynamic process with changing shear rate. The frequency of the dynamic process can be estimated based on how often we blink. The muscle that lets our eye blink is the fastest muscle in our body. It allows us to blink five times a second. However, on average we blink 15,000 times a day. Women blink twice as much as men[35]. Given the highest blink rate, five times a

second, the highest frequency can be estimated as 5 Hz. In this section, both steady and dynamic properties were studied.

3.1.3.1 Steady shear rheological properties

Viscosity is a measure of a solution's resistance to flow and is a function of the molecular attraction that resists flow. It is defined as the ratio of the shearing stress applied to a solution to the velocity gradient in that solution. The relationship between ophthalmic solutions' retention time in the eye and their viscosity is easily understood. For example, blinking causes high shear rate to the solution applied into the eye. If the viscosity of the solution is high, it can lead to high shear stress between the solution and the conjunctiva around the immediate contact area with the tear film, which is the cause of irritation and damage. On the other hand, when the viscosity of the solution is too low and the shear rate between blinks is relatively low or even zero, the ophthalmic solution will not be able to remain on the ocular surface and this will result in increased drainage. Therefore, to decrease the drainage between blinks the viscosity at low shear should be high. For a solution, how the apparent viscosity changes as a function of shear rate is an important rheological parameter. In this study, we tried to obtain solutions that had relatively high viscosity under low shear rate and relatively low viscosity under high shear rate. Increased viscosity, only when it is not too high and causes irritation, can increase retention time, reduce the drainage rate, and increase the bioavailability on the ocular surface. A long contact time, achieved by a high viscosity of the ophthalmic solution is usually favorable, since it increases the bioavailability and therefore reduces the number of applications required to control symptoms and signs.

A solution can have Newtonian or non-Newtonian characteristics, depending upon how the apparent viscosity changes with the shear rate. If a solution's viscosity is independent of the shear rate, it is defined as Newtonian fluid and consequently, a non-Newtonian fluid is defined as a fluid in which the viscosity changes with the shear rate. When a fluid's viscosity is high under conditions of low shear rate and low under conditions of high shear rate, it is defined by the term "shear-thinning". Water and silicone oils are Newtonian fluids and have a constant viscosity regardless of the shear rate, but normal human tears[40] are a non-Newtonian fluid, with viscosity falling from about 5 mPa.sec at 2 s^{-1} to about 1.5 mPa.sec at 160 s^{-1}. Shear-thinning behavior is a typical property of solutions containing long polymeric macromolecules, which are not strongly bonded into a globular form, such as HPMC (Hydroxypropyl Methyl Cellulose) and CMC (Carboxyl Methyl Cellulose) solutions. The random orientation and interaction of these molecules produce high resistance to flow when the shear rate is low. At higher shear rates, the molecules become aligned in the direction of the shearing force and offer much less resistance. Thus, solutions become less viscous when the shear rate increases. Shear-thinning solutions are more comfortable in the eye than Newtonian solutions of the same viscosity since at high speed blinking shear-thinning solutions offer the advantage of low viscosity and have less dragging effect on the ocular surface.

Non-Newtonian behavior is a typical characteristic of polymer solutions. The solution has a Newtonian viscosity, which is high at very low rates of shear. However, over much of the usual accessible shear rate range, the viscosity decreases nearly linearly with a shear rate in the log-log plot. Their apparent viscosity decreases as the rate of shear increases. In this linear range, the so-called power law equation holds where:

$$\eta = K\dot{\gamma}^{n-1} \quad (3.10)$$

where K and n are constants.

For Newtonian liquids, n=1 and K=Consistency coefficient; the value of n is less than one for non-Newtonian polymer solutions. At last, when the shear rate is higher than a certain value, the viscosity is again independent of the shear rate. Considering the properties of human tear, this non-Newtonian behavior is of tremendous practical importance for ophthalmic solution formulation.

3.1.3.1.1 Literature Review

The basic cause for the non-Newtonian behavior of polymer solutions is the orientation of molecular segments by the flow field. Molecular entanglements with an appreciable lifetime exist above a critical molecular weight. Entanglements greatly enhance the possibility of orienting molecular segments in a flow field. The entanglements act as temporary crosslinks, so that the polymer solutions may have many of the characteristics of crosslinked rubbers. At very low rates of shear, the entanglements have time to slip and become disengaged before enough stress can develop in them to orient the molecules. At higher shear rates the segments between entanglements become oriented before the entanglements can disappear. As a load-bearing entanglement disappears another entanglement, that does not carry any load, develops somewhere else in the solution. Thus, a steady state condition is developed in the solution in which the rates of formation and destruction of entanglements is equal.

From the above discussion, a polymer solution at rest should have a higher concentration of entanglements than that of a polymer solution that is flowing. The change in

concentration of entanglements has two effects: first, once the shear rate is higher than a certain value, the viscosity of a polymers' solution should decrease when the shear rate increases. Second, at very high rates of shear practically no entanglements can exist. At this point the viscosity should reach a relatively small value, which becomes independent of the shear rate.

There are several theories that are often used to describe the shear rate dependence on the viscosity. Besides the power law introduced above, the Cross equation is another general empirical equation for fitting curves, which have a sigmoidal shape. The Cross equation for the effect of shear rate on the apparent viscosity is:

$$\eta = \eta_{\infty} + \frac{\eta_0 - \eta_{\infty}}{1 + (C\dot{\gamma})^m} \qquad (3.11)$$

Where η_0 is the Zero Shear Viscosity, the magnitude of the viscosity at the lower Newtonian plateau. It is a critical material property. Zero shear viscosity of a polymer solution is a function of molecular weight, chemical structure, temperature, and concentration.

η_{∞} is the Infinite Shear Viscosity. This tells us how our product is likely to behave in very high shear processing situations.

The parameter m is known as the (Cross) Rate Constant. It represents how fast the viscosity drops. It is dimensionless and is a measure of the degree of dependence of viscosity on shear rate in the shear-thinning region. A value of zero for m indicates Newtonian behaviour with m tending to unify for increasingly shear thinning behaviour. It is affected by the molecular weight distribution.

C is known as the Cross Time Constant (or sometimes the Consistency) and has dimensions of time. It represents the shifting from zero viscosity to infinite viscosity and is proportional to zero viscosity.

So, the Cross model not only provides us with a simple way of quantifying the "full" viscosity/shear rate profile for a shear thinning fluid, but also it helps us to obtain the desired steady flow profile by engineering polymers' structure accordingly.

3.1.3.1.2 Method

The flow properties of the samples were examined using a Haake RS100 RheoStress equipped with a Haake circulation bath and temperature controller. All experiments were run at 25 °C. Steady state flow curves were recorded automatically. Although the shear rate associated with the eye has been estimated to range from 0 to as high as 28500 $1/s$[40], we tested the viscosity at shear rates varying from 15 to 300 due to internal limitations of this rheometer.

3.1.3.2 Viscoelastic behaviors

Viscoelasticity describes materials that exhibit both viscous and elastic characteristics when undergoing unsteady state deformation. Viscous materials will flow when a stress is applied and do not recover their original structures after the stress is removed. Elastic materials strain instantaneously when a stress is applied and quickly return to their original state once the stress is removed. Viscoelastic materials have elements of both of these properties. They have both flowing and deforming behaviors when a stress is applied.

In addition to the flow properties, the viscoelastic properties of ophthalmic solutions are also important, especially at low shear in oscillatory experiments. This is the

case since these conditions will impact how well a solution stays in the eye as it most likely dependent not only on the flow properties but also on the dynamic properties, that is, how well the carrier, polymers in our case, is held together in situ. As previously mentioned, the polymer has to undergo dynamic process because of blinking. How it behaves under varying frequency is important.

3.1.3.2.1 Literature review

According to Steffe's work[36], all materials are viscoelastic, but the viscous or the elastic character may dominate in certain situations. The Deborah number proposed by Marcus Reiner[37] is a means to distinguish between solids (elastic) and liquids (viscous). He recognized that whether a substance is a solid or a liquid depends on the time of the characterization process. The Deborah number is defined as

$$N_{De} = t_{material}/t_{process} \quad (3.12)$$

Where $t_{material}$ is the characteristic time of the material and $t_{process}$ is the characteristic time of the process.

Pipkin[38] suggested that the $t_{material}$ may be provisionally considered as an order-of-magnitude estimate for how long it takes the substance to complete a stress relaxation process. If a material is ideally elastic, $t_{material}$ tends to be infinite and no relaxation occurs. If a material is ideally viscous, $t_{material}$ equals 0, meaning immediate relaxation occurs. In our application, the viscoelastic properties of systems containing polymer molecules arose from three factors: (1) the length of the polymer molecules, (2) the flexibility of the molecular chains, and (3) the interactions of the segments of a polymer molecule with other segments of the same or different polymer molecules[39]. The $t_{process}$

can be seen as inversely proportional to the frequency in a dynamic test. During the ocular drug delivery process, the $t_{process}$ varies over a large range, depending on the status of the eye. When the eye stays open or closed $t_{process}$ can be seen as infinite and when the eye blinks $t_{process}$ can be as low as 0.2 second.

Therefore, the Deborah number can be estimated and used as a measure of the degree of viscoelasticity. If it is less than 1, the material shows more viscous character than elastic character. If it is greater than 1, the material shows more elastic character than viscous character.

3.1.3.2.2 Method

Oscillatory shear experiments were performed to evaluate the viscoelastic properties of the ophthalmic solutions. The shear storage modulus or elastic modulus (G') and the shear loss modulus or viscous modulus (G") were evaluated as function of frequency. G' gives information about the elasticity or the energy stored in the material during deformation, whereas G" describes the viscous character or the energy dissipated as heat.

Strain sweep measurements were made for all samples to determine the maximum strain amplitude for the solution that would allow all measurements to be made in the range of linear viscoelastic behavior. Measurements above this level do not measure the physical properties relevant for a gel at rest under the lower eyelid. All further measurements of rheological properties were made within the linear region, i.e. below this maximum strain. The oscillation frequency ranged from 0.46 to 100 Hz and the experiments were run at 25 °C.

In oscillation experiments the stress response to a sinusoidally varying strain is recorded as a function of frequency. The shear strain, the stress, and the phase angle are determined in the measurement. The parameters obtained are the complex modulus, G*, and the phase angle, δ. Complex Dynamic modulus G^* can be used to represent the relations between the oscillating stress and strain:

$$G^* = \sigma_0/\gamma_0 = (G'^2 + G''^2)^{1/2} \quad (3.13)$$

$$G' = G^*\cos\delta \quad (3.14)$$

$$G'' = G^*\sin\delta \quad (3.15)$$

where

σ_0: amplitudes of stress

γ_0: amplitudes of strain

δ: phase angle

G': storage modulus

G": loss modulus

3.1.4 *In vitro* release test

Controlled release is an important step toward improving the delivery of drugs to the inner part of the eye. In this work, hydrogel was used as a polymer matrix to control drug release. In the context of this paper, the term hydrogel will be used in its broader sense. That is, a matrix formed by either a water-swellable material (usually a cross-linked polymers with limited swelling capacity) or a water-soluble material (usually a hydrophilic polymer that swells indefinitely and eventually undergoes complete dissolution)[40]. Most of the mucoadhesive polymer materials belong to one of these two

categories. For the design of new controlled drug release systems, it is essential to know the exact mass transport mechanism involved in drug release and to predict the resulting drug release kinetics.

3.1.4.1 Literature review

Based on rate-limiting step for controlled release, three models are developed and categorized as follows: (1) Diffusion-controlled, (2) Swelling-controlled, and (3) Chemically-controlled models. The release of the drug from hydrogel is believed to be diffusion-controlled.

Fick's law of diffusion with either constant or variable diffusion coefficient is commonly used in modeling diffusion-controlled release. Drug diffusivities are generally determined empirically or estimated a priori using free volume, hydrodynamic, or obstruction-based theories[41]. *Free volume theory* is based on the assumption that the free volume is the major factor controlling the diffusion rate of molecules. In this theory, the solute diffuses by jumping into voids formed in the solvent space by the redistribution of the free volume within the liquid. It is assumed that the free volume can be redistributed without any energy change. The voids are pictured as being formed by a general withdrawal of the surrounding liquid molecules due to random thermal motion. These holes are then filled in by the reverse process. *Hydrodynamic theory* takes the hydrodynamic interactions into account. These interactions include frictional interactions between solute and the polymer, between the solute and the solvent, and also between the solvent and the polymer. It includes the effect of overlapping of polymer chains, which is omitted in the obstruction model. According to this model, major factors determining diffusion coefficients include drug size, molecular weight, and polymer concentration.

Obstruction theory is based on the assumption that the polymer chains are regarded as motionless relative to the diffusing molecules, which leads to an increase in the mean path length of the diffusing molecules between two points in a system. Therefore, the diffusion coefficient is a function of polymer fraction.

Baker and Lonsdale model

Peppas[42] describes the release of drugs from a hydrogel matrix as a three step process. The first is the *initial burst* when the liquid dissolves the drug present at the immediate surfaces of the matrix, creating a small "burst" effect. At this time the water or biological fluids begin to penetrate the gel at a rate that is dependent on the porosity of the matrix. The second phase is classified as the *stationary phase*, where the water continuously penetrates the matrix at a constant rate. This penetration is accompanied by an expansion of the gel layer in the direction of the external medium. This phase accounts for the majority of the drug release. It is generally accepted that the release of the drug is controlled by diffusion process, not by the rate of drug dissolution or the rate of penetration of the front for hydrophilic matrices. The third phase is the *exhaustion period* which begins when the penetration front has reached the center of the matrix and the drug concentration has dropped below its solubility limit in water. During this stage the release rate rapidly falls.

These controlled release systems can either be classified as systems with suspended drugs or systems with dissolved drugs. Mathematical models for both have been developed and adapted by various authors and a model developed by Baker and Lonsdale for the case in which the drug is dissolved in the polymer can be used for this research. This model is presented for the case that the system is homogenous, there is one

plane of diffusion, there is no diffusion boundary layer present, and there are sink conditions. In this situation, the initial concentration of the drug in the hydrated matrix is less than the drug solubility in it ($C_0 < C_m$). Setting $C_0 = M_\infty/V$, where M_∞ is the initial drug loading (the total amount of drug release at infinite time) and V is the effective volume of the hydrated matrix, the following expressions are valid for $0 \leq M_t/ M_\infty \leq 0.6$:

$$M_t = 2AC_o\left(\frac{D_m}{\pi}\right)^{1/2} \bullet t^{1/2} \qquad (3.16)$$

The rate of release is:

$$\frac{dM_t}{dt} = 2AC_o\left(\frac{D_m}{\pi}\right)^{1/2} \bullet t^{-1/2} \qquad (3.17)$$

where:

M_t = the amount of drug released at any time

M_∞ = the initial drug loading

A= the diffusional area

C_0= the initial concentration of the drug in the system

D_m = the apparent diffusion coefficient

These equations are for the planar case, but can be modified for other shapes. All of these cases will also show a $t^{0.5}$ dependency. Peppas[45] brings up faults with this model due to the following assumptions:

1. This model was not developed for systems undergoing dimensional change.
2. A pseudo steady-state analysis was used that ignores the external mass transfer resistance and is only valid when the solute loading is in great excess of it solubility limit.
3. The countercurrent solvent diffusion was not considered
4. Drug diffusion in the gelled matrix was assumed to be the rate limiting step.

However, the shortcoming of these assumptions are not as much a problem with the ocular system being described because the gel is already hydrated when applied, will not undergo dimensional change, and solvent diffusion can be neglected.

Matrix formulations play an important role in the drug release profiles. Release profiles can usually be modified by type and viscosity of the polymers, the polymer concentration, and the drug particle size. The type of polymer is often determined by the solubility characteristics of the drug. For example, hydrophilic matrices are generally used to prolong the release of highly water-soluble drugs. The viscosity of the polymer appears to play a role in drug release. Polymer concentration follows the general rule that increasing the proportion of hydrophilic material decreases the rate of release. Drug particle size affects the dissolution rate of the drug with the smaller particles having larger surface/volume ratios and therefore, faster dissolutions rates. In summary, we have to consider the size of drug, the structure of hydrogel, the polymer composition, the water content, and the size of the molecules in order to design systems offering desired drug release.

3.1.4.2 Method

A USP dissolution method was used for obtaining release profiles. A Hanson EZ-lift dissolution system made with six separate chambers that were all kept at the same constant temperature water bath was used. Each chamber had a rotating paddle attached to the same drive motor. One-liter beakers were used to hold the release medium, simulated tear solution, and they were filled with a specified amount, 600 ml. The formulated drug was placed in a 5 ml well having a diameter of 5 cm and covered with the same dialysis membrane. The concentration of the drug in the release medium was determined by UNICO SQ-2800 Ultraviolet-Visible Spectrophotometer by taking a sample of 0.10 g at specific time intervals and it to maintain a constant volume. The composition of the simulated tear solution release medium is given in Table 7.

Table 7: Simulated Tear Solution

Chemicals	N/mmol	Mass/g
NaHCO3	26. 00	2. 184
NaCl	108. 00	6. 312
KCl	24. 00	1. 789
CaCl2	0. 40	0. 059
MgCl2	2. 50	0. 238
H2O		to 1000

3.1.5 Stability study

The influence of sterilization by autoclaving and storage under various conditions were studied. In this study, viscosity was used to assess the solutions' stability. To test the effect of autoclaving, viscosities of the same solutions were recorded before and after autoclaving and their flow curves were compared. The same method was also utilized to study the effect of pH and temperature on the storage stability.

3.2 Results and discussion

3.2.1 Surface tension

The surface tensions of DHS and DHS ester solutions are shown in Table 8. They were all dissolved in pH 7.4 phosphate buffer to maintain the same pH value. Samples with multiple concentrations were measured until a surface tension plateau was attained. Among samples tested, no significant effect of the concentration on surface tension was detected from 20DHS, 60DHS, and 100DHS solutions. This is believed to be because of all these samples are hydrophilic in nature and only a very small amount of polymers is absorbed at the solution-air interface. Therefore, when the concentration is higher than a certain level, which is no greater than the lowest concentration we tested (e.g. 0.5%), the surface tension does not change as the concentration increases.

In comparison, all DHS esters tended to reduce the surface tension to a various extent. The ST of their solutions decreased as the concentrations increased, until a plateau was reached. These changes are directly related to the hydrophobic nature of methyl and ethyl groups that were grafted onto the DHS backbones and led to the amphiphilic structures. When these amphiphilic polymers were dissolved in water the hydrophobic groups increased the free energy of the system and were more likely to concentrate at the surface. Since less work was needed to bring these polymers to the surface than water, their presence decreased the work needed to create unit area of surface, which consequently reduced the surface tension. After a certain amount of amphiphilic polymers were adsorbed, the surface was saturated with polymer molecules and could not adsorb any more giving rise to the observed plateau at high polymer concentrations.

In addition, as can be seen from Figure 23, these DHS esters showed different surface activities, in the following order: DHSP2 > DHSA2 > DHSP1 > DHSA1. That means that given the same DS, polymers grafted with longer side chains are more active than those grafted with shorter side chains. Furthermore, given the same length of grafted side chains, polymers with higher DS are more active than polymers with lower DS. These observations can be explained by the difference between methyl and ethyl groups, as well as the difference between the degrees of substitution. Both grafted $-CH_2CH_3$ and $-CH_2CH_2CH_3$ are hydrophobic, but an ethyl group is more hydrophobic than a methyl group. So when methyl and ethyl groups are grafted at the same DS, the polymer with ethyl is more susceptible to be present on the interface with a lower overall energy. The same mechanism can be used to explain why polymers with higher DS showed more activity than polymers with lower DS.

Table 8: Surface tension results

Sample	Surface Tension dynes/cm
20DHS	
0.50%	72.4
1%	71.7
2%	72.2
60DHS	
0.50%	71.8
1%	71.7
2%	71.9
100DHS	
0.50%	72.0
1%	71.7
2%	71.6
DHSA1	
0.50%	70.5
1%	69.2
2%	67.3
5%	64.8
10%	64.7
DHSA2	
0.50%	63.6
1%	63.0
2%	61.6
5%	58.6
10%	58.5
DHSP1	
0.50%	68.0
1%	66.7
2%	64.9
5%	61.6
10%	61.6
DHSP2	
0.50%	55.5
1%	54.3
2%	52.0
5%	50.9
10%	51.0

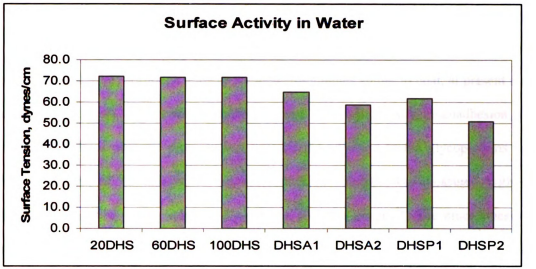

Figure 23: Surface tension of solutions

Tiffany reported that the surface tension of intact cells is much closer to that of water, the cornea/tear system is therefore close to a total wetting situation[25]. However, when we also take kinetics into account, a solution with the same surface tension as water may not be able to spontaneously spread. Additional driving forces contributed by lower surface tension may be required to overcome the retarding forces from viscous resistance. Therefore, a solution with ST lower than water may be needed if its viscosity is higher than water. So, although all substances tested could spontaneously spread on the cornea surface, a low ST is desirable depending on the viscosity of the solution. Meanwhile, a low ST can result in low work of adhesion and therefore weak adhesion strength. Thus, a too low ST should be avoided. The effect of ST will be further investigated by in vivo tests.

3.2.2 Mucoadhesion

The retention time of an ophthalmic solution is influenced by its viscosity, bioadhesion and ST. Although a lower ST indicates a better ability to coat, at present not all of these factors are known. Bioadhesion, and more specifically mucoadhesion, is another important polymer property that impacts the adhesion to the glycoproteins on epithelial surfaces. In this work, the mucoadhesion strength was measured with a rheological method, which was broadly used in previous studies[43]. The mucoadhesion strength of all DHS and DHS ester solutions were tested. Solutions of 20DHS, 60DHS, and 100DHS with the same concentration and viscosity were compared. Also, the mucoadhesion of DHS ester solutions were measured and compared with 100DHS solution.

3.2.2.1 DHS solutions at the same concentration

The mucoadhesion of 20DHS, 60DHS, and 100DHS solutions at concentration 3% is shown and compared in Figure 24, 25, 26, and 27. The upper dots represent the viscosity of the mixed dispersion comprised of 3% DHS and 5% mucin. The lower dots represent the sum of viscosity of 3% DHS and 5% mucin, which were measured separately.

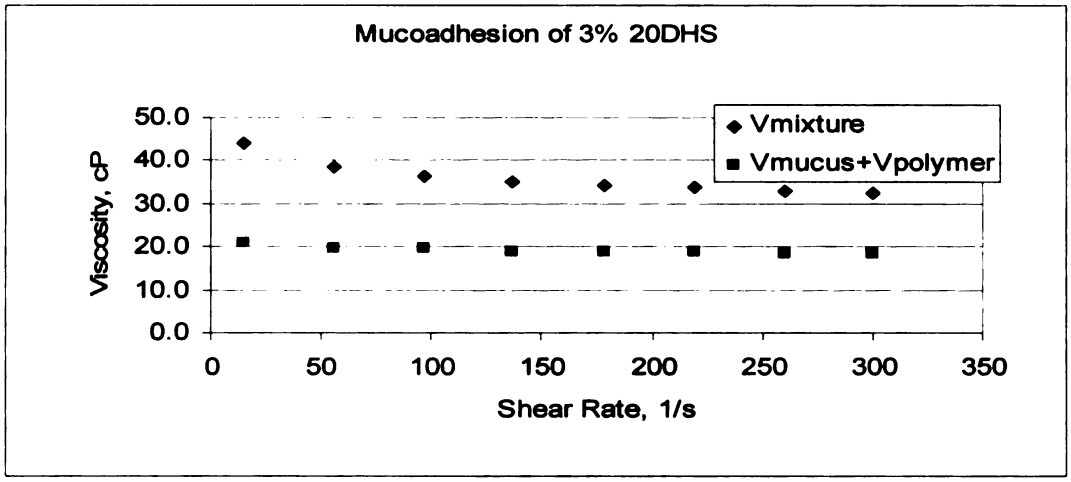

Figure 24: Mucoadhesion of 3% 20DHS

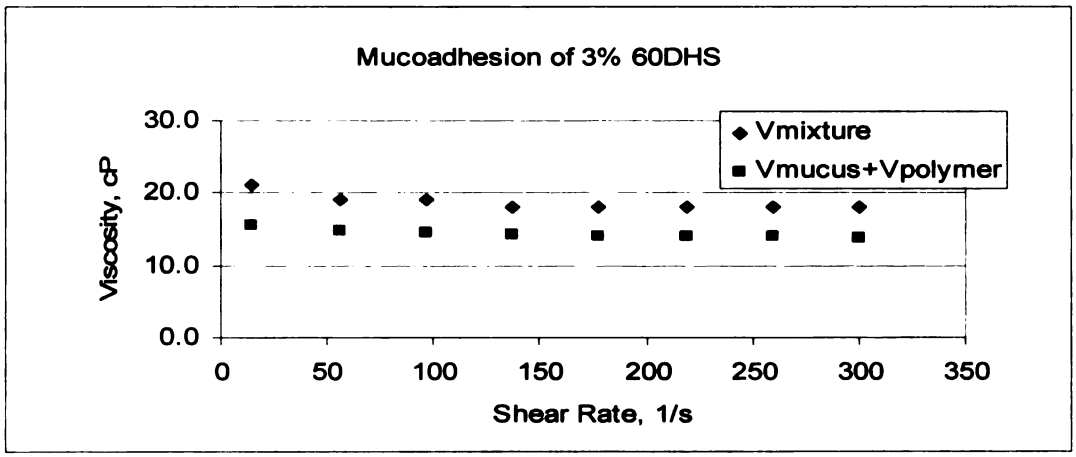

Figure 25: Mucoadhesion of 3% 60DHS

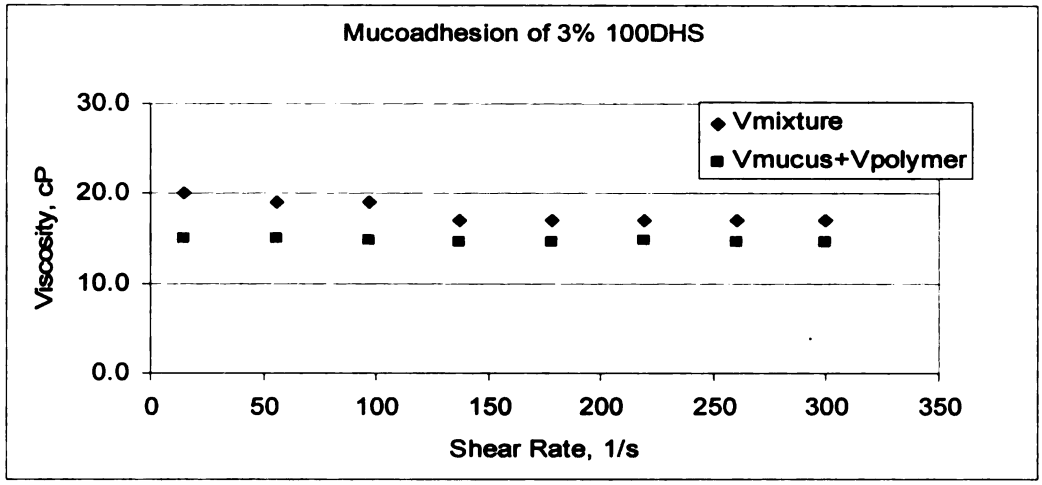

Figure 26: Mucoadhesion of 3% 100DHS

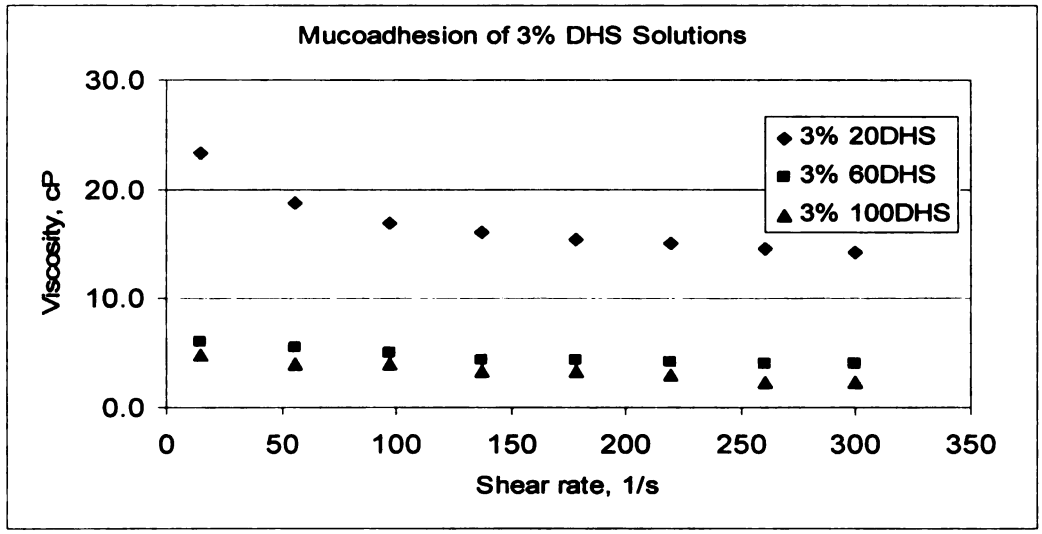

Figure 27: Mucoadhesion comparison of 3% DHS solutions

It is apparent from these figures that all DHS solutions exhibit mucoadhesion with positive η_b contributed by adhesion. This is because of the existence of hydrogen bonding formed between DHS and mucin, both of which consist of substantial amount of hydroxyl groups. The difference in mucoadheison strength between 20DHS, 60DHS, and 100DHS solutions at the same concentration is caused by their molecular weight

difference. At the same DHS concentration, theoretically there should be the same amount of hydrogen bonding formed. However, another factor affecting the adhesion is the molecular weight. This explains why 3% 20DHS, 60DHS, and 100DHS gave different mucoadhesion strengths.

3.2.2.2 DHS solutions with the same viscosity

Since DHS solutions with the same concentration exhibited significantly different mucoadhesion strength, they were further tested and compared as follows. Herein, 8.5% 60DHS and 10% 100DHS were prepared to have the same viscosity as that of 3% 20DHS at the second Newtonian region. The mucoadhesion of 3% 20DHS was shown previously, and the mucoadhesion of 8.5% 60DHS and 10% 100DHS are shown in Figure 28 and 29, and their three solutions are compared in Figure 30.

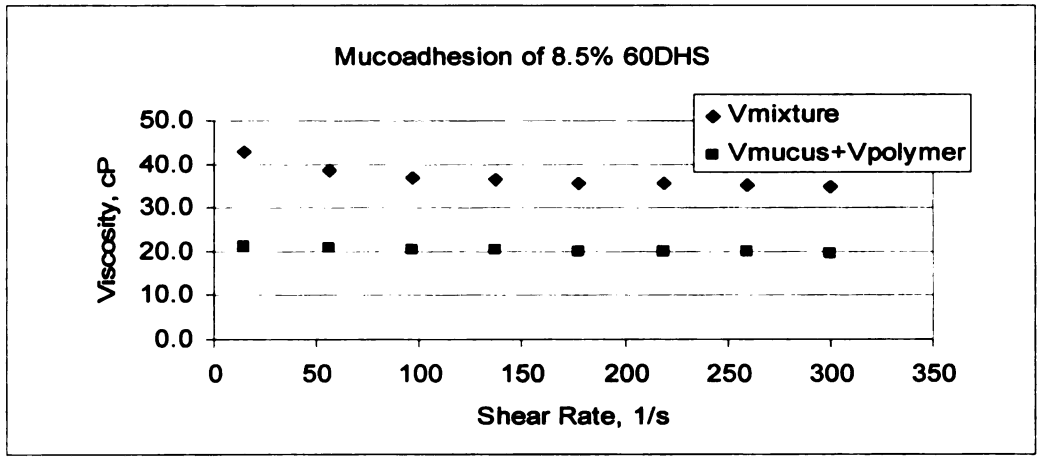

Figure 28: Mucoadhesion of 8.5% 60DHS

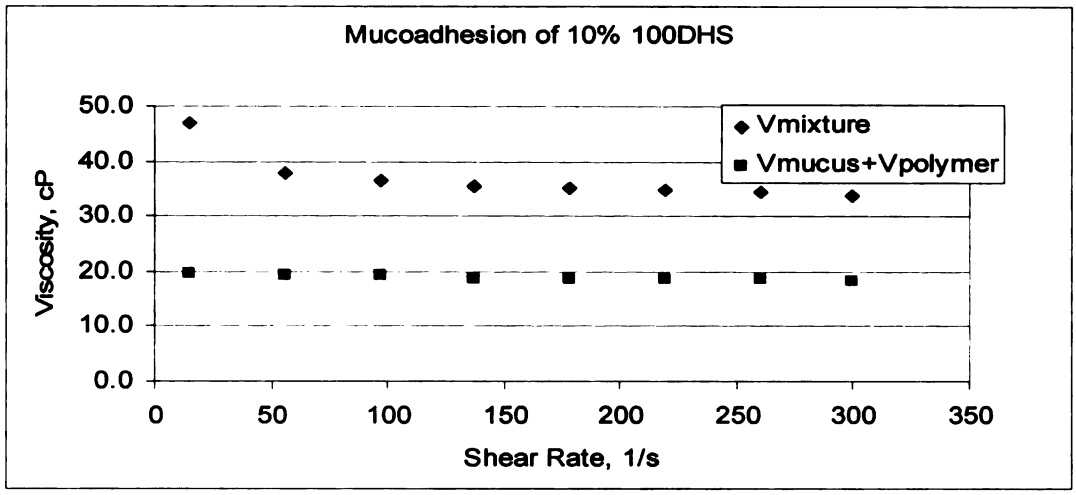

Figure 29: Mucoadhesion of 10% 100DHS

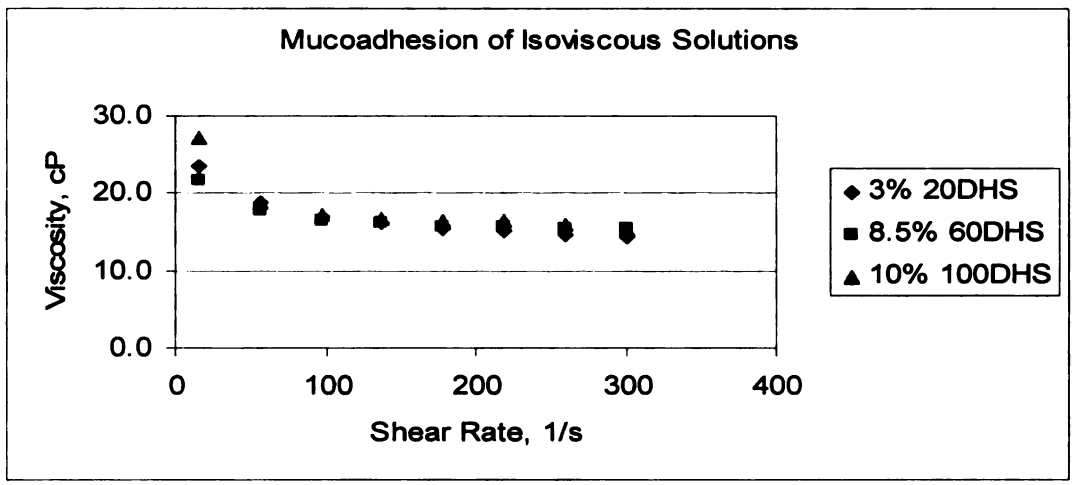

Figure 30: Mucoadhesion comparison of isoviscous DHS solutions

It should be noted that upon matching the viscosity solution of 20DHS, 60DHS, and 100DHS, they exhibited the same strength of mocuadhesion. This further confirmed our conclusion that the adhesion strength is affected by both the molecular weight and the amount of hydrogen bonding. Since viscosity of a polymer solution is also affected by its molecular weight and interaction between chains, it is not surprising to see that solutions with the same viscosity obtained the same adhesion strength.

3.2.2.3 DHSA Esters vs. 100DHS

Mucoadhesion of DHS esters were measured too and their results were compared with that of 100DHS, based on which they were synthesized.

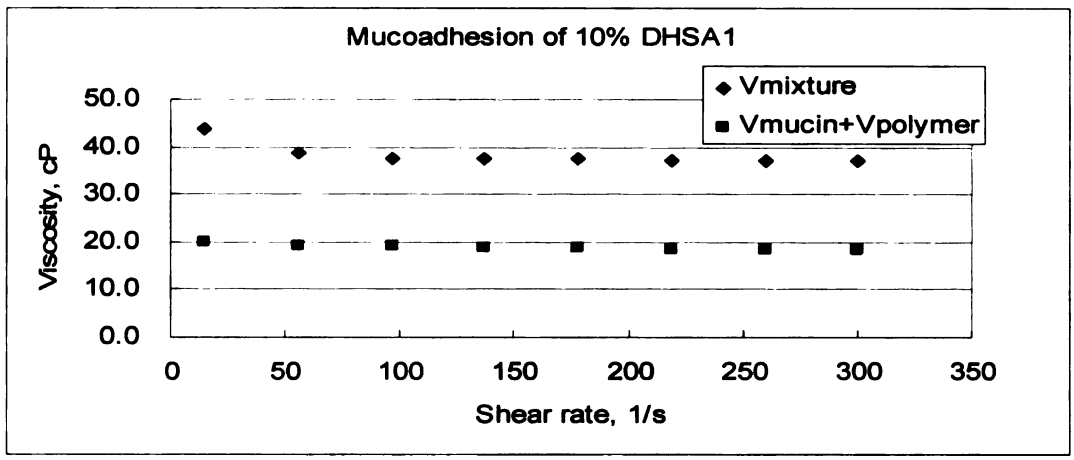

Figure 31: Mucoadhesion of 10% DHSA1

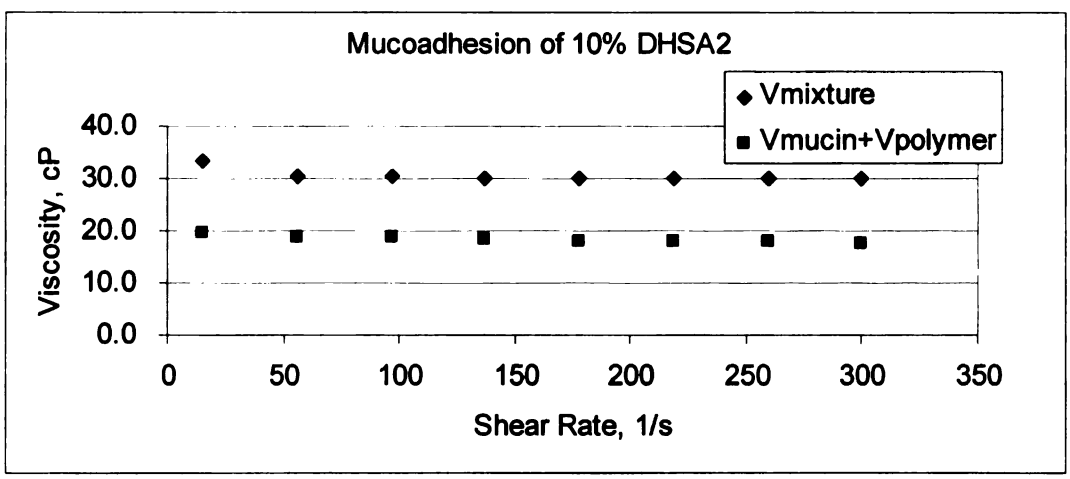

Figure 32: Mucoadhesion of 10% DHSA2

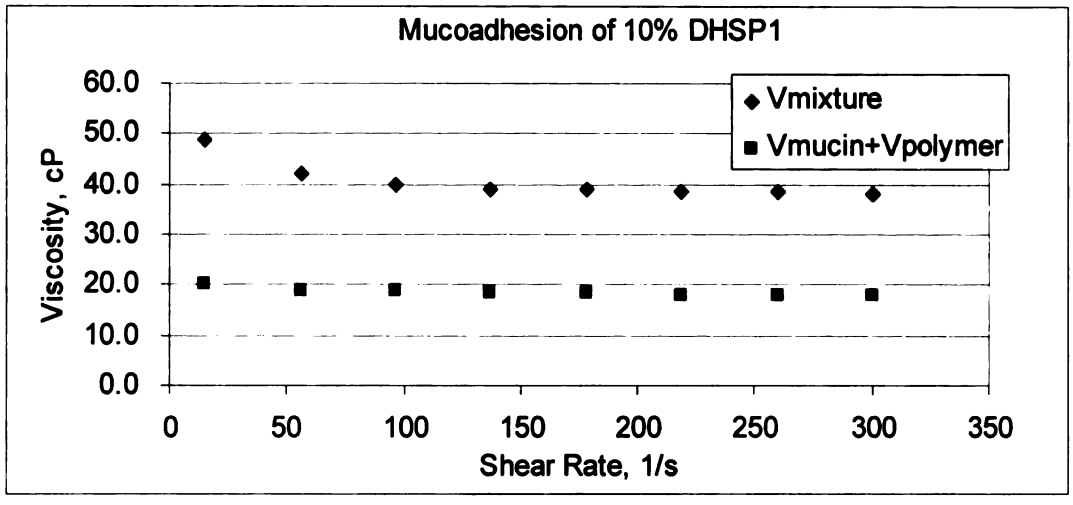

Figure 33: Mucoadhesion of 10% DHSP1

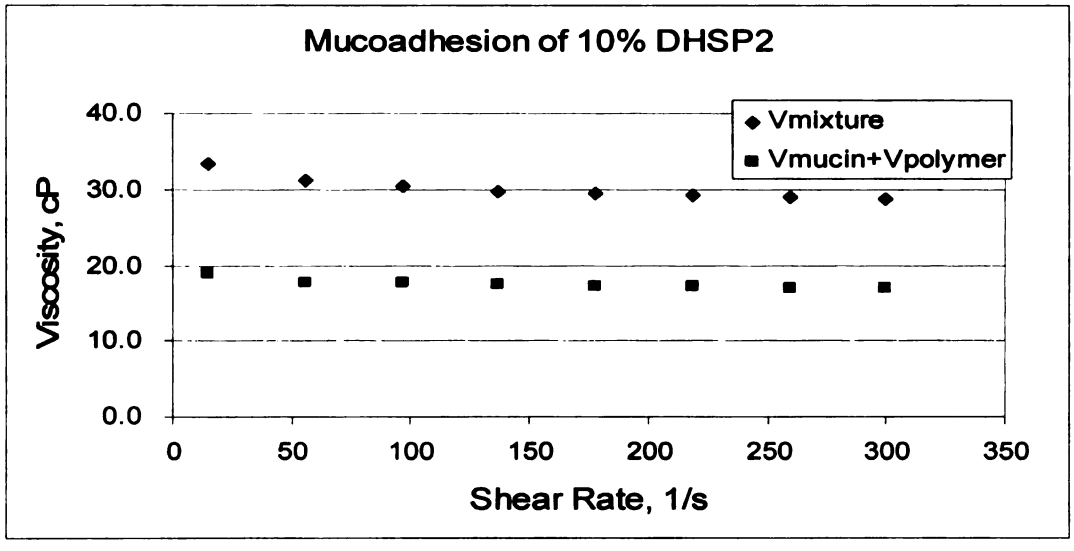

Figure 34: Mucoadhesion of 10% DHSP2

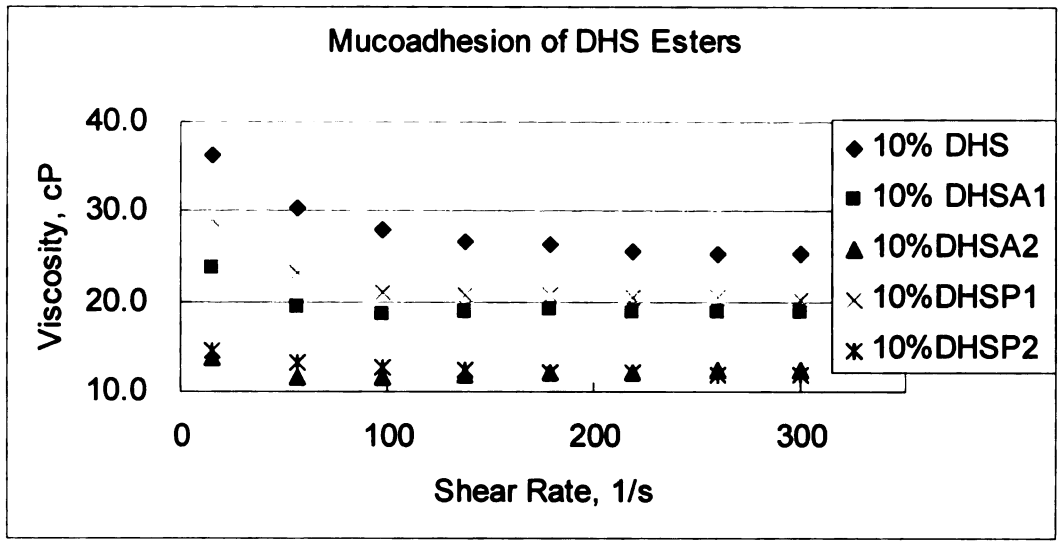

Figure 35: Mucoadhesion comparison of 10% DHS ester solutions

All DHS esters showed positive mucoadhesion, however, when they were compared with 100DHS their mucoadheion was not as high as 100DHS. This lower mucoadhesion is due to the following two reasons: (1) different amount of hydrogen bonding and (2) different surface tension and therefore different work of adhesion. After DHS is esterified, part of hydroxyl groups in the polymer backbone are transferred to ester groups such that less of the primary hydroxyl groups are available to form hydrogen bonding with mucin. In addition, after the hydrophobic methyl or ethyl groups are grafted, the surface tension of the solution is reduced resulting in lower work of adhesion. In conclusion, all the synthesized polymers showed strengthened mucoadhesion and the strength of mocuadhesion is affected by the MW, concentration, ST, and functional groups.

3.2.3 Rheological properties

3.2.3.1 Steady shear flow curve

Figure 36-42 show the rheograms of DHS and DHS ester solutions at different concentrations. Unless noted here, the viscosity in the y-axis of all rheograms refers to apparent viscosity. As can be seen from these rheograms, all samples are concentration dependent.

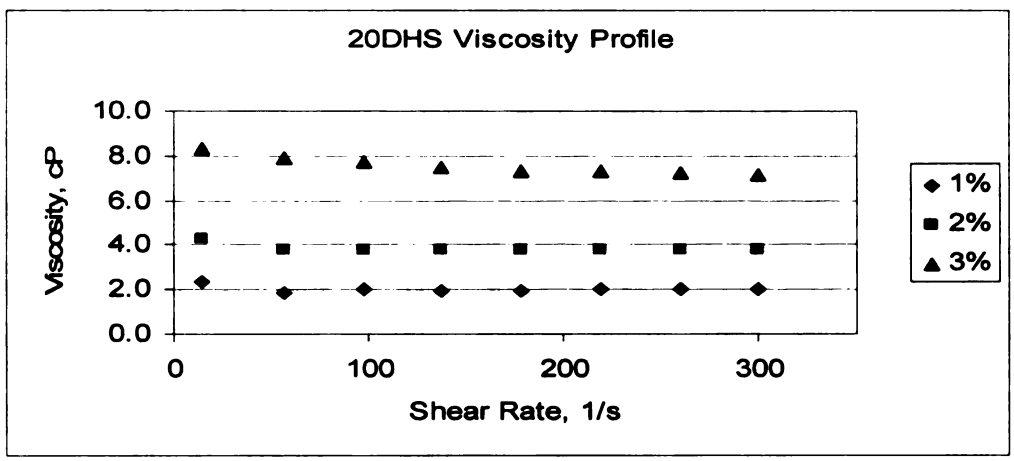

Figure 36: Rheogram of 20DHS

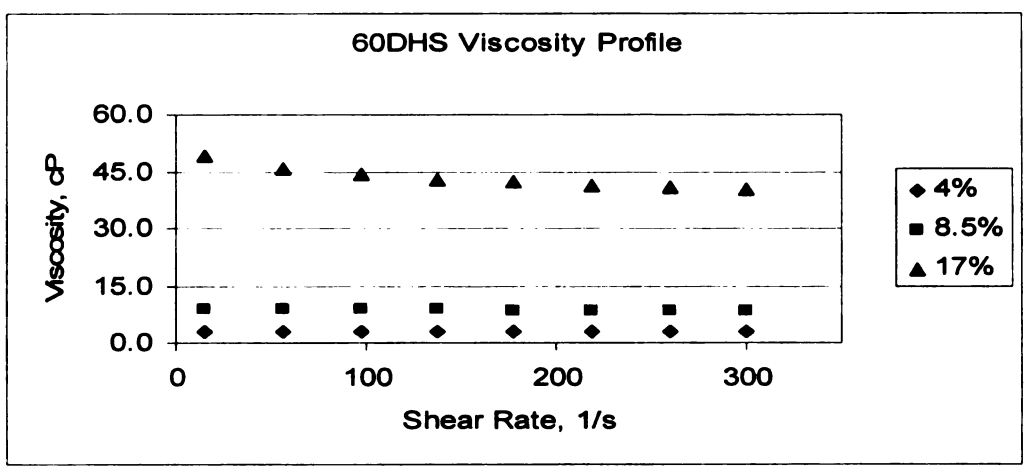

Figure 37: Rheogram of 60DHS

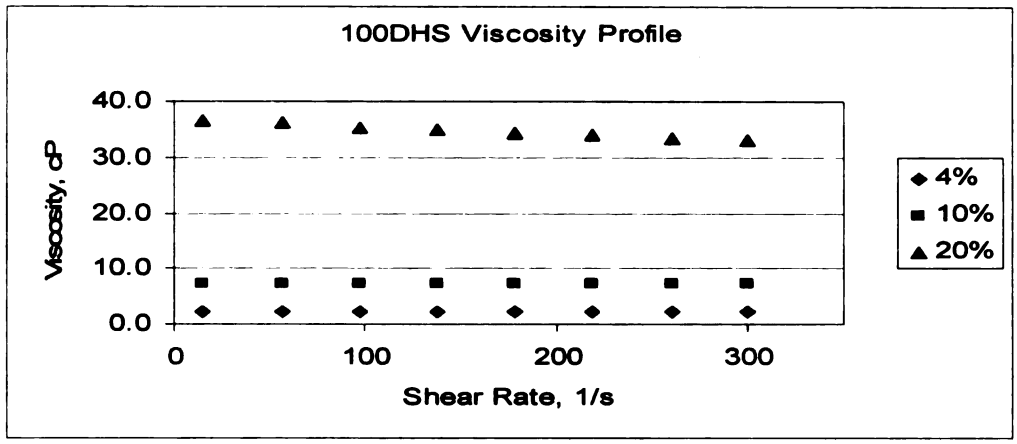

Figure 38: Rheogram of 100DHS

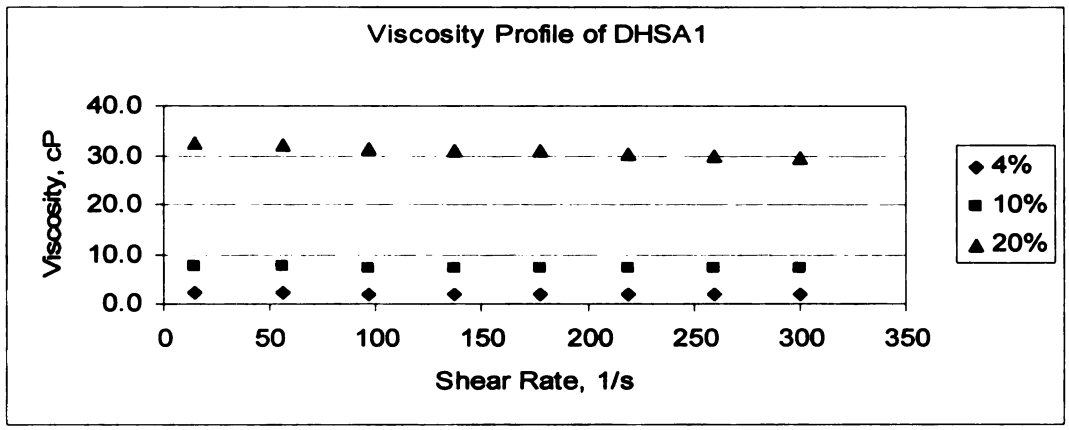

Figure 39: Rheogram of DHSA1

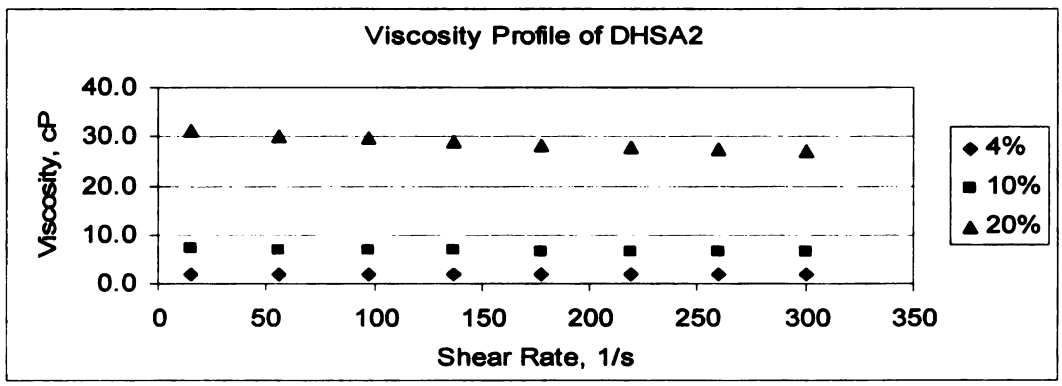

Figure 40: Rheogram of DHSA2

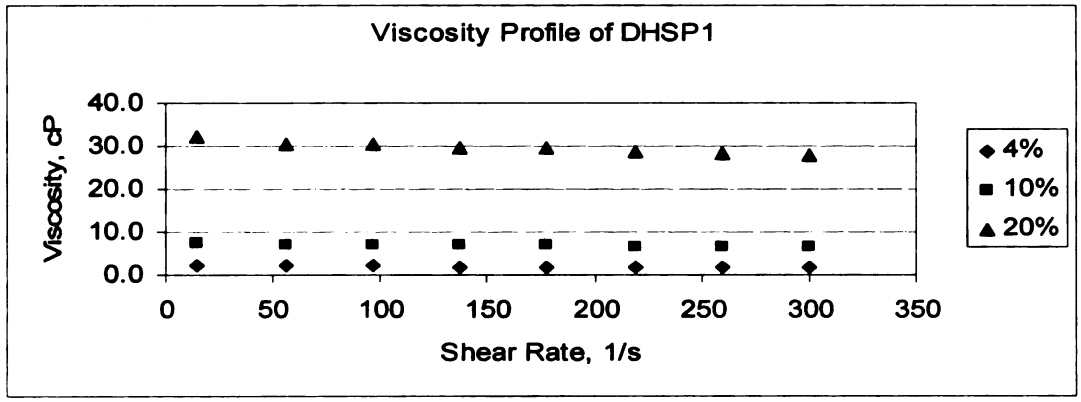

Figure 41: Rheogram of DHSP1

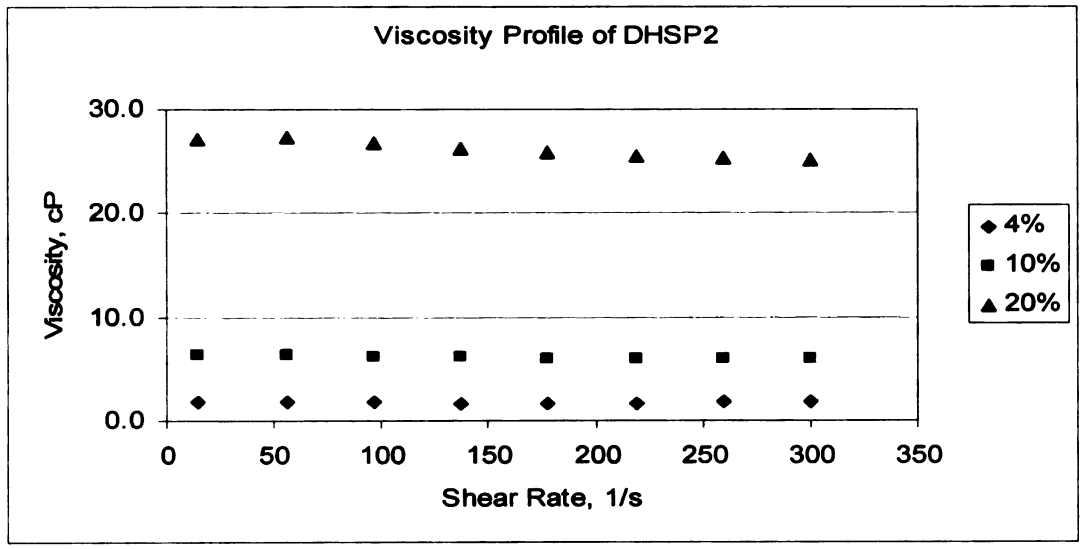

Figure 42: Rheogram of DHSP2

The relationship between viscosity and shear rate was studied for all samples to investigate the non-Newtonian property. The model used to fit shear rate/shear stress experimental data was the Ostwald model. It relates the apparent viscosity of the solution and the shear rate applied. The Ostwald model is one of the most used to model the behavior of non-Newtonian fluids due to its simplicity.

$$\sigma = K\dot{\gamma}^n \qquad (3.18)$$

where

σ: shear stress

$\dot{\gamma}$: shear rate

K: consistency index

n: flow index

When n>1, n=1, and n<1 the flow patterns denote shear-thickening, Newtonian and shear-thinning patterns, respectively. n, as well as K, were estimated by linear regression according to the Ostwald equation and are listed in Table 9.

Table 9: Regression of steady shear flow data

Polymer	K (Pa.s)	n	R^2
1% 20DHS	0.0025	0.97	0.99
2% 20DHS	0.0048	0.96	0.99
3% 20DHS	0.0096	0.95	0.98
4% 60DHS	0.0029	1.00	0.97
8.5% 60DHS	0.0092	0.99	0.98
17% 60DHS	0.0650	0.93	0.99
4% 100DHS	0.0019	1.00	0.99
10% 100DHS	0.0073	0.99	0.97
20% 100DHS	0.0410	0.96	0.98
4% DHSA1	0.0017	1.00	0.99
10% DHSA1	0.0070	0.99	0.99
20% DHSA1	0.0380	0.94	0.98
4% DHSA2	0.0015	1.00	0.98
10% DHSA2	0.0064	0.99	0.97
20% DHSA2	0.0351	0.95	0.99
4% DHSP1	0.0014	1.00	0.99
10% DHSP1	0.0065	1.00	0.98
20% DHSP1	0.0352	0.96	0.98
4% DHSP2	0.0012	0.99	0.98
10% DHSP2	0.0052	0.99	0.99
20% DHSP2	0.0300	0.97	0.97

It is apparent that the Oswald model is appropriate here since all of the correlation coefficients (R^2) are higher than 0.97, indicating a good fit to the data. In accordance with the viscosity data shown in above figures, the consistency index also increases with an increase in the concentration. Also, shear-thinning behaviors are observed from most solutions. Because of the equipment limitation, we were only able to measure the viscosity under shear rate no less than 15 1/s, which might be beyond the non-Newtonian range of some low viscosity samples. The viscosity drops more quickly with a dilute solution than that of a solution with higher concentration. This explains why n decreases with all DHS solutions when concentration is increased.

In addition, DHS and DHS ester solutions at the same concentrations were compared with each other. Figure 43 shows the rheograms of 3% 20DHS, 60DHS, and 100DHS solutions. Among them, 20DHS showed the highest viscosity, followed by 60DHS, and 100DHS, respectively. This difference is most likely due to the different molecular weights of these solutions. Figure 44 shows the rheograms of 10% DHS esters as well as 100DHS solutions. All DHS ester solutions had lower viscosity than 100DHS; DHSP solutions had lower viscosity than the DHSA solution with the same degree of substitution. The viscosity of an ester solution with higher degree of substitution is lower than that of an ester with lower degree of substitution. These differences are due to the fact that less hydrogen bonding is formed when hydroxyl groups are substituted by ester groups during esterification.

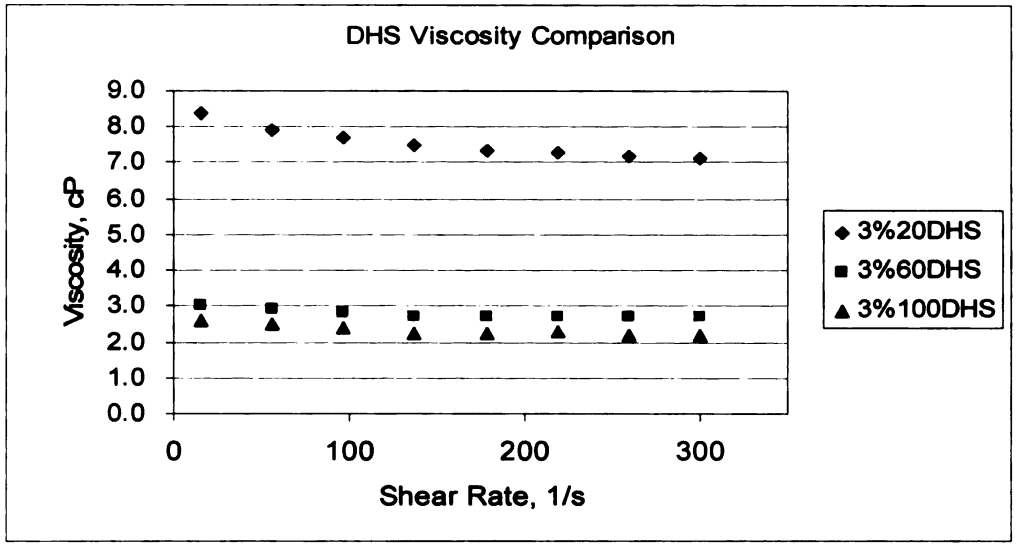

Figure 43: Viscosity comparison of DHS solution at the same concentration

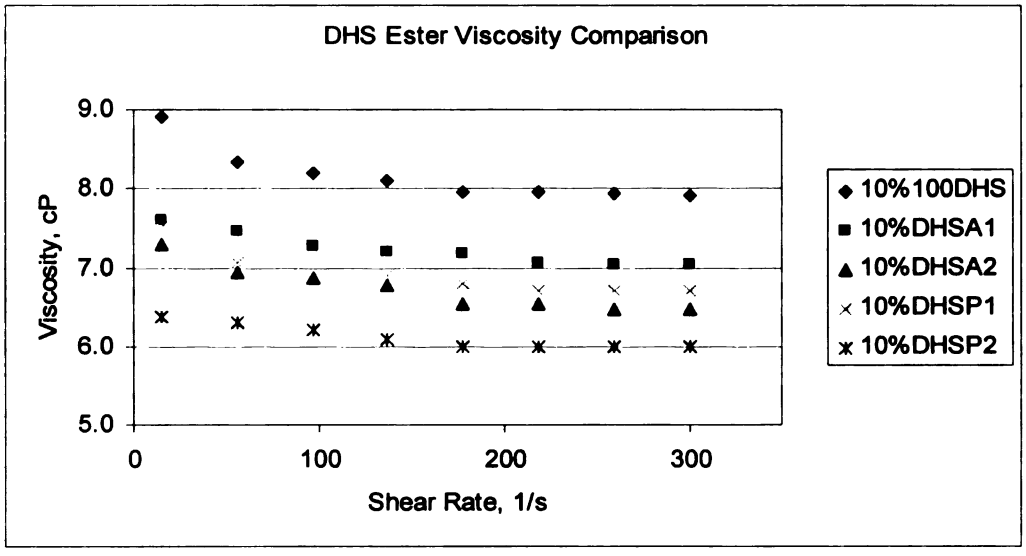

Figure 44: Viscosity comparison of DHS ester solutions at the same concentration

3.2.3.2 Viscoelastic behavior

Storage moduli and loss moduli, G' and G", at different frequencies of DHS and DHS esters are reported in Tables 10-16. The loss tangent curves as a function of frequency for the same systems are reported in Figure 45-51.

Table 10: Viscoelastic property of 20DHS

20DHS	1%		3%		5%	
f, Hz	G', Pa	G", Pa	G', Pa	G", Pa	G', Pa	G", Pa
0.46	0.00	0.01	0.00	0.04	0.00	0.11
0.68	0.00	0.02	0.00	0.04	0.01	0.16
1.00	0.00	0.03	0.00	0.06	0.04	0.24
1.47	0.00	0.04	0.00	0.09	0.15	0.35
2.15	0.00	0.05	0.00	0.15	0.36	0.66
3.16	0.00	0.07	0.00	0.28	0.82	0.74
4.64	0.00	0.12	0.00	0.21	1.75	1.64
6.81	0.00	0.34	0.30	1.37	5.34	3.34
10.00	0.00	0.69	0.45	1.73	7.38	4.95
14.70	0.55	1.49	2.34	7.00	18.68	12.15
25.10	6.35	11.49	37.63	35.88	141.13	56.22
39.00	48.47	68.64	158.00	110.00	332.29	155.25
61.00	467.22	448.12	600.00	460.00	865.64	487.49
100.00	4852.44	1883.55	6000.00	2401.25	8654.15	3265.15

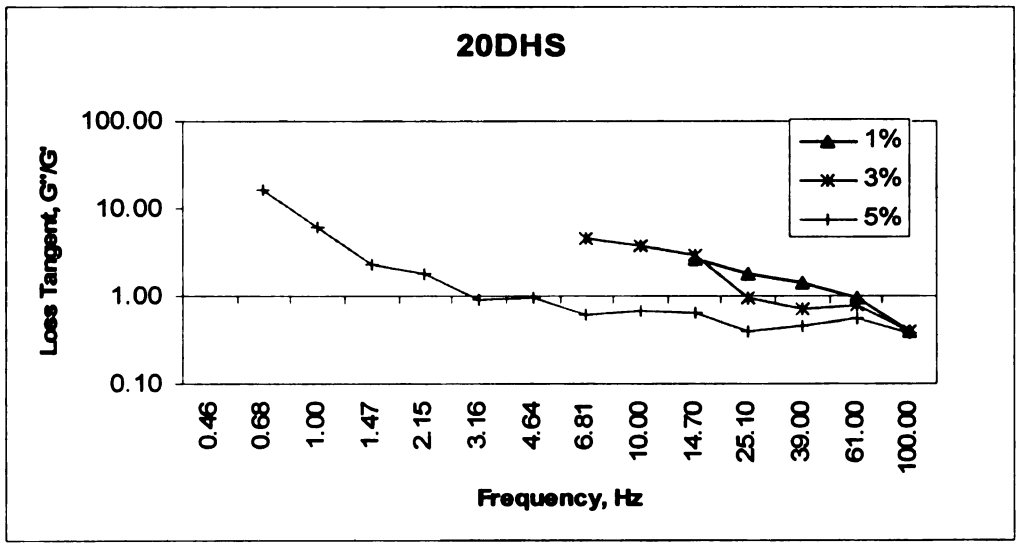

Figure 45: Loss tangent of 20DHS

Table 11: Viscoelastic property of 60DHS

60DHS	4%		8.5%		17%	
f, Hz	G', Pa	G", Pa	G', Pa	G", Pa	G', Pa	G", Pa
0.46	0.00	0.02	0.00	0.04	0.00	0.06
0.68	0.00	0.02	0.00	0.04	0.00	0.09
1.00	0.00	0.04	0.00	0.06	0.04	0.18
1.47	0.00	0.06	0.00	0.09	0.11	0.27
2.15	0.00	0.09	0.00	0.13	0.66	0.52
3.16	0.00	0.12	0.00	0.19	1.52	1.02
4.64	0.00	0.16	0.00	0.22	2.54	2.16
6.81	0.00	0.55	0.00	0.99	4.32	3.34
10.00	0.00	1.05	0.42	1.76	7.16	5.27
14.70	0.42	1.64	1.94	5.32	18.53	12.22
25.10	7.86	18.22	64.75	41.79	78.24	51.32
39.00	36.17	36.24	147.75	61.50	152.22	96.15
61.00	2877.35	1524.21	5238.00	2388.75	5328.19	2732.65
100.00	9537.48	2634.16	13938.50	3693.50	13925.22	5124.26

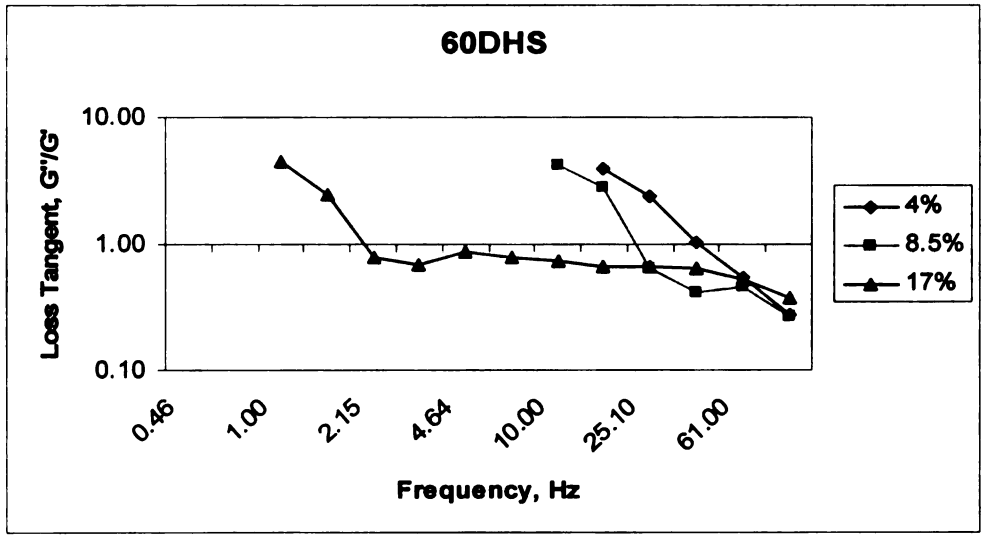

Figure 46: Loss tangent of 60DHS

Table 12: Viscoelastic property of 100DHS

100DHS	4%		10%		20%	
f, Hz	G', Pa	G", Pa	G', Pa	G", Pa	G', Pa	G", Pa
0.46	0.00	0.03	0.00	0.04	0.00	0.05
0.68	0.00	0.03	0.00	0.04	0.00	0.09
1.00	0.00	0.05	0.00	0.06	0.01	0.19
1.47	0.00	0.08	0.00	0.09	0.13	0.30
2.15	0.00	0.15	0.00	0.15	0.55	0.45
3.16	0.00	0.28	0.00	0.28	1.25	0.75
4.64	0.00	0.29	0.02	0.21	2.84	1.81
6.81	0.12	1.78	0.15	1.37	3.46	2.50
10.00	0.21	1.86	0.30	1.73	6.75	4.64
14.70	0.54	4.59	2.34	12.00	17.55	10.58
25.10	4.47	26.48	37.63	38.65	73.46	44.45
39.00	39.48	113.18	107.50	100.25	133.17	87.35
61.00	3090.59	982.55	2600.25	531.25	4568.16	2875.84
100.00	11536.22	2685.47	15069.75	2401.25	11253.47	4458.46

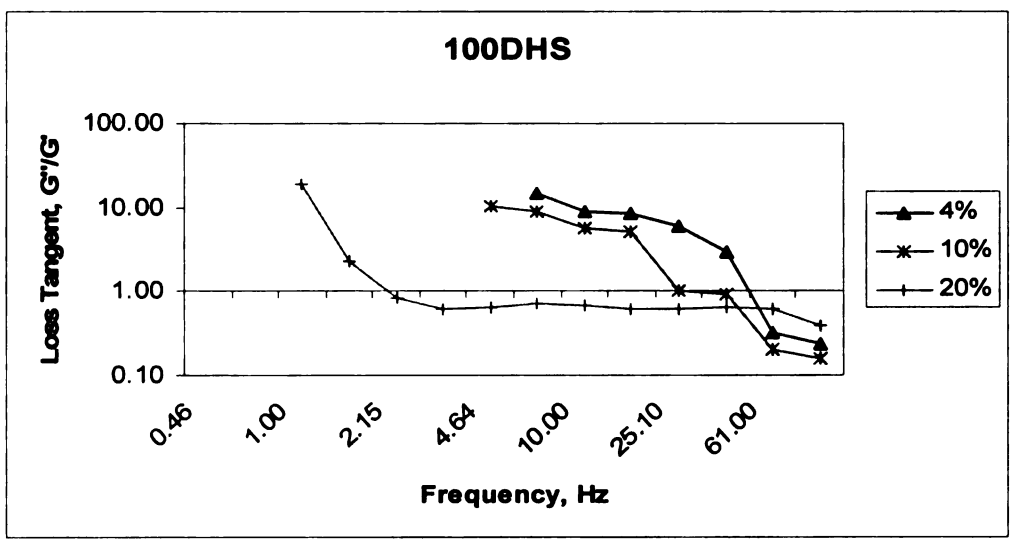

Figure 47: Loss tangent of 100DHS

Table 13: Viscoelastic property of DHSA1

DHSA1	4%		10%		20%	
f, Hz	G', Pa	G", Pa	G', Pa	G", Pa	G', Pa	G", Pa
0.46	0.00	0.03	0.00	0.04	0.00	0.05
0.68	0.00	0.03	0.00	0.04	0.00	0.08
1.00	0.00	0.04	0.00	0.06	0.01	0.19
1.47	0.00	0.07	0.00	0.09	0.08	0.22
2.15	0.00	0.12	0.00	0.14	0.44	0.41
3.16	0.00	0.25	0.00	0.26	1.21	0.82
4.64	0.00	0.26	0.00	0.19	2.16	1.59
6.81	0.00	1.35	0.04	1.21	3.20	2.62
10.00	0.00	1.78	0.25	1.53	5.73	4.05
14.70	0.17	12.69	2.04	11.19	15.19	9.53
25.10	3.25	34.58	33.18	41.45	62.20	40.25
39.00	34.18	121.23	95.35	112.39	117.67	79.65
61.00	2758.15	786.54	2273.64	464.42	4540.45	2993.45
100.00	10054.46	2308.29	14352.47	2118.70	11563.54	4002.45

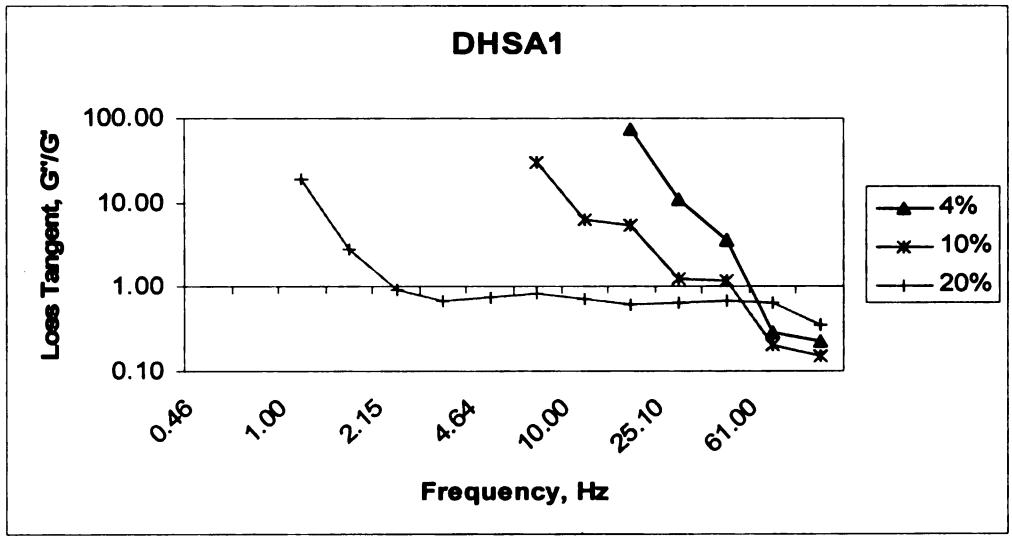

Figure 48: Loss tangent of DHSA1

Table 14: Viscoelastic property of DHSA2

DHSA2	4%		10%		20%	
f, Hz	G', Pa	G", Pa	G', Pa	G", Pa	G', Pa	G", Pa
0.46	0.00	0.02	0.00	0.04	0.00	0.03
0.68	0.00	0.03	0.00	0.04	0.00	0.05
1.00	0.00	0.04	0.00	0.06	0.02	0.18
1.47	0.00	0.07	0.00	0.08	0.08	0.25
2.15	0.00	0.11	0.00	0.13	0.40	0.38
3.16	0.00	0.23	0.00	0.24	0.98	0.84
4.64	0.00	0.17	0.00	0.29	2.16	1.51
6.81	0.00	1.32	0.00	1.15	3.17	2.35
10.00	0.00	1.62	0.23	1.43	5.64	3.98
14.70	0.59	10.17	2.24	10.62	15.17	9.01
25.10	6.17	23.22	31.49	30.13	58.38	36.16
39.00	44.35	113.07	88.17	59.50	111.49	74.88
61.00	2618.55	684.55	2005.22	433.17	3902.56	3305.36
100.00	8400.49	1795.57	10254.19	2014.55	11353.46	3821.13

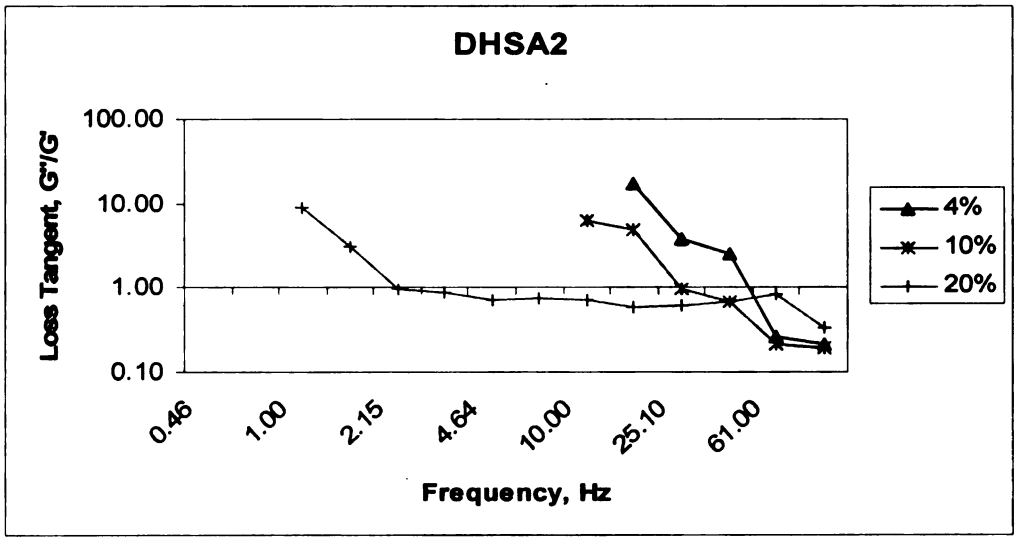

Figure 49: Loss tangent of DHSA2

Table 15: Viscoelastic property of DHSP1

DHSP1	4%		10%		20%	
f, Hz	G', Pa	G", Pa	G', Pa	G", Pa	G', Pa	G", Pa
0.46	0.00	0.04	0.00	0.03	0.00	0.02
0.68	0.00	0.04	0.00	0.04	0.00	0.06
1.00	0.00	0.05	0.00	0.05	0.03	0.16
1.47	0.00	0.09	0.00	0.06	0.07	0.23
2.15	0.00	0.17	0.00	0.12	0.44	0.33
3.16	0.00	0.23	0.00	0.22	1.05	0.69
4.64	0.00	0.26	0.00	0.15	2.35	1.52
6.81	0.00	1.32	0.00	1.30	3.07	2.32
10.00	0.00	1.63	0.24	3.69	5.33	3.85
14.70	0.63	12.05	1.86	11.02	14.02	8.90
25.10	3.54	32.14	27.63	30.24	60.31	37.25
39.00	32.06	114.17	112.35	105.36	111.53	75.86
61.00	2568.46	695.06	2036.95	443.65	3778.29	2865.03
100.00	8512.43	2144.86	13151.24	2015.42	10862.22	3814.33

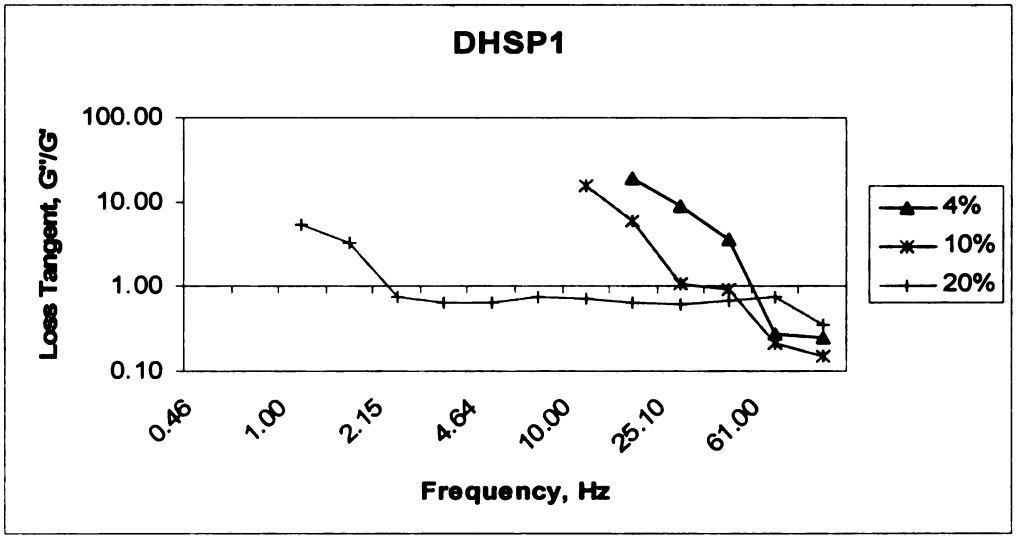

Figure 50: Loss tangent of DHSP1

Table 16: Viscoelastic property of DHSP2

DHSP2	4%		10%		20%	
f, Hz	G', Pa	G", Pa	G', Pa	G", Pa	G', Pa	G", Pa
0.46	0.00	0.03	0.00	0.03	0.00	0.03
0.68	0.00	0.04	0.00	0.04	0.00	0.06
1.00	0.00	0.04	0.00	0.04	0.01	0.13
1.47	0.00	0.06	0.00	0.08	0.07	0.19
2.15	0.00	0.13	0.00	0.13	0.39	0.35
3.16	0.00	0.25	0.00	0.24	0.87	0.66
4.64	0.00	0.19	0.00	0.25	1.98	1.33
6.81	0.00	1.12	0.21	1.04	2.56	2.10
10.00	0.00	1.38	0.60	1.31	4.77	3.41
14.70	0.49	10.55	5.12	10.12	12.35	8.30
25.10	2.77	28.69	14.98	29.58	56.28	34.23
39.00	28.36	104.37	79.35	73.53	98.68	70.12
61.00	2318.42	598.65	1954.24	401.65	3658.49	2193.53
100.00	7763.64	1954.63	10982.33	1796.35	9534.51	3215.25

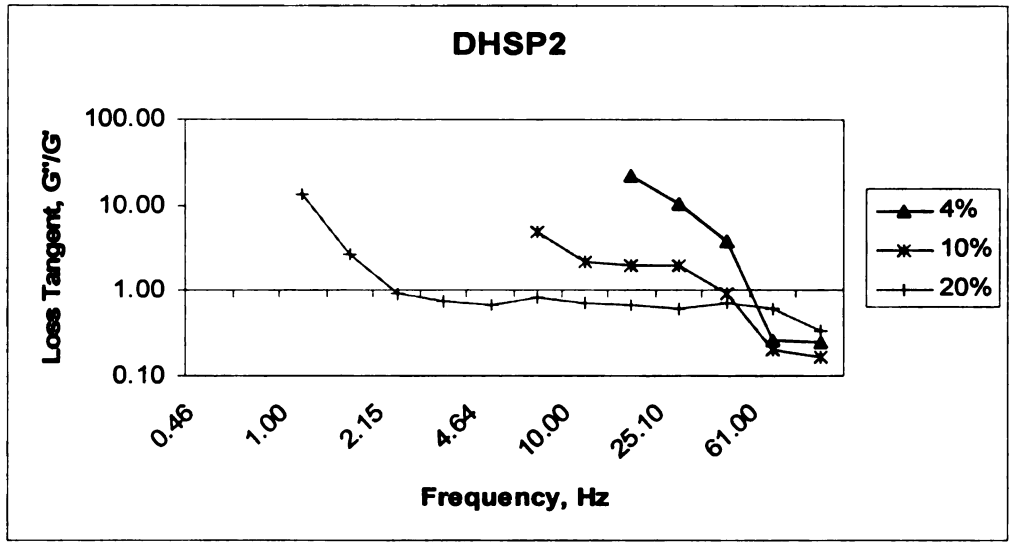

Figure 51: Loss tangent of DHSP2

All the systems display elastic and viscous moduli that are frequency dependent. Furthermore, in all cases both modulus increased as the frequency increased. At low frequency all the formulations show a predominant viscous character (G" > G') but as the frequency is increased, the elastic modulus increases faster than the viscous modulus so

that G' curve crosses G" curve at a certain frequency called the cross-over frequency. Even with higher frequencies than the cross-over frequency the elastic modulus remains high and the systems show a predominant elastic characteristic. This rheological behavior is a feature of an entangled network that can further be seen in the loss tangent curves. For the solutions at the cross-over frequency the loss tangent is equal to 1, while it is greater than 1 at low frequency and lower than 1 at high frequency. What should be particularly pointed out is the cross-over point, which means the material demonstrates equal viscous and elastic characters. At frequencies lower than the cross-over point, the relaxation time of the material is shorter than the process time and the material has sufficient time to relax. Thus, it shows more viscous behavior. When the frequency is higher than the cross-over point, the process time is shorter than the material relaxation time and there is not sufficient time for the material to relax, resulting in a more elastic behavior.

The cross-over points of all the solutions we tested are dependent on concentration. Namely, the concentration is inversely proportional to the cross-over frequency. This is due to the fact that when the concentration is high there is more entanglement and interactions between polymer chains and longer relaxation time is needed when a stress is applied.

One of the key objectives in this study was to obtain ophthalmic solutions that show an entangled solution behavior. Since such solutions are characterized by the important feature of flowing as viscous fluid (G" > G') when stressed at low frequency therefore adapting to the ocular surface just like a natural tear and behaving elastically

when stressed quickly, therefore the entangled DHS should be able to stay together in presence of quick stress change.

3.2.4 *In vitro* release profile of Ofloxacin

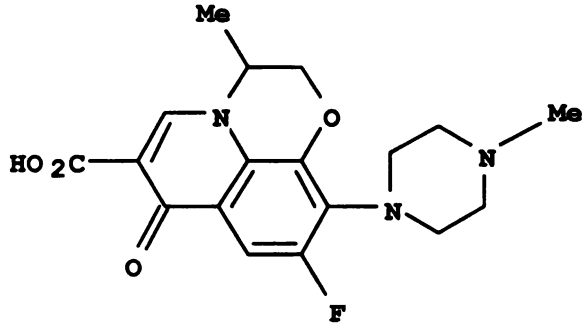

Figure 52: Structure of ofloxacin

Ofloxacin is an antibacterial agent belonging to the fluoroquinolone family with a molecular weight of 361.37. Of the available fluoroquinolones, ofloxacin is usually administered as a single agent and has been shown to have the best aqueous humor penetration. As an ophthalmic formulation, ofloxacin is formulated as a 0.3% solution and is known by the trade name OCUFLOX®. According to Allergan's prescribing information packet, OCUFLOX solution is unbuffered and formulated with a pH of 6.4 (range - 6.0 to 6.8). Ofloxacin is a fluorinated 4-quinolone which differs from other fluorinated 4-quinolones in that there is a six member pyridobenzoxazine ring from positions 1 to 8 of the basic ring structure.

The drug release profiles were studied using a UNICO SQ-2800 Ultraviolet-Visible Spectrophotometer. The absorbance spectrum for the drug ofloxacin is shown in Figure 53.

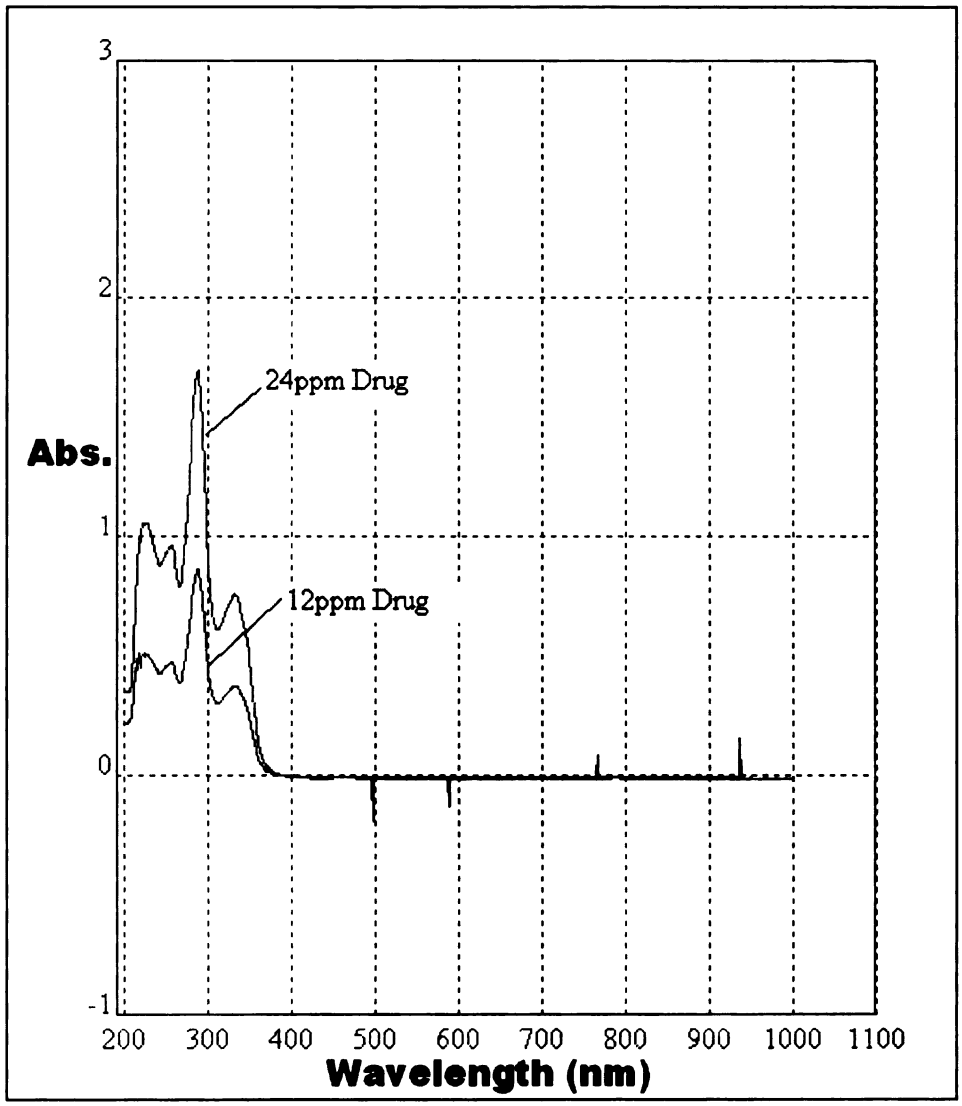

Figure 53: UV/Vis Spectrum of ofloxacin

The strongest peak, at 288 nm, was used to determine the concentration of ofloxacin as compared to a calibration curve (Figure 54). The absorbance at concentrations of 0.0036% w/v to 0.00075%w/v was found linearly dependent and measurable using the parameters described in the analytical technique chapter. A fixed-point measurement method was used so that only the absorbance at 288 nm was recorded. This eliminated the need to develop a full spectra for all of the samples.

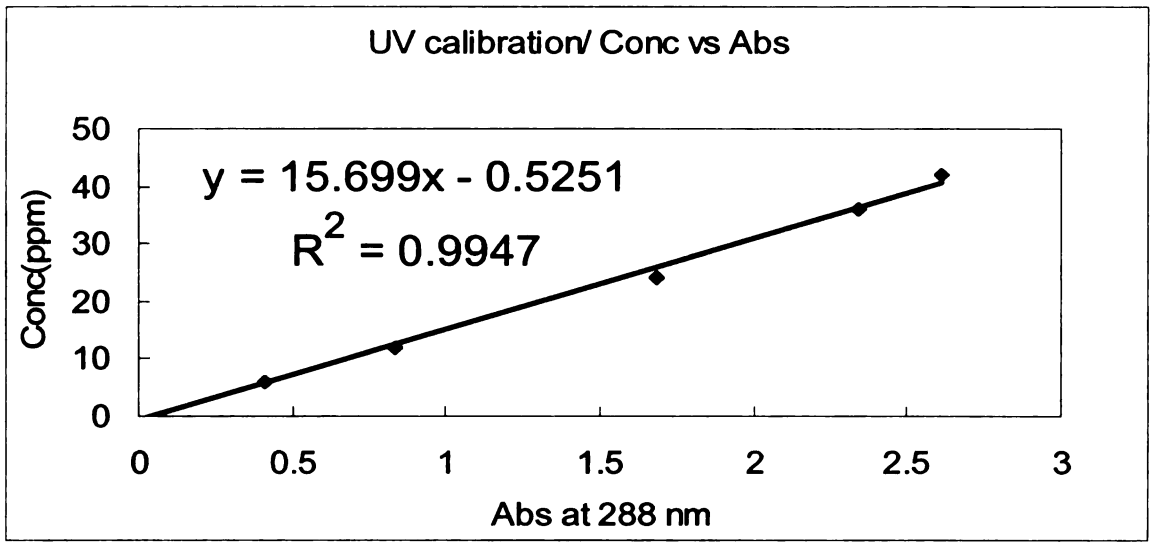

Figure 54: Calibration curve for Ofloxacin

3.2.4.1 Release from isoviscous solutions

Figure 55 shows the release profiles from seven isoviscous DHS and DHS ester solutions and phosphate buffer as control at pH 7.4 using phosphate buffer.

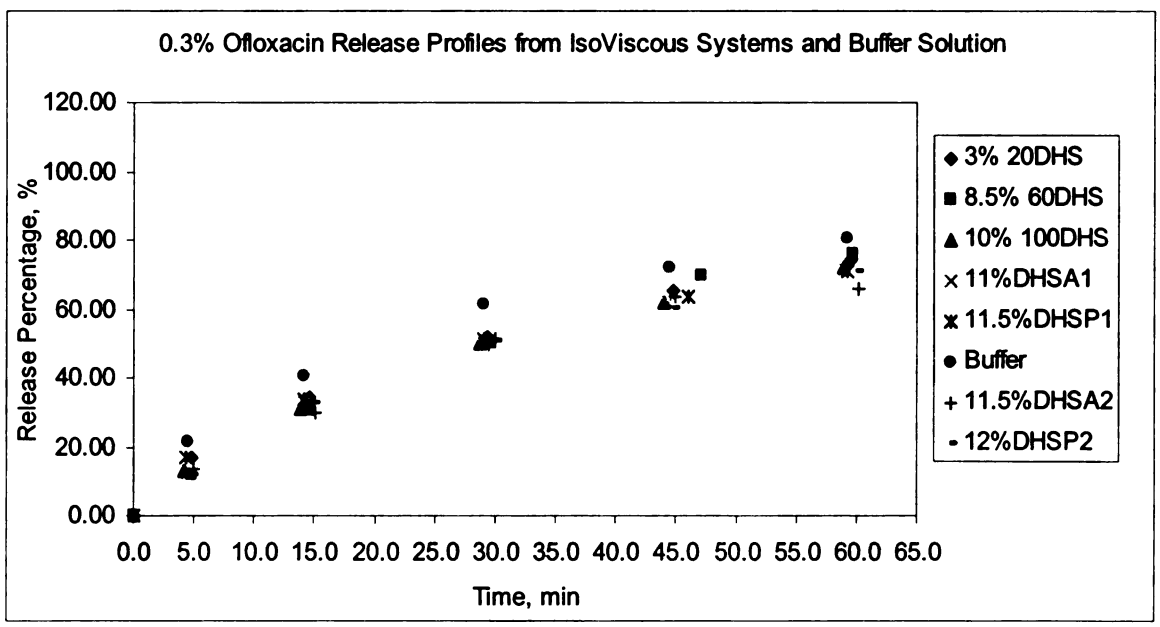

Figure 55: Release profiles of ofloxacin from isoviscous solutions

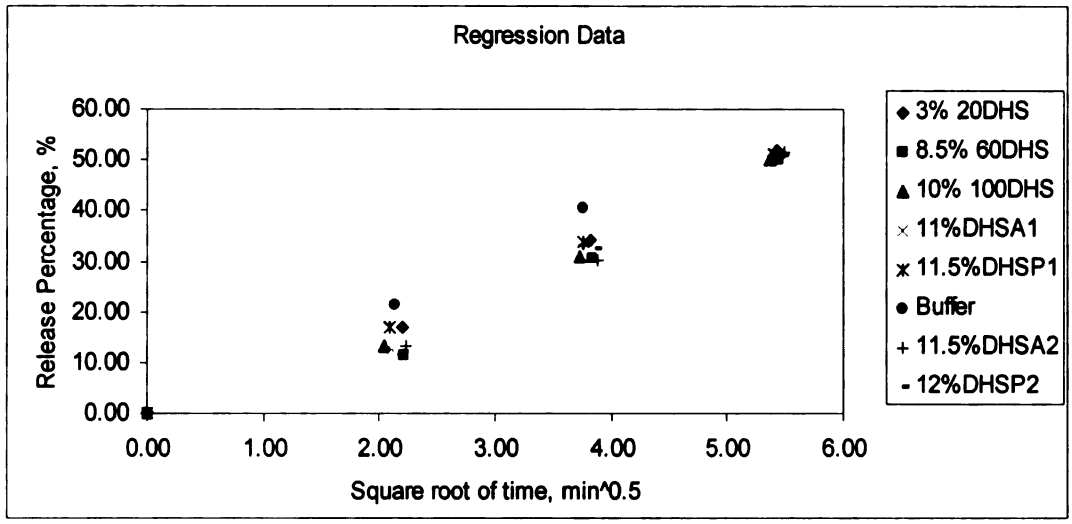

Figure 56: Release Percentage from Isoviscous Solutions vs. Square Root of Release Time

Table 17: Regression Data of Ofloxacin Release from Isovisous Solutions

Solution	Slope	R^2	p value	Dm (10^(-4)cm^2/g)
3% 20DHS	9.54	0.9915	0.027	1.95
8.5% 60DHS	9.17	0.9639	0.010	1.87
10% 100DHS	9.36	0.9813	0.011	1.91
11% DHSA1	9.20	0.9772	0.034	1.87
11.5% DHSA2	9.46	0.9957	0.016	1.93
11.5% DHSP1	9.29	0.9975	0.021	1.89
12% DHSP2	9.33	0.9936	0.013	1.90
Buffer solution	11.35	0.9978	1.000	2.31

The release percentage is also plotted in Figure 56 as a function of the square root of the release time to fit the Baker and Lonsdale model and it appears to yield a linear correlation. The slope, R^2 values, p value, and diffusion coefficients, Dm are listed in Table 17.

It is apparent that all R^2 values are greater than 0.95, confirming the fit of the release profiles from DHS and DHS ester solutions to Baker and Lonsdale model. Furthermore, the slopes, which are proportional to diffusion coefficients of DHS as well

DHS esters, were compared with that of the blank buffer solution by T test. The p values shown in Table 17 are all less than 0.05, which indicates that the release profiles of all isoviscous samples are significantly different from that of buffer solution.

Also, an ANOVA test was done to study whether there was a significant difference between the release profiles of these isoviscous samples. The p value is 0.78473, which is greater than 0.05, indicating that there is no significant difference of release profiles between these isoviscous solutions.

3.2.4.2 Release from solutions with different viscosity

Figure 57 shows the release from 100DHS at different concentrations (e.g. different viscosities).

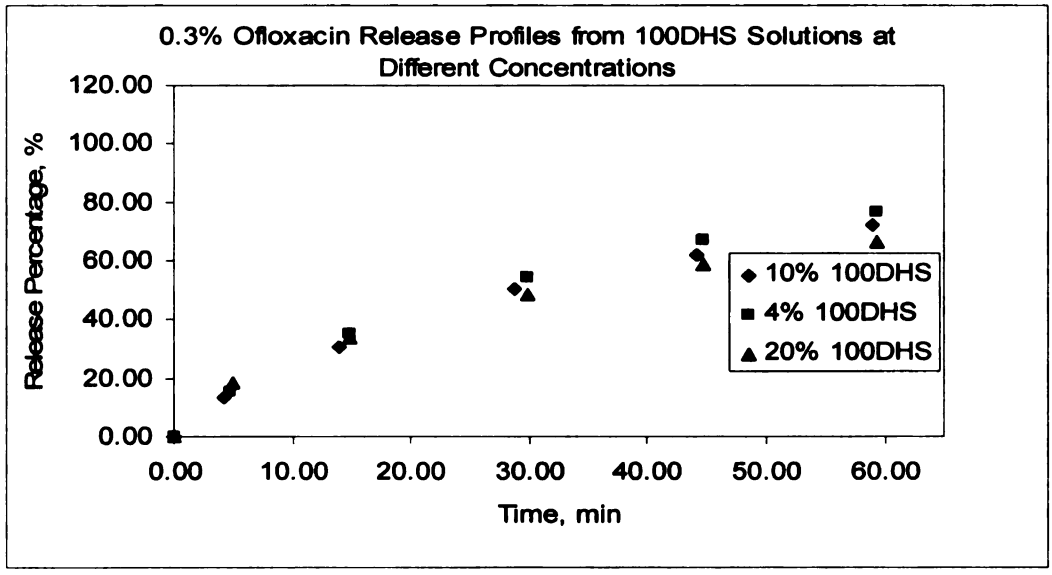

Figure 57: Release Profiles of Ofloxacin from 100DHS at Different Concentrations

These data are also plotted as before as a function of the square root of the release time yielding a linear correlation. The linear regression parameters (e.g. slope and R^2 values) are listed in Table 18.

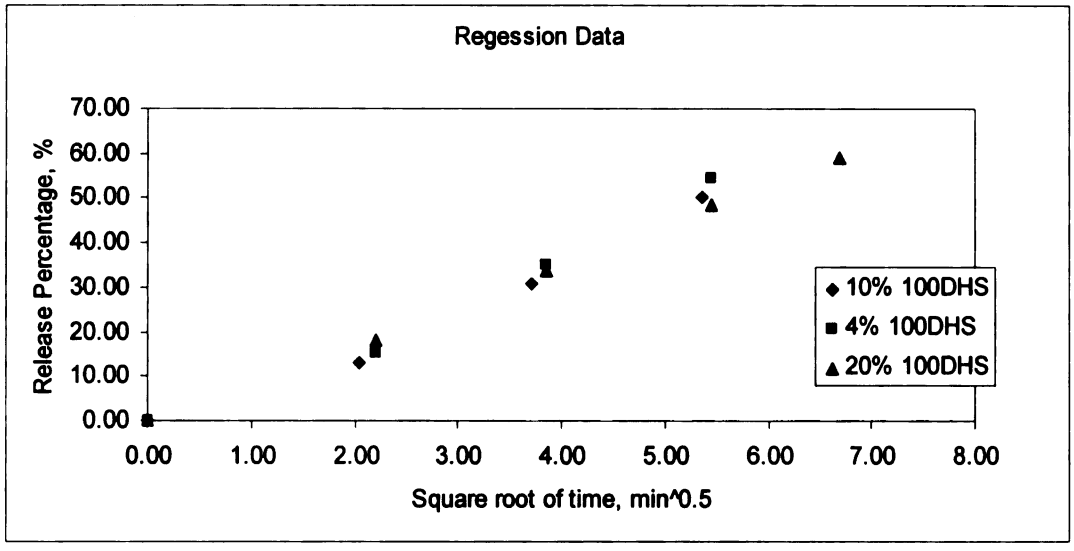

Figure 58: Non Isoviscous Release Percentage vs. Square Root of Release Time

Table 18: Regression Data of Ofloxacin Release from Solutions with Different Viscosity

Solution	slope	R^2	Dm (10^(-4)cm^2/g)
4% 100DHS	9.94	0.981	2.03
10% 100DHS	9.36	0.981	1.91
20% 100DHS	8.91	0.999	1.82

All R^2 values are greater than 0.95, indicating a good fit to Baker and Lonsdale model. T tests were examined between solutions at concentrations of 4% and 10%, 10% and 20%, as well as 4% and 20% (Table 12). They all have p values less than 0.05, indicating that they are significantly different from each other statistically. As shown in Table 11, 20% 100DHS has the lowest diffusion coefficient and 4% 100DHS has the highest diffusion coefficient.

Table 19: T Test Results of Solutions with Different Viscosities

T test between	P value
4%, 10%	0.034
10%, 20%	0.044
4%, 20%	0.020

Based on the *in vitro* release tests, we found that viscosity was a factor that significantly affected the incorporated drug release profile. The drug diffused faster in low viscosity solutions than in high viscosity solutions. However, this does not necessarily agree with their *in vivo* release profile. In this test the effects of drug-eye contact time and interaction with mucus were not included, while they can significantly affect *in vivo* drug release as well.

3.2.5 Stability Data

3.2.5.1 Storage stability

In this project, the effects of pH and temperature on the polymers' storage stability were studied. Samples 20DHS, 60DHS, 100DHS, DHSA1, DHSA2, DHSP1, and DHSP2 were dissolved in pH 4, 7, and 9 buffer solutions. Six samples of each solution were made. Three of them were stored at 4 °C and the other three were stored at room temperature (22 +/- 2 °C). Their apparent viscosity was recorded at a shear rate of 300 1/s immediately after they were prepared and then compared with the viscosity measured 30 days later. The results are shown in the Table 20-26.

Table 20: Storage stability of 3% 20DHS

Viscosity, cPs	4 °C	Room temp.
pH 4	2.1--1.4	2.1--1.2
pH 7	8.0--7.5	8.0--7.5
pH 9	8.0--7.5	8.0--7.5

Table 21: Storage stability of 8.5% 60DHS

Viscosity, cPs	4 °C	Room temp.
pH 4	1.8--1.4	1.8--1.4
pH 7	7.7--7.5	7.7--7.7
pH 9	7.5--7.5	7.5--7.4

Table 22: Storage stability of 10% 100DHS

Viscosity, cPs	4 °C	Room temp.
pH 4	2.4--1.1	2.4--1.2
pH 7	7.8--7.8	7.8--7.7
pH 9	7.5--7.5	7.5--7.4

Table 23: Storage stability of 10% DHSA1

Viscosity, cPs	4 °C	Room temp.
pH 4	4.3--2.0	4.3--2.1
pH 7	7.2—7.0	7.2—7.3
pH 9	7.4—7.3	7.4—7.4

Table 24: Storage stability of 10% DHSA2

Viscosity, cPs	4 °C	Room temp.
pH 4	3.9--2.1	3.9--2.0
pH 7	6.7—6.8	6.7—6.7
pH 9	7.2—7.3	7.2—7.1

Table 25: Storage stability of 10% DHSP1

Viscosity, cPs	4 °C	Room temp.
pH 4	4.4--2.2	4.4--2.1
pH 7	6.8—6.8	6.8—6.7
pH 9	7.1—7.0	7.1—7.1

Table 26: Storage stability of 10% DHSP2

Viscosity, cPs	4 °C	Room temp.
pH 4	3.6--2.1	3.6--2.0
pH 7	6.3--6.4	6.3--6.3
pH 9	7.2—7.2	7.2—7.1

No difference was observed between the data collected at 4 °C and room temperature, indicating these solutions can be stored at room temperature. However, the pH had a significant effect on the conditions these solutions were dissolved and stored. At pH 4 the viscosity of DHS solutions was much lower than that of the solutions at pH 7

and 9. This agrees with Sihtola's conclusion[22] that DHS hydrolyzes at acidic environment. At pH 7 and 9 solutions of samples 60DHS, 100DHS, and DHS esters showed excellent stability with no viscosity change. However, we did observed a viscosity drop of 20DHS solutions. Apparently, the structure of 20DHS is very close to that of starch and retrogression takes place as in a starch solution.

3.2.5.2 Effect of autoclaving

The purpose of this test was to study the effect of autoclaving (121 °C, 20 min) on the polymer molecular weight. In this test the viscosity was measured as an indicator of the molecular weight change. DHS and DHS ester solutions were tested at pH 7. The viscosity of these samples was measured with shear rate set at 300 1/s by a Haake rheometer. The viscosity measurement was repeated twice before and after autoclaving and the results are shown as follows.

Table 27: Viscosity drop after autoclaving

Viscosity, cPs	Before autoclaving	After autoclaving	%(viscosity drop)
3% 20DHS	8.0	4.5	43.8
8.5% 60DHS	7.7	5.8	24.7
10% 100DHS	7.3	5.9	19.2
10% DHSA1	7.1	5.1	28.2
10% DHSA2	6.9	4.7	31.9
10% DHSP1	6.8	4.6	32.4
10% DHSP2	6.2	5.0	19.4

A drop in the viscosity was observed with all DHS solutions, with 20DHS having the largest drop indicating that hydrolysis occurred under the high temperature and pressure conditions. However, this hydrolysis should not affect the performance of ophthalmic solutions too much, as long as autoclaving does not impact their rheological

properties too much. We also observed that the viscosity drop takes place in CMC solutions, which is one of the most commonly used polymers in ophthalmic solutions.

In summary, based on the property characterizations described in this chapter, the synthesized polymers showed very good properties. The variable studied allowed us to control the surface activities, mucoadhesnion, rheological behaviors, sustained drug release, and storage stability. *In vivo* tests would be conducted to further investigate their potential as ophthalmic applications.

Chapter 4 Performance Characterization

Based on the property characterizations described in the previous chapter, the modified starch products were shown to be good candidates for ocular drug delivery applications. In this chapter, we report the results of our in vitro performance tests and the results of in vivo irritancy tests that were run to confirm safety issues. Specifically, the following tests will be discussed: in vitro EpiOcular test, in vivo irritancy test, Tear Break-up Time (TBUT) test, and Timolol release test. All these tests were conducted in cooperation with Dr. Wendy Townsend.

4.1 Experiments

4.1.1 EpiOcular *in vitro* test

The EpiOcular™ model provides a predictive, morphologically relevant *in vitro* means to assess ocular irritancy. In this study, the Epi Ocular *in vitro* test was run with the MatTek's EpiOcular™ corneal model in Dr. Wendy Townsend's lab using the following the SOP:

1. Pre-warm the MatTek assay medium to 37 °C by placing it in an incubator for one hour
2. Use sterile technique pipet 0.9 ml of assay medium into each well of sterile six well plates
3. Transfer EpiOcular samples using sterile forceps into the six well plates containing the prewarmed assay medium
4. Place at 37 °C and 5% CO_2, humidified chamber for one hour prior to dosing.
5. Remove the assay media and replace with 0.9 ml/well of fresh media

6. Pipet 100 ul of test material into cell culture insert atop the EpiOcular sample. For negative controls dose with 100 ul of deionized water. Perform in triplicate for each material. Use Triton X as positive control at same time exposures.

7. Exposure time is 16 minutes initially, if viability > 90% then 64 minutes and 256 minutes

8. Before the end of the exposure period, thaw the MTT concentrate and place 2 ml of concentrate in with 8 ml of MTT diluent. Filter to remove any precipitate. Store remaining MTT in the dark at 4 °C

9. Prepare a 24 well place by pipetting 300 ul of the MTT solution into each well needed for an insert and label the 24 well plate top.

10. Discard liquid atop EpiOcular tissues. Submerge each insert to fill with PBS and decant. Repeat three times. Submerge cell culture, insert in a well of a 12 well plate containing 5 ml of assay media for 10 minutes at 37 °C and 5% CO_2

11. Decant and shake off assay medium. Place EpiOcular sample in the MTT containing 24 well plate. Return to the incubator at 37°C and 5% CO_2 for 3 hours

12. Remove each insert and gently rinse with PBS. Shake the insert and blot with a Kimwipe. Place in pre-labeled 24 well extraction plate.

13. If test article is colored then pipet 1 ml into the well and place the insert in each well (If it is not colored pipet 2 ml into the cell culture insert itself).

14. Place cover and wrap in aluminum foil. Place on counter overnight in a sealed plastic bag.

15. If placed test material in each well then remove insert and add 1 ml of extractant. If placed test material in the cell culture insert then decant into the well and discard the insert.
16. Pipet extractant solution up and down three times to mix well
17. Pipet 200 ul to a 96 well plate, perform in triplicate for each well
18. Measure optical density (OD) at 540 nm. Blank is 200 ul of extractant.

Calculate % viability = 100 x [OD sample / OD negative control] (4.1)

4.1.2 *In vivo* irritation test

In vivo irritation tests were done before any other *in vivo* tests to ensure the test substances were accepted by the test animals. Both short-term and long-term irritation tests were carried on as described below.

4.1.2.1 Assessment of ocular irritation after a single administration of the test formulations

Eighteen rabbits were divided into six groups evenly. The groups were composed of rabbits receiving either a saline control, Gellan gum™ control, or the DHS formulations. One drop (50 ul) was administered to one eye of each rabbit. The rabbits were examined via slit-lamp biomicroscopy and fluorescein staining (as needed) pre-administration and at 15 minutes, 30 minutes, 1 hour, 2 hours, 3 hours, and 5 hours post-administration. Scoring of ocular signs was performed according to the Hackett-McDonald Ocular Scoring System [44]. Any complications or irritation from the preparations was treated as required [either topical antimicrobial ophthalmic medication (neomycin/polymyxin/bacitracin ophthalmic ointment ¼ inch strip q4-8 hours) if corneal or conjunctival ulceration developed or topical anti-inflammatory ophthalmic

medications (1% prednisolone acetate ophthalmic suspension 1 drop q4-12 hours) if inflammatory responses developed]. Any pain associated with corneal ulceration or severe inflammation was treated with ketoprofen administered subcutaneously at 3 mg/kg q24h and butorphanol tartrate administered at 0.25 mg/kg subcutaneously every four hours until resolved. When any systemic signs of toxicity or disease should arise they were addressed by the attending laboratory animal veterinarian.

4.1.2.2 Assessment of ocular irritation after multiple doses of the test formulations

In this long-term irritation test we followed a similar procedure as the short-term irritation test. The differences were that the doses were administrated every 2 hours from 7 AM until 7 PM for a period of 7 days and the rabbits were examined at pre-administration, day 2, and day 7.

4.1.3 Tear break-up time test

The normal tear film is continuous. Blinking maintains the tear film continuity. If the eye is kept open long enough, without blinking, the tear film will start breaking up. The eye will feel uncomfortable and be forced to blink. In subjects with dry eyes the tear film is unstable and breaks up faster. Therefore the tear breakup time in subjects who have dry eyes is shorter. However, an effective artificial tear can extend the tear breakup time. In this study tear break-up test was used to assess the feasibility of DHS and DHS esters for use of dry eye solutions.

There were 10 rabbits in a group. The group was composed of rabbits receiving initially balanced salt solution (BSS) and then the polymer solutions. Each rabbit was anesthetized by mask administration of isoflurane and oxygen. One drop (50ul) of balanced salt solution containing 1.25mg/ml of fluorescein was administered to one eye

of each rabbit once. The lid was manually closed twice to distribute the fluorescein stain. The lids were then manually kept open for measurement. Immediately after the second blink a timing instrument was started. The tear film was scanned using a broad beam slit lamp (Kowa SL-15) in a darkened room using a cobalt blue filter. The timer was stopped when the film disruption occured first The ocular surface was flushed with BSS. The polymer formulations were then tested by an identical procedure. If any post-operative discomfort was noted as detected by the presence of blepharospasm, rubbing at the eye, decreased activity, or inappetance, butorphanol tartrate was administered at 0.25 mg/kg subcutaneously (can be repeated every 4 hours if needed). Any complications or irritation from the preparations was treated as required [either topical antimicrobial ophthalmic medication (neomycin/polymyxin/bacitracin ophthalmic ointment ¼ inch strip q4-8 hours) if corneal or conjunctival ulceration developed or topical anti-inflammatory ophthalmic medications (1% prednisolone acetate ophthalmic suspension 1 drop q4-12 hours) if inflammatory responses developed]. If any systemic signs of toxicity or disease should arose was addressed by the attending laboratory animal veterinarian.

4.1.4 *In vivo* Timolol release test

4.1.4.1 *In vivo* drug release profiles

Timolol is a drug used to lower pressure in the eye for glaucoma patients by reducing aqueous production. *In vivo* Timolol release tests were used to evaluate the performance of synthesized polymers as ocular drug delivery systems. Sixty rabbits were divided into three groups evenly. The groups were composed of rabbits receiving either a timolol 0.5% commercial ophthalmic solution (topical glaucoma agent) or timolol 0.5% in our polymer solutions. One drop (50 ul) was administered to one eye of each rabbit

once. At each time point (15, 30, 60, 90, and 120 minutes) post-administration, four rabbits from each group were anesthetized by mask administration of isoflurane and oxygen. Topical proparacaine (a topical anesthetic agent) was applied to the cornea. A sample of 60-80ul of aqueous humor was obtained from the anterior chamber. The sample was stored at –20°C. The concentration of Timolol present within the sample was then determined using high pressure liquid chromatography (HPLC). Prior to recovery, ketoprofen was administered subcutaneously at 3 mg/kg. Also, 250 ml of warmed subcutaneous fluids was administered while anesthetized to decrease the risk of GI stasis. If any post-operative discomfort was noted as detected by the presence of blepharospasm, rubbing at the eye, decreased activity, or inappetance butorphanol tartrate was administered at 0.25 mg/kg subcutaneously (can be repeated every 4 hours if needed). If signs of ocular inflammation resulted from the aqueouscentesis either topical anti-inflammatory agents (1% prednisolone acetate ophthalmic suspension 1 drop q4-12 hours) was administered or systemic anti-inflammatory agents (ketoprofen subcutaneously at 3 mg/kg q24h) was administered to alleviate the inflammation. If any signs of intra-ocular infection were noted, systemic antibiotics (enrofloxacin 10 mg/kg per os q 12 hours) was administered after consultation with the attending lab animal veterinarian.

4.1.4.2 Intra-Ocular Pressure test

Timolol is the drug being delivered to decrease in intra-ocular pressure (IOP). Therefore by serially measuring the IOP one should have a measure of whether the drug is being delivered for a sustained period of time. Measurement of IOP is a very non-invasive procedure and can be completed with the use of a topical anesthetic. The IOP of

each eye of ten rabbits will be evaluated at time 0 and then 2 hours, 6 hours, and 8 hours after the administration of one drop (50 ul) of solution. One drop of proparacine hydrochloride will be administered before the IOP is measured utilizing the TonoPenVet applanation tonometer. A one day recovery period will be utilized after the application. The IOP of each eye of ten rabbits will then be evaluated as above after the administration of one drop (50 ul) of either commercial Timolol eye drop or polymer solution containing 0.5% timolol maleate in both eyes. A one week washout period will occur between measurement series. A sample size of 10 animals was selected based on the following calculations. If one assumes a 0.9 mmHg difference between the BSS control and the trial solution, with a standard deviation of 2.5 mmHg and a $p<0.05$ then to achieve a power of 80%, a sample size of 10 is required[45].

4.2 Results and Discussion

4.2.1 EpiOcular

The viability data, with 256 minutes exposure time, of 20DHS and 100DHS at concentrations 1%, 3%, 5%, and 10% were collected and are shown in Figure 59. They all had satisfactory results with viabilities higher than 80%, which indicate minimal irritancy. The same tests were also done with 10% DHS esters and they showed viabilities close to 100%.

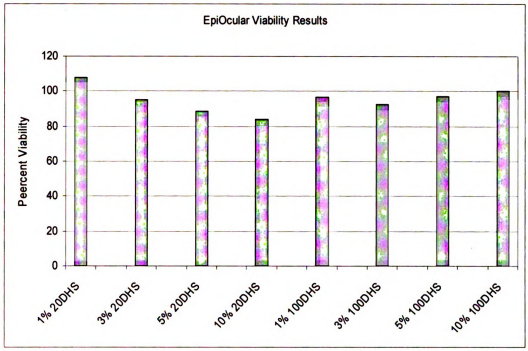

Figure 59: EpiOcular results of 20DHS and 100DHS

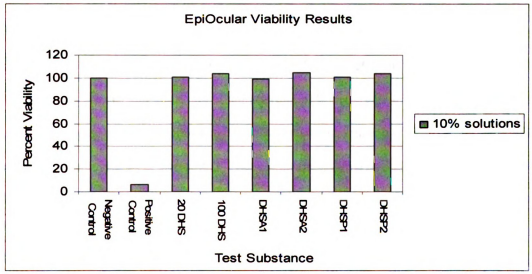

Figure 60: EpiOcular results of DHS Esters

4.2.2 *In vivo* irritation test

There were two irritation tests performed on the rabbits. For the short-term irritancy the drops were applied once and then the animals were evaluated with the slit lamps at 15 min, 30 min, 60 min, 2 hours, 3 hours, and 5 hours post-application. Samples tested included solutions of DHS, DHSA2, and DHSP2. The scores were recorded as 0 (normal) or 1-4. The scores were all 0 at all time points, which meant everyone was as normal as the control eye (the other eye). The same polymers were also tested with the long-term method. For the long-term irritancy the drops were applied six times daily for seven days and evaluated pre and at days 2 and 7. The scores were the same as before. All had a total score of 0, which meant normal.

4.2.3 Tear Break-up time

In this section the solutions of DHS and DHS esters were tested. According to the previous discussion, a prolonged TBUT is helpful for stabilizing the tear film. For comparison some commercial products (Advance Eye Relief from Bausch & Lomb and Systane from Alcon) and solutions of commercial polymers, which were commonly used in ophthalmic solutions, (carboxymethylcellulose, hydroxylpropyl methylcellulose, and sodium hyaluronate) were also tested. The results are summarized as following.

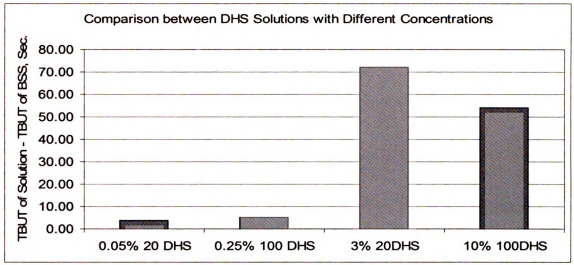

Figure 61: TBUT comparison of DHS solutions with different concentrations

In Figure 61 20DHS and 100DHS were tested under different concentrations. The solutions with high concentrations had much longer TBUT than those with low concentrations. This can be contributed to multiple reasons. Comparing with low concentration solutions, high concentration solutions have higher viscosity, lower relaxation time, and stronger mucoadhesion therefore, they are able to resist shear caused by blinking and stay in the eye for a prolonged time as an unbroken surface.

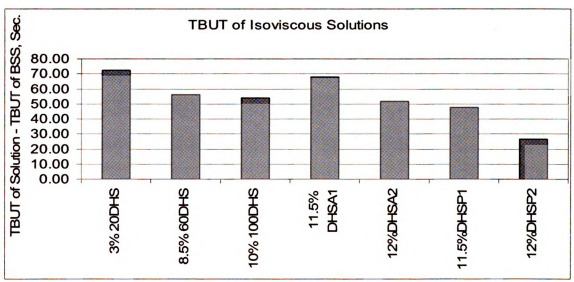

Figure 62: TBUT of Isoviscous solutions

In Figure 62, the isoviscous solutions made of DHS and DHS esters are compared. Among the three DHS solutions, 3% 20DHS had the longest TBUT, and 60DHS and 100DHS had similar TBUT, which was lower than that of 20DHS. Given that they have similar surface tension, rheological properties, and mucoadhesion strength it is not clear why the performance of 3% 20DHS is different. The performance of DHS ester solutions was compared with that of 100DHS. Among them, DHSA1 had the best performance with a TBUT at 69 seconds. It is followed by DHSA2, which had a similar TBUT as 100DHS. Both DHSP1 and DHSP2 had shorter TBUT than 100DHS and DHSP2 had the shortest one at only 27 seconds. The most important reason for these differences is most likely related to the difference in different surface tension between these samples. The results confirm our prediction that a surface tension lower than that of water should help an ocular drug delivery system to remain in the eye for a prolonged time. These results further explain the reason DHSA1 had much longer TBUT than 100DHS. In addition, we also predicted previously that if the surface tension was lower than a certain level, it would not help any more and may even turn to be a negative factor. This explains why the TBUT of DHSA2, DHSP1, and DHSP1 is shorter than TBUT of 100DHS and their TBUT is in the order of DHSA2 > DHSP1 > DHSP2. This means when the surface tension decreases, although it helps spontaneous spreading on the cornea, it also lowered the work of adhesion, and therefore, the surface tension of an ophthalmic solution should be only slightly lower than that of water.

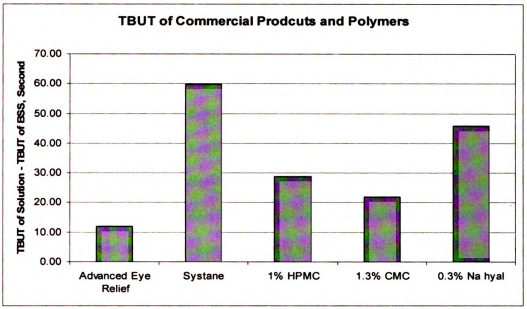

Figure 63: TBUT of commercial products and polymers

In addition, in order to examine the performance of our polymers when comparing with available products, we tested two commercial products and three commercial polymers that are commonly used in ophthalmic solutions. It was exciting to see that several of our polymers had a better performance than commercial products.

Based on the above TBUT results, we found that in order to obtain improved tear film stability a tear substitute formulation should have the following characteristics: (1) optimized viscosity, if the viscosity is too low, the solution is not able to stay on the cornea, if the viscosity is too high irritancy can be caused, which thereafter results in increased blinking frequency; (2) optimized surface tension, if the surface tension is too high, it prevents spontaneous spreading on the cornea, if the surface tension is too low, it will result in low adhesion strength; and (3) mucoadhesion, which keeps the polymer on the cornea for prolonged time.

4.2.3 *In vivo* Timolol release results

Timolol release profiles were measured with selected polymers to make sure that Timolol entered the inside of the eye. Afterwards, IOP tests were done to determine their performance. The results are as follows.

4.2.3.1 *In vivo* Timolol release profiles

The in vivo Timolol release profiles of 20DHS and 100DHS solutions were collected. 3% 20DHS, 3% 100DHS, and 10% 100DHS were tested, along with a commercial Timolol eye drop as a control. In this test, 3% 20DHS and 10% 100DHS had much higher concentrations at all of the time points, this means they were able to stay in the eye for a longer time compared with the commercial control. Their performance is believed to be contributed by its (1) stronger mocuadhesion, which helps drug stay in the eye with longer retention time in the eye; (2) relatively higher viscosity, which means slower drug release compared with 3% 100DHS and the control; and (3) lower relaxation time, which means more elastic character during blinking. In contrast, 3% 100DHS did not help because of its low viscosity and mucoadhesion strength. The results are shown in Figure 64. Based on these results, we confirmed that our polymers had the ability to deliver Timolol into the eye. However, although the drug was detected in the eye, it did not mean our goal (to decrease the ocular pressure) was achieved. In the next section IOP results are presented to show the performance of our polymers in terms of decreasing ocular pressure.

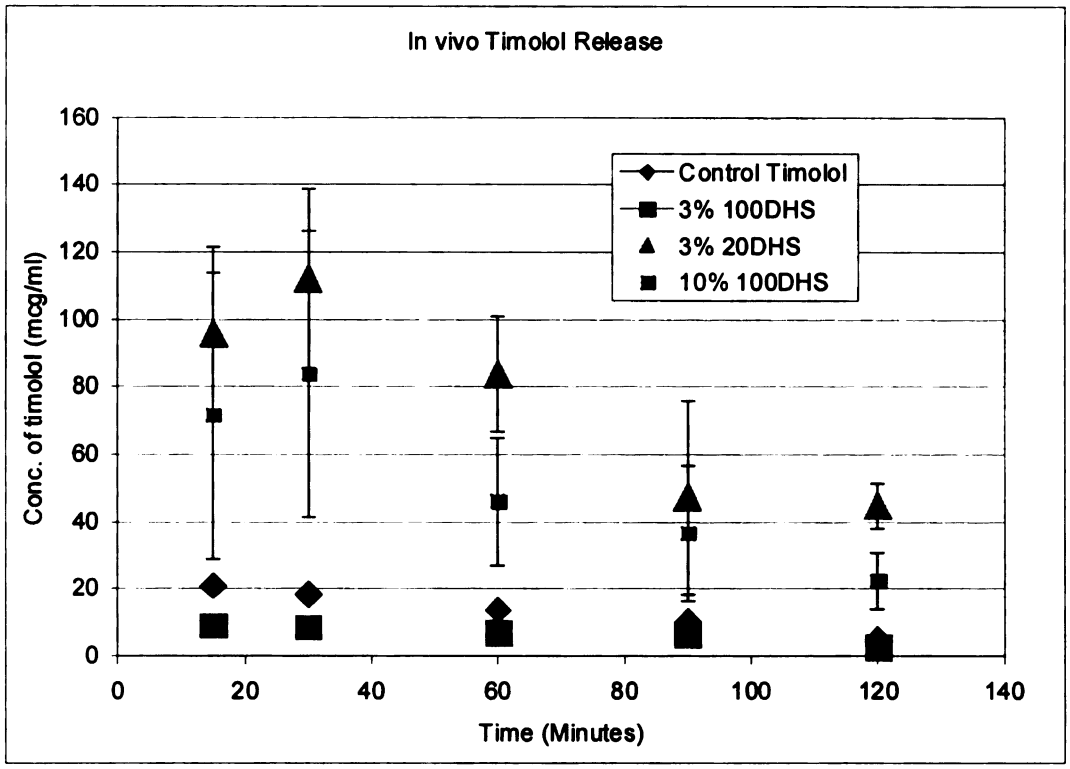

Figure 64: First set of Timolol release test

4.2.3.2 IOP results

Change in IOP (ΔIOP) for each eye is expressed as follows:

$$\Delta IOP = IOP_{zero\ time} - IOP_{time,\ t} \quad (4.2)$$

In this test, besides our selected solutions (4% 20DHS, 5% 20DHS, 20% 100DHS, and 20% DHSA1), two commercial products were also tested as controls plain Timolol and Gel Forming Solution (GFS). According to their Indications and Dosage information, the plain Timolol should be applied twice a day and the GFS should be applied once a day. In this test, all solutions with 0.5% Timolol were applied once and the IOP were measured at 2 hours, 6 hours, and 8 hours. Their IOP change calculated according to Equation (4.2) and the standard deviations were listed in the following table. ΔIOP is

plotted as a function of time. The results can be seen in Figure 65. The IOP measurement of plain Timolol showed a drop at 2 hours but did not sustain and diminished afterwards. This is because there was no carrier in the plain Timolol solution and only a small fraction of drug diffused into the eye at the beginning due to the high drug concentration in the precorneal region right after the solution was applied. The measurement of GFS did not show any IOP drop at any time point. This might be caused by its short retention time in the eye. When the GFS was dropped into the eye the aqueous solution of xanthan gum in the presence of tear protein (lysozyme) formed a gel with elastic rather than viscoelastic character, which might cause irritancy and the irritancy further caused fast and frequent blinking, therefore resulted in a short retention time in the eye. When compared with either of the commercial products, our polymers showed sustained effect. At 2 hours, 4% 20DHS had significantly better performance than the GFS and comparable performance as plain Timolol. At hour 8, 4% 20DHS showed significantly greater IOP drop from both of the commercial products. At 6 hours, it is not clear what caused the poor performance. The performance of 5% 20DHS was not as good as that of 4% DHS. This might be due to its higher viscosity and more elastic character when comparing with 4% 20DHS. Although, the average IOP drop of 5% 20DHS showed a sustained trend. Similar as 5% 20DHS, 20% 100DHS and DHSA1 also showed slight IOP drop at all times. What needs to be particularly pointed out is the performance of DHSA1. It did not show better performance than 100DHS, as in the TBUT test. This observation means that surface tension is a more important factor for tear film stability than Timolol delivery. This is because that surface activity is a key factor for spreading and spreading determines how the ophthalmic solution covers on the cornea. However,

instead of targeting the outer surface of the cornea the polymers stays in the corner of eye for Timolol delivery, therefore spreading is not as important as for TBUT.

Table 28: IOP change

	IOP Change					
	Hour 2		Hour 6		Hour 8	
Sample	Average, mmHg	Std. Dev.	Average, mmHg	Std. Dev.	Average, mmHg	Std. Dev.
Plain Timolol	0.9	1.3	-0.4	1.6	-0.1	1.4
GFS	-1.6	1.6	0	1.4	0	1.1
4% 20DHS	0.7	1.2	-0.2	1.4	1.4	2.2
5% 20DHS	0.5	1.6	0.4	1.5	0.4	1.3
20% 100DHS	0.3	1.3	0.2	1.3	0.2	1.4
20% 100DHSA1	0.2	1.6	0.6	1.3	0.3	1.2

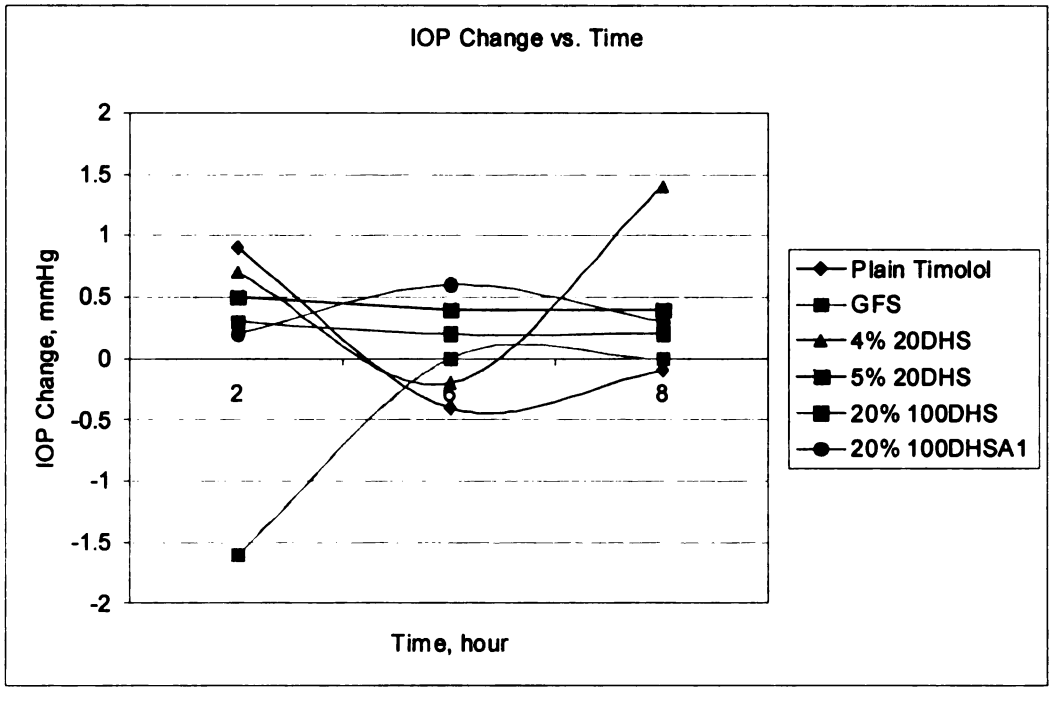

Figure 65: IOP change vs. Time

Based on the above Timolol release test results, we can draw the following conclusions: (1) in order to obtain effective treatment and minimized instillation frequency drug delivery systems with controlled drug release are needed. (2) Comparing with drug delivery systems that forms gel in the eye a system with optimized viscoelastic

character has more advantage by offering low irritancy under low frequency of blinking and high stability under high frequency of blinking, therefore maximized effective treatment and patient acceptance. (3) Comparing with TBUT, surface tension is not a significant factor for Timolol delivery.

In summary, given the prolonged TBUT and sustained drug release from *in vivo* tests, our polymers demonstrated a good potential for ophthalmic solutions, either as drug delivery systems or dry eye solutions. Therefore, commercialization of these polymers should be further pursued. In addition, the data confirm our prediction that the ocular drug delivery process should be improved though a multidisciplinary approach. All factors including surface tension, mucoadhesion, rheology, and controlled drug release work together to determine the performance as an ocular drug delivery system. Such approach will help others and us in this field to design effective ocular drug delivery systems.

Chapter 5 Conclusions and Recommendations

5.1 Conclusions

- The synthesized polymers, DHS and DHS esters, can be characterized by FTIR, NMR, and chemical method to analyze the structure and degree of modification, qualitatively and/or quantitatively.
- The degree of modification is controllable by varying reaction conditions.
- The polymers are water dispersible or soluble, depending on the controlled degree of modification.
- The DHS ester solutions can reduce the surface tension of an ophthalmic solution, which helps them spreading on the corneal surface.
- The polymers show strengthened adhesion with mucin, which can offer the drug delivery system prolonged retention time when in contact with mucin.
- The polymer solutions have desired flow and viscoelastic properties for application of ophthalmic formulations.
- The polymer solutions have controlled drug release profiles consistent of hydrogel matrices.
- The products have acceptable irritation test results from both *in vitro* and *in vivo* tests.
- *In vivo* Tear Break-Up Time Tests show some candidates have prolonged TBUT, which indicates that they can be used to stabilize the tear film.
- *In vivo* Timolol release tests provide promising results for sustained drug release, which offers the potential for effective ocular drug delivery.

5.2 Fundamental Contribution

Our fundamental contribution is the building of a structure-property-performance relationship for polymer-based ocular drug delivery systems. According to our work, the performance of an ocular drug delivery system is determined by properties such as surface tension, adhesion, and rheology. The surface tension is important for spreading and strength of adhesion, mocuadhesion is essential for the retention of prolonged retention time in the eye, and rheological properties regulate resistance to the shear stress, which further affects the retention time, and drug release profile. In addition, all these properties can be optimized according to specific needs by engineering polymers with various structures. By understanding the structure-property-performance relationship, it will help designing of effective polymer-based ocular drug delivery systems.

5.3 Recommendations

- Study the temperature's effect on polymers' rheological properties.
- IOP tests with prolonged test time.
- Further investigation for dry eye application with corneal topographic modeling system.

References

[1] Kaur, I. P. and Kanwar, M. (2002). "Ocular preparations: The formulation approach." Drug Development and Industrial Pharmacy 28(5): 473-493.

[2] Mindel, J. S. (1982) Bioavailability. Biomedical Foundations of Ophthalmology: Chapter 22.

[3] Burrows, J., Tsibouklis, J., and Smart, J. (2002) "Drug delivery to the eye." The Drug Delivery Companies Report 2002 (Pharmaventures)

[4] Robinson JC. (1993) "Ocular anatomy and physiology relevant to ocular drug delivery." Ophthalmic Drug Delivery Systems, Marcel Dekker: New York, US, 29-57

[5] Davies, N.M. (2000). "Biopharmaceutical considerations in topical ocular drug delivery." Clinical and Experimental Pharmacology and Physiology 27:558-562.

[6] Brewitt, H. and Sistani, F. (2001) "Dry Eye Disease: The Scale of the Problem" SURVEY OF OPHTHALMOLOGY VOLUME 45 SUPPLEMENT 2 MARCH 2001

[7] Albietz, J. M. (2001). "Dry eye: an update on clinical diagnosis, management and promising new treatments." Clin Exp Optom 84(1): 4-18.

[8] Geerling, G., and Liu, C.S. et al. (2002). "Costs and gains of complex procedures to rehabilitate end stage ocular surface disease." Br J Ophthalmol 86(11): 1220-1.

[9] Baudouin, C. (2001). "The pathology of dry eye." Surv Ophthalmol 45 Suppl 2: S211-20.

[10] Calonge, M. (2001). "The treatment of dry eye." Surv Ophthalmol 45 Suppl 2: S227-39.

[11] Bach, F. C., J. B. Adam, et al. (1972). "Ocular retention of artificial tear solutions. Comparison of hydroxypropyl methylcellulose and polyvinyl alcohol vehicles using an argyrol marker." Ann Ophthalmol 4(2): 116-9.

[12] Sugiyama, T., S. Miyauchi, et al. (1991). "The effect of sodium hyaluronate on the migration of rabbit corneal epithelium. II. The effect of topical administration." J Ocul Pharmacol 7(1): 53-64.

[13] Sullivan, D. A., H. Ariga, et al. (1994). "Androgen-induced suppression of autoimmune disease in lacrimal glands of mouse models of Sjogren's syndrome." Adv Exp Med Biol 350: 683-90.

[14] Rieger, G. (1990). "Lipid-containing eye drops: a step closer to natural tears." Ophthalmologica 201(4): 206-12.

[15] Urtti, A. (1995). "Kinetic Aspects in the Design of prolonged action ocular drug delivery systems." Advances in Pharmaceutical Sciences.

[16] Rolando M, Zierhut M, (2001). The Ocular Surface and Tear Film and Their Dysfunction in Dry Eye Disease, Survey of Ophthalmology Volume 45 , Pages S203 - S210.

[17] Lindberg, B.; Misiorny, A. Quantitative analysis of reducible carbohydrates by means of sodium borohydride. *Svensk. Papperstidn.* 1952, *55*, 13-14.

[18] Miladinov,V.D. and Hanna,M.A. (2000) Starch esterification by reactive extrusion, Industrial Crops and Products 11 (2000) 51–57

[19]Solomon, O. F. and Ciuta,I. Z. (1962) Determination of the intrinsic viscosity of polymer solutions by a simple determination of viscosity , J. Appl. *Polym. Sci.*, 6,683.

[20] Sihtola, H. Chemical properties of modified cellulose. 2003 Die Makromolekulare Chemie Volume 35, Issue 1. Pages 250 – 265

[21] Narayan, R. cellulose modification Engineering, L. o. R. R. (1983). Conversion of cellulose and xylan into glycols. NSF Grant No. 8022426AI.

[22] Billmers, R. L. and Tessler, M. M. Method of preparing intermediate DS starch esters in aqueous solution, United States Patent 5321132

[23] Holly, F. J. and M. A. Lemp (1971). "Wettability and wetting of corneal epithelium." Exp Eye Res 11: 239-250.

[24] Cope, C., Dilly, P. N. et al. (1986). "Wettability of the corneal surface: a reappraisal." Curr Eye Res 5(10): 777-85.

[25] Tiffany, J. M. (1990). "Measurement of wettability of the corneal epithelium. I. Particle attachment method." Acta Ophthalmol (Copenh) 68(2): 175-81.

[26] Girifalco, L. A. and Good, R. J. (1957) A Theory for the Estimation of Surface and Interfacial Energies. I. Derivation and Application to Interfacial Tension, R. J. , *J. Phys. Chem.*, 61, 904.

[27] Rose, M.C. (1992) Mucins: structure, function, and role in pulmonary diseases, *Am J Physiol Lung Cell Mol Physiol* 263: L413-L429,

[28] Smart, J.D. (1999) "The role of water movement and polymer hydration in mucoadhesion" Bioadhesive Drug Delivery Systems: Chapter 2

[29] Checkering, D.E. and Mathiowitz E. (1999) "Definitions, mechamisms, and theories of bioadhesion" Bioadhesive Drug Delivery Systems: Chapter 1

[30] Voyutskii, S.S. Autohesion and adhesion of high polymers. 1st edition. 1963 P272

[31] Mikos, A.G, and Peppas, N.A. Systems for controlled release of drugs. V. Bioadhesive systems. S T P Pharmacol 2:705-716, 1986

[32] Huntsberger, J. R.. Locus of adhesive failure. Journal of Polymer Science, Part A: General Papers (1963), 1 1339-44.

[33] Hassan, E.E. and Gallo, J.M., 1990. A simple rheological method for the in vitro assessment of mucin–polymer bioadhesive bond strength. *Pharm. Res.* 7, pp. 491–495.

[34] Carpenter RHS. Movements of the eyes. 2nd ed. London: Pion, 1988: 55-131

[35] Ravn K., A better faux teardrop, Los Angeles Times, Health, February 12, 2007

[36] Steffe, J. Rheological methods in food process engineering, 2nd Edition. Chapter 5.

[37] Reiner, M. 1964, The Deborah number, Physics today, Jan.: 62.

[38] Pipkin, A.C. 1986, Lectures on viscoelasticity theory, 2nd Edition

[39] Tobolsky, A.V. , Dunell, B.A., and Andrews R.D. Relaxation and Dynamic Properties of Polymers Textile Research Journal, Vol. 21, No. 6, 404-411 (1951)

[40] Cáramella, C.M., Rossi, S., and Bonferoni M.C. (1999) "A rheological approach to explain the mucoadhesive behavior of polymer hydrogels" Bioadhesive Drug Delivery Systems: Chapter 3

[41] Amsden, B., Solute Diffusion within Hydrogels. Mechanisms and Models *Macromolecules,* 31 (23), 8382 -8395, 1998

[42] Peppas, N.A. and Lustig S.R., Solute diffusion in hydrophilic network structures. In: N.A. Peppas, Editor, *Hydrogels in Medicine and Pharmacy 1*, CRC Press, Boca Raton (1986), pp. 57–84.

[43] Allen, A., Foster SNE, Person JP. 1986. Br J Pharmacol 87: 126p

[44] Munger, RJ. "Veterinary ophthalmology in laboratory animal studies" *Veterinary Ophthalmology.* 2002. 5 (3): 167-175

[45] Cao y, Zhang C, et al " Poly (N-isopropylacrylamide)-chitosan as thermosensitive in situ gel-forming system for ocular drug delivery" J. of Controlled Release, 2007, vol. 120, p. 186-194